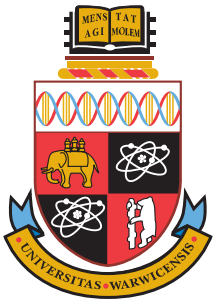

Mathematical Modelling of Epidemic Systems Influenced by Maternal Antibodies and Public Health Intervention

by

James D Chapman

Thesis submitted to the University of Warwick

in partial fulfilment of the requirements

for admission to the degree of

Doctor of Philosophy

School of Engineering

September 2010

THE UNIVERSITY OF WARWICK

Contents

List of Tables

List of Figures

List of Symbols

General Modelling Terms

$\Sigma(p)$	Postulated state space model
$x(t,p)$	Vector of state variables
$x^0(p)$	Initial condition
$y(t,p)$	Output function
p	Vector of unknown model parameters

Analysis

$\hat{x}$	Steady state value of $x(t,p)$
$\tilde{p}$	Alternative parameter vector indistinguishable from p
α	Vector of normalised parameters, $\ln p$
$\sim$	Denotation of indistinguishability between components
Ω	Open set of all possible parameter vectors
$\mathcal{N}(p)$	Open neighbourhood in parameter space
$\mathbb{R}$	Set of real numbers
T	Invertible linear map
ϕ	Smooth mapping between state trajectories of p and $\tilde{p}$
θ	Specific substitution relevant only to preceding expression
M_i	Monomials of a multivariate polynomial expression
W	Wronskian determinant
S	Sensitivity matrix
$Q(p)$	Sum of squares deviation due to some change in p
ψ	Principal component

State Variables

$M(t,a)$	Protected by maternally acquired immunity
$S(t,a)$	Susceptible to infection
$E(t,a)$	Infected but not yet infectious
$I(t,a)$	Infective and infectious to others
$R(t,a)$	Recovered
$Ab^+(t,a)$	Seropositive to disease specific antibodies
$Ab^-(t,a)$	Seronegative to disease specific antibodies

Model Parameters

N	Total population size
$N(a)$	Population distribution with respect to age
μ	Combined birth/mortality rate coefficient (yr^{-1})
$\mu_b(a)$	Age dependent birth rate (yr^{-1})
$\mu_d(a)$	Age dependent mortality rate (yr^{-1})
L	Life expectancy (yr)
A_v	Average age at primary infection (yr)
A_T	Target age (yr)
R_0	Basic reproduction number
R_E	Effective reproduction number
c	Average contact rate between individuals (yr^{-1})
ρ	Probability of transmission upon contact with an infective
$\beta(t, a_s, a_i)$	Transmission function (yr^{-1})
β_0	Annual average transmission rate (yr^{-1})
β_1	Magnitude of seasonal variation
ϕ	Phase or annual timing of seasonality
$\lambda(t, a)$	Force of infection
v	Recovery rate coefficient (yr^{-1})
ω_M	Rate of loss of maternally acquired protection (yr^{-1})
ω_R	Rate of waning active immunity (yr^{-1})
σ	Partial immunity/reduced susceptibility parameter (proportion)
γ	Reduced infectivity parameter (proportion)
P_v	Effective birth-targeted vaccine coverage (proportion)
P_m	Proportion of newborns maternally immunised
ϑ	Proportional interaction between vaccination & MAb
k	Observation gain
k_i	Ageing rate coefficient (yr^{-1})
$Q(t, a)$	Age specific loss of maternally acquired protection (yr^{-1})
Ab	Log antibody titre (log AU)
$C(t, Ab)$	Population cord log antibody titre distribution
$C_v(t, Ab)$	Post-vaccine titre distribution
$V_M(t, Ab)$	Maternal immunisation function
τ	Threshold in Ab distinguishing immunity & susceptibility (log AU)

Acknowledgements

I would like to thank my supervisor Dr Neil Evans for his guidance and continual support throughout the duration of this project. In addition, I would like to thank Prof Graham Medley, Dr Lisa White and Dr James Nokes, as well as all of our group, including but not limited to Prof Keith Godfrey, Dr Mike Chappell and in particular Dr John Hattersley, for sharing their wealth of knowledge and insightful discussion.

I would also like to extend my appreciation to the School of Engineering at the University of Warwick and to the Engineering and Physical Sciences Research Council (EPSRC) for funding this research and for the opportunity to promote my work at a number of international conferences and events.

Finally, I am hugely indebted to all my family and friends who have provided enormous support and encouragement throughout my studies.

Declarations

This thesis is the original work of the author. The following publications have arisen from specific sections of the work, where the role of the co-authors, in all cases, has been supervisory:

Chapter 4

J.D. Chapman & N.D. Evans, The structural identifiability of susceptible-infective-recovered type epidemic models with incomplete immunity and birth targeted vaccination. Biomedical Signal Processing and Control, 4 (4) 2009 278-284.

J.D. Chapman & N.D. Evans, The structural identifiability of SIR type epidemic models with incomplete immunity and birth targeted vaccination. In Proceedings of the 17th IFAC World Congress, Seoul, Korea, July 6-11, 2008.

Chapter 5

J.D. Chapman, M.J. Chappell & N.D. Evans, The use of a formal sensitivity analysis on epidemic models with immune protection from maternally acquired antibodies. Computer Methods and Programs in Biomedicine, In Press.

J.D. Chapman, M.J. Chappell & N.D. Evans, The use of a formal sensitivity analysis on epidemic models with immune protection from maternally acquired antibodies. In Proceedings of the 7th IFAC Symposium on Modelling and Control in Biomedical (Biological) Systems, Aalborg, Denmark, August 12-14, 2009.

Chapter 6

J.D. Chapman & N.D. Evans, A prospective model framework for the study of mass maternal immunisation. The IMA Journal of Mathematical Medicine and Biology, submitted Jan 2010.

Abstract

The general subject area of research considered in this thesis is population level epidemic modelling of infectious diseases, with specific application to the problems of model indeterminacy and systems that include processes associated with maternally acquired immunity. The work presents the derivation and analysis of a lumped systems model framework to study the influence of maternal antibodies on the population dynamics of infection among neonate and young infant age classes. The proposed models are defined by sets of ordinary and partial differential equations that describe the variation of distinct states in the natural history of infection with respect to time and/or age.

The model framework is extended to explore the potential population level outcomes and consequences of mass maternal immunisation: an emerging targeted vaccine strategy that utilises the active transfer of neutralising antibodies during pregnancy in order to supplement neonatal immunity during the first few months of life. A qualitative analysis of these models has highlighted the importance of interaction with early childhood targeted vaccination campaigns, the potential to invoke transient epidemic behaviour and the prospective advantages of seasonal administration.

The work considers the implications of structural identifiability, indistinguishability and formal sensitivity analyses on a number of fundamental model structures within the proposed framework. These methods are used to establish whether a postulated model structure, or the individual parameters within a known structure, are uniquely determinable from a given set of empirical observations. The main epidemiological measures available for the validation of epidemic models are inherently based on records of clinical disease or age serological surveys, which are not explicitly representative of infection and provide a very limited observation of the full system state. The analyses suggest that these issues give rise to problems of indeterminacy even in the most simple models, such that certain system characteristics cannot be uniquely estimated from available data.

Chapter 1

Introduction

The implementation of mass immunisation campaigns has long been recognised as an effective strategy for preventing severe morbidity and mortality inflicted by a variety of infectious diseases. Neonatal and young infant age classes however, remain vulnerable to many of these infections [Englund et al., 1998]. Immunising vaccines are generally unsuccessful in individuals with immature immune systems and their safety in newborns is of ongoing concern. An accumulation of evidence suggesting that passive protection during the first few months of life may be conveyed in the form of maternal antibodies (MAb) could therefore have a significant impact on future health care effort within this context [Munoz and Englund, 2000].

The potential to augment passively acquired immunity in the newborn by stimulating a complementary active immune response in the mother has presented an emerging public health opportunity in the form of maternal immunisation [Glezen and Alpers, 1999]. Interventions of this nature have already been successfully applied in several developing regions with the aim of reducing young infant mortality due to tetanus [WHO, 2002]. Candidate vaccines are currently also being considered for a number of other highly prevalent viral infections, such as human respiratory syncytial virus (hRSV), influenza and pertussis, which are found to

cause a significant burden of disease among neonatal and young infant age classes [Healy and Baker, 2006].

The inherent complexity of host-pathogen interactions at both individual and population levels, and the necessarily stringent processes by which new large scale healthcare intervention strategies are approved, prescribe the use for methods of theoretical analysis [Nokes and Anderson, 1988]. Mathematical modelling provides an abstract framework with which to explore the observed behaviour of real world systems and their potential responses to various environmental conditions, without the constraints typically imposed by real world risk or cost of experimentation. In the context of communicable diseases, these efforts are motivated by a requirement for more accurate predictions regarding the outcome of infection, a greater understanding of the principal biological mechanisms at work and to inform decisions concerned with the governance of public health policy.

Mathematical models are generally classed as either process driven or data driven, depending on whether they represent an analytic description of the underlying physical processes or simply some empirical record of real world system behaviour. The adoption of both approaches is evident throughout the study of mathematical epidemiology, however, process driven modelling methods are generally more favourable since they allow more elemental inferences to be made regarding the fundamental operation of the system. A general procedure for generating and applying mathematical models of this nature to a particular real world problem may be described in the following stages:

- **Problem Definition** - Specify the scope of the problem and capture the requirements of the model.
- **Model Derivation** - Collate relevant hypotheses and prior knowledge of the real world system in order to identify the key physical processes of interest and describe critical interactions between them in an appropriate mathematical form.

- **General System Analysis** - Investigate relations within the fundamental operation of the model using mathematical techniques such as steady state analysis, stability criterion, and bifurcation theory, in order to further understand the characteristic behaviour of the system.

- **Validation** - First, ensure that the model sufficiently describes any qualitative characteristics of the real system using the aforementioned general system analysis. Second, calibrate the model by quantitatively comparing its output with empirical observations and estimating unknown parameters. Validation is performed in order to ensure that the model may be used to accurately infer characteristics of a specific real world system and make meaningful predictions about its future behaviour.

- **Simulation** - Explore the predicted behaviour of the system by simulating the model with a series of input conditions and perturbations that may be representative of critical and interesting scenarios.

It is the application of this modelling methodology to epidemic systems, including those that describe characteristics associated with maternally acquired immunity and intervention, that is the subject of this work.

Problem Statement

The benefits of maternally acquired immunity and maternal immunisation to the individual are becoming increasingly well established through studies such as those described by Vandelaer et al. [2003], Puck et al. [1980], and Mulholland [1998]. However, the influence of these processes on population level infection characteristics remains largely unknown.

The epidemiology of infectious diseases is markedly different to that of noninfectious diseases. Since each infective individual is a potential source of infection to

others, the risk of disease to any one member of a host population is inherently dependent on the status of all those with whom they may potentially come into contact [Medley and Nokes, 2005]. The spread of an infectious agent throughout a large population of hosts is therefore principally driven by community-wide patterns of susceptibility/immunity and the prevalence of infection. Epidemiological characteristics and interventions that may influence these variables subsequently have indirect population level consequences beyond those of the individual to which they directly relate. Furthermore, heterogeneous interactions between these factors, such as seasonal, demographic and immunological dependencies, often lead to highly complex system behaviour.

Population dynamics of communicable diseases are frequently explored using lumped system models, where individuals within a population are grouped according to some common epidemiological characteristic and considered as a single homogeneous unit [Jacquez, 1996]. Individual level complexities may be reduced according to risk factors such as immunological experience, age or spatial distribution, in order to make analysis of the resulting model more tractable. In this instance, the appropriate selection of model structure and the identification of essential system processes are crucial and have a significant impact on the applicability of the model to a specific problem.

In order for mathematical models to accurately describe particular real world systems, they must first be rigorously validated. However, the validation of complex population level infection based models is often a markedly non-trivial task. The main epidemiological measures available are typically based on records of clinical disease or age serological surveys, which are not necessarily representative of infection and provide only a very limited observation of the full system state [White et al., 2005]. The notification of many infectious agents is also incomplete and heavily biased depending on awareness, severity of symptoms and social stigma [Thacker et al., 1983]. These issues give rise to the problem of indeterminacy, where certain system characteristics may not be uniquely determined from the

available set of empirical observations.

It is the objective of this work to derive and consider the validation of a series of population level epidemic model structures that may be used to estimate the influence of processes and interventions associated with maternally acquired immunity on the epidemiology of infectious disease. Significant and original contributions in both these subject areas are presented, where it is hoped that the resulting framework will ultimately contribute to the assessment and optimal implementation of future public health policies within this context.

Thesis Structure

The thesis is structured into two chapters that describe the derivation of both existing and novel epidemic model structures, three chapters of analysis and a brief overall discussion that includes suggestions for future research. Each technical chapter contains an introduction, a review of relevant literature and a discussion of the key findings and implications of the work.

Chapter 2 provides a pedagogical review of current epidemic compartmental systems and the basic modelling principles required by the reader. A number of fundamental model structures are described in detail since they are applicable to the derivation of new models in Chapter 3 and their subsequent analysis in Chapters 4 and 5 is novel. **Chapter 3** presents the development and preliminary analysis of models that incorporate processes associated with maternally acquired immunity and maternal immunisation.

Chapters 4 and **5** describe the application of techniques used to address issues of indeterminacy that arise during the validation of the discussed models. These methods are namely structural identifiability/indistinguishability and sensitivity analysis, which aim to establish, first, whether it is even theoretically possible

to ascertain unique parameter estimates from a particular set of measurements (structural identifiability), and second, how well a particular estimation is determined or supported by an experimental observation (numerical identifiability and sensitivity analysis). The results from these analyses are also interpreted to give an indication of the likely influence of maternally acquired immunity over population level system behaviour and discussed in the context of model reduction and future experimental design.

Chapter 6 describes additional qualitative analysis of the models derived in Chapter 3 and presents a series of examples demonstrating their applicability to epidemiological problems arising from maternally targeted intervention. Simulation is performed using nominal characteristic parameter estimates extracted from the literature in order to establish what the potential static, dynamic and seasonal implications of these processes might be.

Chapter 2

Mathematical Modelling of Communicable Diseases

In reality, all epidemic system processes are inherently stochastic in nature since they are primarily driven by individual-level events and interactions between hosts. However, the analysis of epidemic models that include probabilistic descriptions of such random processes can be a complex and challenging task, and often only considered following a preliminary analysis of more tractable deterministic models [Andersson, 2000]. At a population level, stochastic variations are generally most critical when considering the progression of minor outbreaks within small isolated cohorts or the persistence of pathogens that are close to the threshold of extinction. As a result, deterministic models provide a useful approximation to the epidemic evolution of highly infectious agents that appear ubiquitous throughout large populations [Anderson and May, 1991].

The most common approach to deterministic modelling of population level microparasite transmission dynamics is through a compartmental representation of the various stages in the natural history of infection, written as a system of ordinary differential equations (ODEs). Analogous examples of compartmental analysis are

also frequently found throughout the literature relating to other scientific contexts, such as chemical and drug kinetics, where a large base of applicable techniques have been documented [Godfrey, 1983]. Models of this type comprise a finite number of interconnected subunits (compartments) that consist of homogeneous and well-mixed material, where all flow of material between compartments, and to and from the environment, adheres to the principle of mass balance. For epidemic systems, the compartmentalised material corresponds to a large population of individual hosts, through which an infectious agent may be transmitted. In this instance, compartments in the model structure represent subpopulations of hosts residing in a common state of disease.

Compartmental based epidemic models were first developed by Kermack and McKendrick [1927] and have since been extended to incorporate a wide range of complex epidemiological characteristics such as incomplete immunity [Gomes et al., 2004], altered secondary infection [Glass and Grenfell, 2004; Greenhalgh et al., 2000] and multiple-strain variants [White et al., 2005]. For the general application of these models see the texts by Anderson and May [1991], Capasso [1993] and Jacquez [1996], and for specific examples see the work by Medley et al. [2001] and Edmunds et al. [1996] for hepatitis-B virus (HBV), Weber et al. [2001] and White et al. [2007] for human respiratory syncytial virus (hRSV), and Keeling and Grenfell [2002] for measles.

2.1 SIR Framework Models

The general SIR model [Kermack and McKendrick, 1927], shown in Figure 2.1, is used to characterise epidemic systems where the natural history of infection can be reasonably approximated into three distinct stages. The host population is therefore divided into three non-overlapping classes that distinguish an individual's state of disease as either *susceptible*, *infective* or *recovered*, which are delineated

by the state variables $S(t)$, $I(t)$ and $R(t)$, respectively.

The susceptible class includes all individuals who are able to contract the disease and become infectious; the infective class represents only individuals who are currently infected and infectious to susceptibles; and the recovered class contains all individuals who have recovered from infection and have consequently acquired solid lifelong immunity. In this instance, latency incubation periods are neglected, whereby all infected individuals are immediately considered to be infectious. It is also assumed that recovered individuals are no longer able to transmit or re-contract the pathogen, hence, the structure is most appropriate for modelling diseases such as measles, mumps and rubella (MMR), where evidence suggests that lifelong immunity to the entire pathogen population is induced following recovery from natural infection [Jansen et al., 2003].

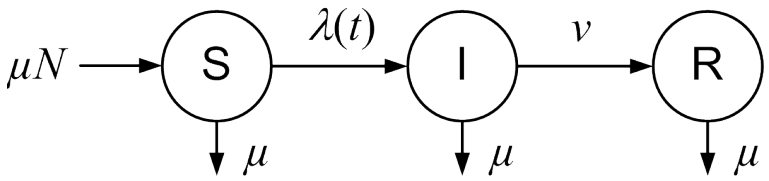

Figure 2.1: General SIR Compartmental Model

Individuals are born into the susceptible class at a net birth rate, μN, where N is the total population size. It is assumed that the average duration of infection, v^{-1}, is small with respect to the average life expectancy, μ^{-1}, such that the net mortality rate, $\mu(S(t) + I(t) + R(t))$, can be assumed to equal μN, hence maintaining a constant size population.

Transmission of the infectious agent throughout the population is modelled using a frequency dependent approximation to mass action mixing. This method is generally accepted for the spread of pathogens among humans, although alternative approximations also exist [McCallum et al., 2001]. Assuming a constant average contact rate, c, per individual, between all individuals within a particular

population, the rate at which infectives, $I(t)$, make contact with the susceptible proportion, $S(t)/N$, is equal to $cS(t)I(t)/N$. For each of these contacts there is then a constant probability, ρ, that the infectious agent will be successfully transmitted. Therefore, the incidence of infection, that is the rate at which susceptible hosts become infected, can be modelled as $\beta S(t)I(t)/N$, where $\beta = c\rho$. The function $\lambda(t) = \beta I(t)/N$ is often used to represent the *force of infection* [Jacquez, 1996], where the average age at primary infection can be approximated by $\lambda(t)^{-1}$.

The resulting transmission dynamics predicted by the SIR model are subsequently described by the following system of ordinary differential equations:

$$\dot{S}(t) = \mu N - \lambda(t)S(t) - \mu S(t), \qquad S(0) = S^0, \tag{2.1}$$

$$\dot{I}(t) = \lambda(t)S(t) - (\mu + v)I(t), \qquad I(0) = I^0, \tag{2.2}$$

$$\dot{R}(t) = vI(t) - \mu R(t), \qquad R(0) = R^0, \tag{2.3}$$

where

$$\lambda(t) = \beta I(t)/N. \tag{2.4}$$

It should also be noted that the model structure is strictly a two state system, since any one of the three state variable equations may be trivially found from the assumption that the population size is constant, i.e. $N = R(t)+S(t)+I(t)$.

2.1.1 The Basic Reproduction Number R_0

The *basic reproduction number*, denoted R_0, is often considered to be the most important quantity in mathematical epidemiology of infectious diseases. It is primarily defined as the average number of secondary cases of infection induced by a single primary case in a completely susceptible (naive or virgin) population [Dietz, 1993], and is expressed as a product of the transmission parameter, β, and the

average duration of time an individual remains infectious:

$$R_0 = \frac{\beta}{\mu + v}. \tag{2.5}$$

This definition gives rise to an invasion threshold at $R_0 = 1$ that determines whether or not an infectious agent can successfully sustain within a particular host population. If the average infective case leads to more than one secondary case, i.e. $R_0 > 1$, then the infection has the ability to invade the host population and cause an epidemic. Given that transmission is heavily dependent on social and environmental variables, which differ between demographically and geographically distinct populations, R_0 is unique for both different diseases and different populations within which it is being considered [Anderson and May, 1991].

2.1.2 Transmission Dynamics & Endemic Equilibrium

Following the introduction of an infectious agent into a fully naive population, the initial growth of a resulting invasion is depicted by the basic reproduction number, R_0. However, once an epidemic has become established, the host population is no longer completely susceptible to infection since a significant proportion of the population are either infective or recovered. In this instance, the number of secondary cases per primary case is defined by the *effective* reproduction number, $R_E = XR_0$, where $X = S/N$ represents the subsequently reduced proportion of the population susceptible.

The typical time course of a resulting epidemic can be described in terms of four distinct stages (see Figure 2.2). The first stage corresponds to a rapid initial increase in transmission due to an abundant availability of susceptible hosts present within an inexperienced population. As the number of available susceptibles di-

minish with the spread of infection, the growth of the invasion begins to stall. An epidemic peak in prevalence is reached at the point where X equals a critical value $X^* = R_0^{-1}$; at which point $R_E = 1$ (i.e. only one new infection arises from each existing case) and there are generally a greater number of individuals recovering from infection per unit of time than there are new cases emerging. Subsequently,

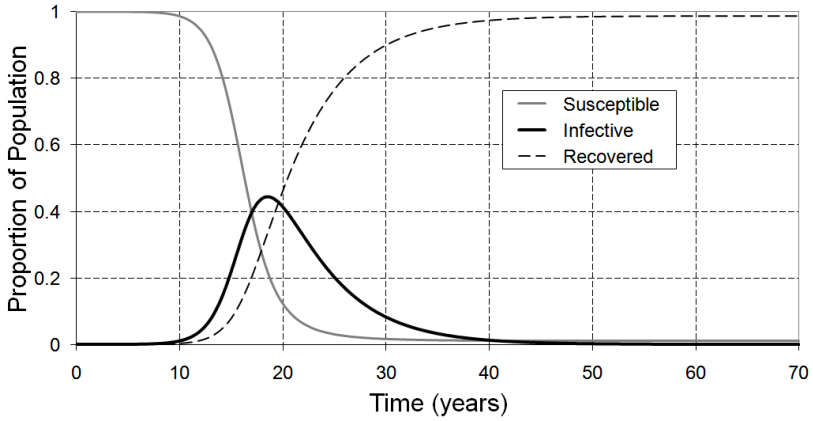

Figure 2.2: Typical epidemic curve for a closed population SIR-type system.

during the third stage, the number of infective individuals begins to fall at a rate largely determined by the average duration of infection. This leads to a reduction in the force of infection and a further decrease in the proportion of the population infective. Finally, the invading pathogen population will either continue to decline and become extinct, or, if there is sufficient replenishment of susceptibles, settle into a stable endemic equilibrium where X is sustained at X^*.

Steady state analysis of the general SIR model may be applied by initially setting the system equations (2.1)-(2.2) equal to zero:

$$\dot{S}(t) = \mu N - \frac{\beta}{N}\hat{S}\hat{I} - \mu\hat{S} = 0, \tag{2.6}$$

$$\dot{I}(t) = \frac{\beta}{N}\hat{S}\hat{I} - (\mu + v)\hat{I} = 0, \tag{2.7}$$

and solving explicitly in terms of the model parameters. It is found that two steady state solutions exist, which correspond to either a disease free or endemic state of invasion, given respectively by

$$\begin{bmatrix} \hat{S} \\ \hat{I} \end{bmatrix} = \begin{bmatrix} N \\ 0 \end{bmatrix} \qquad \text{and} \qquad \begin{bmatrix} \hat{S} \\ \hat{I} \end{bmatrix} = \begin{bmatrix} \frac{N}{R_0} \\ \frac{\mu N}{\mu+v}(1-\frac{1}{R_0}) \end{bmatrix}. \tag{2.8}$$

Since all state variables must be non-negative, it can be seen that the endemic equilibrium is only valid for $R_0 > 1$. Therefore, the threshold $R_0 = 1$ gives rise to a bifurcation point, at which the number of valid steady states and their associated stability is subject to change. These characteristics may be determined through an eigenvalue analysis of the system Jacobian matrix, given by:

$$\begin{bmatrix} -(\mu + \frac{\beta}{N}I) & -\frac{\beta}{N}S \\ \frac{\beta}{N}I & \frac{\beta}{N}S - (\mu + v) \end{bmatrix}. \tag{2.9}$$

Since all parameter values are also real and non-negative, eigenvalues for the disease free and endemic steady states are found respectively to be of the form:

$$\lambda_{1,2} = -\mu, \quad \beta-(\mu+v), \tag{2.10}$$

$$\lambda_{1,2} = -\frac{1}{2}\left(\mu R_0 \pm \sqrt{\mu(\mu(R_0-2)^2 - 4v(R_0-1))}\right). \tag{2.11}$$

It can be seen from (2.10) that the disease free eigenvalues are always real and that the corresponding steady state is asymptotically stable (i.e. has negative real parts) for $R_0 < 1$ (that is $\beta < \mu + v$) and unstable for $R_0 > 1$ (that is $\beta > \mu + v$), which re-iterates the invasion threshold discussed in Section 2.1.1. The endemic steady state is stable throughout its valid range of $R_0 > 1$, however, the associated eigenvalues are seen to become complex for certain values of R_0 determined by the following conditions:

$$\frac{2(\mu + v - \sqrt{v(\mu+v)})}{\mu} < R_0 < \frac{2(\mu + v + \sqrt{v(\mu+v)})}{\mu}. \tag{2.12}$$

In this instance, the analysis implies that the system will display damped oscillatory behaviour while it converges to endemic equilibrium.

2.1.3 Recurrent Epidemics & Seasonal Forcing

Many common infections such as measles, mumps and rubella (MMR), influenza and hRSV tend to display large seasonal oscillations about their endemic equilibrium (for example see Figure 2.3). All epidemic behaviour is primarily driven by susceptibility. Therefore, recurrent epidemics are usually caused by a degree of antagonism between a relatively slow rate of susceptible supply and a high rate of recovery from infection, which is sustained by some element of periodic external forcing. For the unforced SIR example, where R_0 adheres to the conditions for complex endemic eigenvalues given by (2.12), the natural inter-epidemic time period may be expressed by the following approximate form:

$$T \approx \frac{2\pi}{\sqrt{\mu(\beta - v)}}. \tag{2.13}$$

In general, it is found that systems with higher net birth rates and more rapid loss of immunity exhibit shorter inter-epidemic time periods. In contrast, infections with a carrier state or a large duration of infection with respect to net birth rate tend not to display significant (underdamped) oscillatory behaviour. Similarly, infections that induce very limited immunity, such as most sexually transmitted infections, also do not show recurrent epidemic cycles without significant periodic forcing.

Recurrent epidemic cycles can in theory be sustained purely by stochastic variation [Alonso et al., 2007], although most recurrent epidemic systems are found to oscillate in clear annual or biennial cycles [Hawker et al., 2005]. This strongly suggests the influence of external seasonal forcing given that the natural frequency of oscillation is highly parameter dependent and it is unlikely that these values will coincidently combine to give a consistent time period corresponding to a natural number [White et al., 2005].

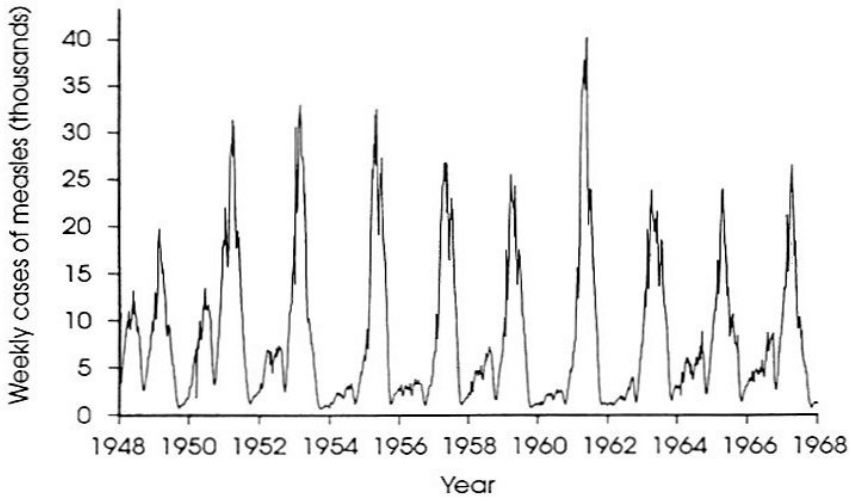

Figure 2.3: Weekly case notifications of measles in England and Wales for the period 1948 to 1968, prior to the introduction of mass vaccination [Anderson and May, 1991]

The most commonly considered mechanisms for seasonal forcing are associated with the transmission parameter, $\beta(t)$, since both the effects of human behaviour, $c(t)$, and the contagiousness of the infectious agent, $\rho(t)$, are potentially governed by recurring seasonal trends. For example, seasonality in measles is primarily driven by the annual school term-time pattern of increased contact between individuals in the classroom (see Keeling et al. [2001], and Fine and Clarkson [1982]), and the prolonged survival of pathogens such as rotavirus, norovirus and influenza (see Cook et al. [1990], Mounts et al. [2000], and Hemmes et al. [1960]) outside the host can be affected by a number of climatic conditions such as temperature, humidity and exposure to sunlight (see also the reviews by Altizer et al. [2006], and Grassly and Fraser [2006]). Temporal variation is typically included in basic SIR type models as a simple sinusoidal function of time of the form:

$$\beta(t) = \beta_0\big(1 + \beta_1 \cos\big[2\pi(t - \phi)\big]\big), \tag{2.14}$$

where β_1 defines the magnitude of the annual variation and ϕ corresponds to the phase (annual timing).

2.1.4 Models With Incomplete Immunity

In reality, most pathogens are able to evade natural immunity and re-infect their hosts through either static antigenic variability or antigenic evolution over time. The consequence of significant antigenic variability within a pathogen population is that natural immunity acquired through experience of infection serves only to protect an individual against a proportion of the circulating infectious agents, leading to only partial immune protection within the host population [Gomes et al., 2004]. Similarly, if the pathogen population experiences a rapid rate of antigenic evolution then any acquired immunity following infection will appear only temporarily effective. It should be noted that the extreme case of incomplete immunity is the SIS (Susceptible, Infected, Susceptible) model structure, in which all individual hosts recover directly back into the fully susceptible state and are immediately able to re-contract the infection. SIS type structures are most appropriate for diseases such as gonorrhoea, which does not produce sufficient immunity against reinfection [Capasso, 1993].

In order to model an epidemic system where immune hosts experience waning of acquired immunity with time since previous infection, the general SIR model is extended to include an additional transfer of individuals from compartment R to compartment S, with rate coefficient ω_R. This describes the rate at which

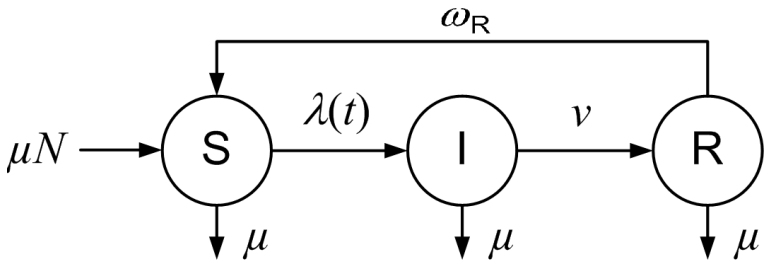

Figure 2.4: SIRS Temporary Immunity Model

recovered (immune) hosts return to being fully susceptible (note that the average

duration of immunity is then ω_R^{-1}) where they are able to re-contract the infection upon contact with an infective individual. It is assumed that before waning off, acquired immunity is solid and provides protection against all current variants of the infectious agent. The model connectivity diagram is shown in Figure 2.4, from which the system equations can be stated as follows:

$$\dot{S}(t) = \mu N - \lambda(t)S(t) - \mu S(t) + \omega_R R(t), \qquad S(0) = S^0, \tag{2.15}$$

$$\dot{I}(t) = \lambda(t)S(t) - (\mu + v)I(t), \qquad I(0) = I^0, \tag{2.16}$$

$$\dot{R}(t) = vI(t) - (\mu + \omega_R)R(t), \qquad R(0) = R^0, \tag{2.17}$$

where

$$\lambda(t) = \beta I(t)/N. \tag{2.18}$$

A partial immunity model describes the situation when immunity serves only to protect the individual against a proportion of the current pathogen population, and an element of susceptibility to some antigenic variants is always retained. The

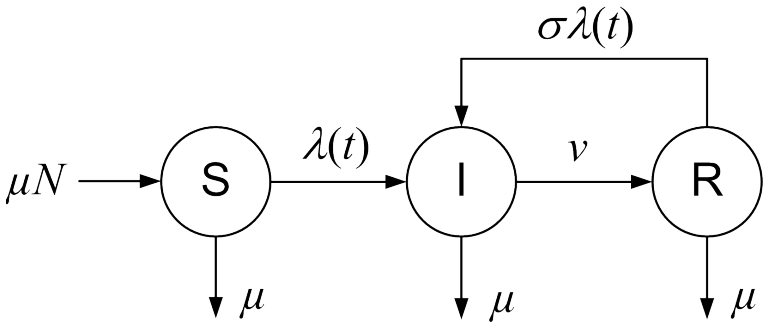

Figure 2.5: SIRp Partial Immunity Model

model can be considered as a combination of an SIR submodel (primary infection) and an SIS submodel (secondary infection), hence the recovered class now acts as a second susceptible class where hosts have a reduced susceptibility to the force of infection governed by the parameter $\sigma \in [0, 1]$. The model structure is shown

diagrammatically in Figure 2.5 and is defined by the following system equations:

$$\dot{S}(t) = \mu N - \lambda(t)S(t) - \mu S(t), \qquad S(0) = S^0, \tag{2.19}$$

$$\dot{I}(t) = \lambda(t)(S(t) + \sigma R(t)) - (\mu + v)I(t), \qquad I(0) = I^0, \tag{2.20}$$

$$\dot{R}(t) = vI(t) - \sigma\lambda(t)R(t) - \mu R(t), \qquad R(0) = R^0, \tag{2.21}$$

where

$$\lambda(t) = \beta I(t)/N. \tag{2.22}$$

It is assumed that any acquired immune protection does not wane with time and is not altered by subsequent re-infections. The dynamic behaviour and endemicity of the system is dually dependent on the contributing characteristics of the SIR and SIS components of the system. The skewing of this dependence towards either primary or secondary infection is governed by the re-infection threshold [Gomes et al., 2004], which describes a limit for R_0 with respect to the partial immunity parameter σ, beyond which re-infection becomes dominant and a significant increase in transmission can occur.

2.2 Vaccination Models

Vaccination strategies are employed to protect susceptible hosts, both at individual and population level, against parasite infection and subsequently reduce the prevalence or burden of disease [Anderson and May, 1991]. Vaccines work by presenting a foreign antigen to the immune system in order to evoke a specific immune response with less morbidity than the naturally occurring infection. At a population level, immunisation can be considered as a process of fast-tracking a proportion of all susceptible hosts to a state of immunity without experiencing infection and hence a period of time during which they are infectious to others. The work documented in this study focuses on the analysis of models where vac-

cination is assumed to induce identical properties of immunity to that of natural infection, such that vaccinated hosts are included within the recovered population class, $R(t)$. In this instance, mechanisms such as antigenic variability and evolution that allow the infectious agent to evade natural immune protection also apply to vaccine induced immunity. In cases where vaccine induced immunity characteristics differ significantly from those produced by natural infection, an additional state variable is typically included to represent individuals protected by the vaccine (for a useful introduction to models of mass vaccination see the review by Scherer and McLean [2002]).

The simplest form of immunisation program is that of an untargeted blanket vaccination of a proportion of the total population. In this instance the vaccination is applied to a random selection of individuals in the population regardless of which state (experience of infection) they reside in. This is a particularly inefficient strategy given that some individuals who have already attained a degree of immune protection through natural infection, or who are currently infected, will receive the vaccine to no effect. This approach can often be the only applicable strategy given the frequent difficulties that arise with identifying an individual vaccinee's prior experience of infection (for example in cases of wild animal vaccination).

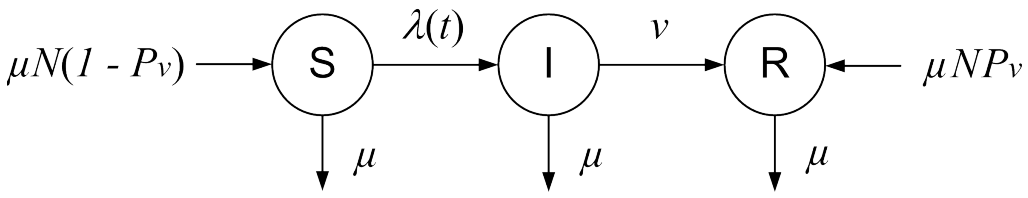

Figure 2.6: SIR Model With Birth Targeted Vaccination

One of the most common examples of a targeted vaccination strategy is to administer immunisation to a proportion of individuals at a particular age. This type of program, typically employed for childhood immunisations such as the MMR, can be easily implemented and monitored within a typical healthcare infrastructure. The most simple realisation of this strategy for an SIR-type epidemic model is

to assume that a proportion of all newborn individuals are vaccinated at birth. Although in reality, vaccination is very rarely administered to neonates due to complications associated with a highly immature immune system, this assumption provides a useful approximation to situations where vaccination is targeted below the average age of primary infection, without the otherwise necessary inclusion of age dependency within the model. A strictly time domain description of this strategy can therefore be implemented within the SIR framework structure (2.1)-(2.4) by replacing the inflow of births, μN, into the susceptible compartment (2.1), by an inflow of susceptibles, $\mu N(1 - P_v)$, and an inflow of vaccinated individuals, $\mu N P_v$, to the recovered compartment (2.3) (see Figure 2.6), where the parameter P_v is the *actual* proportion of newborns that successfully take the vaccine and develop immunity to infection.

Following either the introduction of an infectious agent (discussed in Section 2.1.2), or the implementation of a birth targeted vaccination campaign, the corresponding population is no longer completely susceptible, and the number of secondary cases per primary case is subsequently described by $R_E = XR_0$. Considering the case of a disease free population where $I(t) = 0$ and $S(t) = N$, vaccination serves to reduce the proportion susceptible from $X = 1$ to $X = 1 - P_v$ (provided immunity is solid and lifelong, for example in the case of the general SIR). Hence the effective reproduction number becomes $R_E = (1 - P_v)R_0$. Given that R_E is required to be greater than unity for an epidemic to occur, a potential pathogen invasion can be prevented through vaccination provided the following inequality is achieved:

$$P_v \geq 1 - \frac{1}{R_0}. \tag{2.23}$$

The expression also provides a threshold for the eradication of an established endemic infection and illustrates how diseases with a relatively low R_0 such as smallpox can be eradicated much more easily than those with a high R_0 such as measles. This concept is often referred to as *herd immunity* [Anderson, 1992] and shows how population level protection against an infection can be achieved without

necessarily vaccinating all individual hosts within it (see also the comprehensive article by Nokes and Anderson [1988]).

2.2.1 Vaccination & Eradication Thresholds

The invasion threshold, which determines the basic reproduction number R_0, and the minimum vaccination threshold can both be derived from an eigenvalue analysis of the stability of the disease free equilibrium. Given that $P_v \in [0, 1]$ is a proportion, it can be seen from the expression for herd immunity (2.23) that eradication of an SIR type infection is always possible provided 100% vaccination coverage can be achieved. For the general SIR model with birth targeted vaccination (Figure 2.6), the disease free steady state of the reduced two state system is found to be of the form:

$$\begin{bmatrix} S \\ I \end{bmatrix} = \begin{bmatrix} N(1 - P_v) \\ 0 \end{bmatrix}. \tag{2.24}$$

The influence of vaccination on the stability of the disease free equilibrium can be determined from the corresponding eigenvalues of the system Jacobian matrix:

$$Jacobian = \begin{bmatrix} -(\mu N + \beta I)/N & -\beta S/N \\ \beta I/N & \beta S/N - (\mu + v) \end{bmatrix}, \tag{2.25}$$

where the corresponding eigenvalues for the disease free equilibrium are: $\lambda_1 = -\mu$ and $\lambda_2 = \beta(1 - P_v) - (\mu + v)$. It can then be seen that λ_1 and λ_2 are always real, and from rearranging λ_2, that the disease free steady state can be forced stable (i.e. negative) if $P_v \geq 1 - 1/R_0$, hence reiterating the condition for herd immunity (2.23).

SIRS Temporary/Waning Immunity

For the SIRS model (Figure 2.4), where acquired immunity serves only to protect individuals for a limited period of time, the system Jacobian matrix, when evaluated at the corresponding disease free equilibrium, gives rise to the following eigenvalues:

$$\lambda_1 = -\omega_R - \mu \quad \text{and} \quad \lambda_2 = \frac{\beta\left[\mu(1-P_v)+\omega_R\right]}{\omega_R+\mu} - (\mu+v). \tag{2.26}$$

It can be seen that λ_1 is always negative and real. However, the stability of λ_2 is also dependent on the waning immunity parameter, ω_R. Given that $P_v = 1$ indicates ideal 100% vaccination coverage, a new threshold term can be derived that determines the maximum rate of loss of immunity before eradication of the infection through vaccination becomes impossible. For the eradication of endemic or potentially endemic infections (where $R_0 > 1$) to be possible:

$$\omega_R \;<\; \frac{\mu}{R_0 - 1}. \tag{2.27}$$

Provided the temporary immunity parameter, ω_R, satisfies this condition, the critical vaccination coverage required to force the disease free steady state to be stable and hence successfully eradicate the infection is found to be:

$$P_v \;>\; \frac{(R_0-1)(\omega_R+\mu)}{R_0\mu}. \tag{2.28}$$

SIRp Partial Immunity

For the partial immunity model (Figure 2.5), when $P_v = 1$ the model structure can be reduced to that of an SIS given that only secondary infections can occur. This implies that for eradication to be possible, the corresponding basic reproduction

number for the SIS submodel, σR_0, must be less than unity, hence:

$$\sigma \ < \ \frac{1}{R_0}. \tag{2.29}$$

Provided σ does not exceed this threshold, the critical vaccination coverage required to eradicate the infection can be derived from the following eigenvalues, evaluated again at the disease free equilibrium:

$$\lambda_1 = -\mu \quad \text{and} \quad \lambda_2 = \beta\left[1 - P_v(1-\sigma)\right] - (\mu + v). \tag{2.30}$$

The critical vaccination coverage is therefore given by,

$$P_v \ > \ \frac{(1-R_0)}{R_0(\sigma - 1)}. \tag{2.31}$$

2.2.2 Consequences of Vaccination

It can be seen from an endemic steady state analysis of the discussed models that the implementation of a mass vaccination campaign can have a significant effect on the average age of infection [Nokes and Anderson, 1988]. A reduction in endemic prevalence, $\hat{I}$, and hence the force of infection, λ, will result in an increase in the average time taken for newborn individuals to become exposed to and infected with the disease, and therefore a rise in the average age at infection. The approximate average age of infection for the general SIR model with birth targeted vaccination, shown in Figure 2.6, can be derived as follows:

$$A_v \ = \ \lambda^{-1} \ = \ \frac{N}{\beta \hat{I}} \ = \ \frac{L}{R_0(1-P_v) - 1}, \tag{2.32}$$

where $L = \mu^{-1}$ is the average life expectancy at birth. The individual and population level implications of increasing the average age of infection can be varied depending on the age-related nature of the clinical disease and any heterogeneity

within the transmission function, β [Anderson and May, 1985]. If the severity of clinical disease, or the primary route of transmission changes significantly within this region, the resulting shift in the age distribution of infective individuals can be both beneficial or detrimental to the success of the intervention. For example, the risk of intrauterine infection in cases of congenital rubella increases significantly with fertility. In this instance any notable benefit from reducing the overall incidence of infection may be severely undermined by the increased risk of severe disease arising from a greater distribution of cases among child bearing age classes [Anderson and Grenfell, 1985; Knox, 1980].

It should also be noted that the implementation of public health campaigns with the capability to significantly and rapidly reduce the proportion susceptible can also result in significant rebound epidemics prior to a new endemic equilibrium being reached [Scherer and McLean, 2002]. This occurs due to an initial period of reduced incidence driven by the intervention, which allows for an unsustainable accumulation of susceptibles in excess of the epidemic threshold [Medley and Nokes, 2005]. The magnitude of the resulting epidemic behaviour may be particularly pronounced if the perturbed system is highly oscillatory in nature.

2.3 Age Structure

In Section 2.1.3 it was discussed how transmission function properties associated with human behaviour, $c(t)$, and the probability of transmission, $\rho(t)$, have been frequently found to vary as a result of some seasonal forcing with respect to time. However, significant heterogeneity in the transmission of infection can also occur in the form of an age dependency of structured social and intimate mixing patterns, and individual susceptibility/infectivity to circulating infection. The work by Anderson and May [1983] argues for the better representation of heterogeneous transmission patterns in epidemiological models, where the importance of this

structure on transmission dynamics and vaccination design has since been illustrated in a number of high profile examples (see the work by Anderson and May [1985] for measles and rubella, and Gupta et al. [1989] and Sattenspiel et al. [1990] for HIV).

Age dependency may be included in epidemic model structures in one of two ways: either discretely, as additional SIR type compartments that represent key age/risk groups (see the worked example by Jacquez [1996]), or continuously as a system of partial differential equations (PDE) (see Anderson and May [1985; 1991]). The fundamental SIR model (2.1)-(2.4) is therefore extended to give the following set of system equations:

$$\frac{\partial S(t,a)}{\partial t}+\frac{\partial S(t,a)}{\partial a} = -\big[\lambda(t,a)+\mu_d(a)\big]S(t,a), \tag{2.33}$$

$$\frac{\partial I(t,a)}{\partial t}+\frac{\partial I(t,a)}{\partial a} = \lambda(t,a)S(t,a) - \big[v(a)+\mu_d(a)\big]I(t,a), \tag{2.34}$$

$$\frac{\partial R(t,a)}{\partial t}+\frac{\partial R(t,a)}{\partial a} = v(a)I(t,a) - \mu_d(a)R(t,a), \tag{2.35}$$

where

$$\lambda(t,a_s) = \frac{1}{N(a_s)}\int_0^\infty \beta(t,a_s,a_i)\ I(t,a_i)\ da_i, \tag{2.36}$$

with boundary conditions given by:

$$S(t,0) = \int_0^\infty \mu_b(a)N(a)\ da, \qquad I(t,0) = 0, \qquad R(t,0) = 0. \tag{2.37}$$

In this instance, the state variables correspond to (time dependent) age distributions of individuals within a given state of disease, where age dependent mortality is described by $\mu_d(a)$ and the (age dependent) duration of infection is $D(a) = 1/v(a)$. The function $\beta(t,a_s,a_i)$ describes the transmission rate of infection from infectives of age a_i to susceptibles of age a_s, incorporating heterogeneous mixing and susceptibility/infectivity patterns among individuals of different ages, as well as a potential dependency on time. It is assumed that the population as a whole is of

constant size N (i.e constant net birth and mortality rates), and has a constant age distribution with respect to time of the form:

$$N(a) \;=\; \frac{N}{L}\, e^{-\int_0^a \mu_d(z)\, dz}, \tag{2.38}$$

where the average life expectancy is given by $L = NS(t,0)^{-1}$.

If the number of susceptible individuals becoming infective at age a (and time t) is given by $\lambda(t,a)S(t,a)$, then the average age of infection can be calculated from the first moment of this distribution [Anderson and May, 1991], using the following integral equation:

$$A_v(t) \;= \frac{\int_0^\infty a\, \lambda(t,a)S(t,a)\; da}{\int_0^\infty \lambda(t,a)S(t,a) da}. \tag{2.39}$$

2.3.1 Heterogeneity & Basic Reproduction

In most applied situations the value of R_0 is estimated as an average value taken over an integer number of annual cycles, discounting any seasonal fluctuations in contact patterns. Therefore, the transmission function $\beta(a_s, a_i)$ is a matrix that represents average annual (age dependent) transmission rates. In cases with a long duration of infection (i.e. if contact properties or mortality changes significantly during the infectious period), the average number of individuals of age a_s that contract the infection from a single individual infected at age a_i, where $S(a) = N(a)$, during the interval $[a_i, a_i + \delta a_i]$ is given by:

$$\beta^*(a_s, a_i) \;=\; N(a_s) \int_0^\infty \beta(a_s, a_i + u)\{1 - D_{a_i}(u)\} e^{-\int_{a_i}^{a_i+u} \mu_s(z)\, dz} du, \tag{2.40}$$

where $D_{a_i}(u)$ corresponds to the cumulative distribution function of the infectious

period for an infective at age a_i [Farrington et al., 2001]. Hence, if an infected individual is introduced into a non-homogeneously mixing susceptible population, the number of resulting cases (i.e. the initial growth of the invasion) will depend on the age of the initial individual. It should also be noted that for cases with a relatively short infectious period, $\beta^*(a_s, a_i) \approx N(a_s)D\beta(a_s, a_i)$.

According to the work by Diekmann et al. [1990], R_0, now the number of expected cases in a naive population arising from a single *typical* infective introduction, can be defined as the dominant eigenvalue of $\beta^*(a_s, a_i)$. For details on the definition of the effective reproduction number, R, in heterogeneous systems see the work by Farrington and Whitaker [2003].

2.4 Model Validation and Empirical Data

As previously discussed, prospective mathematical model structures must be appropriately validated in order to accurately relate to specific real world systems. One key aspect of this process is often referred to as the 'inverse problem' [Jacquez, 1982], where internal model parameters are assigned numerical values corresponding to an output that best correlates with experimental data. Epidemic models such as those described in this work are based on processes of infection and are regularly fitted to time series data collected from records of clinical disease, or with respect to age in the form of age-stratified serological surveys. The main epidemiological measures considered in this study are:

- **Prevalence** - the number of individuals within the population currently presenting the infection, defined by $y(t, a) = I(t, a)$.
- **Incidence** - current rate of emerging cases, for example, recorded as the number of new cases within a given 4 week period, $y(t, a) = \lambda(t, a)S(t, a)$.

- **Serology** - a qualitative serological survey is used to determine prior experience of infection, implemented as $y(t,a) = Ab^{+}(t,a)$, where $Ab^{+}(t,a)$ corresponds to all seropositive individuals, i.e. $R(t,a)$.

It should be noted that all of these measures can, in principle, be recorded with respect to both time and age. However, for infections that exhibit strong seasonal epidemic patterns, steps must be taken to ensure the correction of any subsequent distortion in the average age distribution resulting from inconsistent sampling throughout the inter-epidemic period [Whitaker and Farrington, 2004]. The work by Keeling and Grenfell [2000] suggests that ignoring the temporal variation in these cases serves to underestimate values for R_0.

2.4.1 Model Indeterminacy

An immediate problem concerning parameter estimation for infection based epidemic models arises from an inherently limited and often biased observation of the full system state, where the main epidemiological measures typically allow access to only the (clinically) infective and/or seropositive populations. Notification of communicable diseases is often found to be incomplete and its bias due to awareness, disease severity, perceived public health importance and social stigma is notoriously difficult to quantify [Harpaz, 2004; Thacker et al., 1983].

In addition, the metrics of infection, disease and serology, although strongly interdependent, are not necessarily concordant, and may depend incongruously on risk factors such as age. This implies that observations arising from the detection of severe clinical symptoms or from the presence of disease specific antibodies are often not accurately representative of circulating infection, and may therefore distort any deductions that might be made from fitting the model to data.

In the study of hRSV it is found that the risk of severe lower respiratory tract infections (LRTI) such as bronchiolitis and pneumonia, and resulting hospitalisation (typical source of time series data) decreases significantly with increasing age. However, it is not known whether this susceptibility to disease is governed by continuous physiological development (e.g. larger airways) or accumulative immunological experience, or if this dependency correlates with that of susceptibility to infection [White et al., 2005]. The vast majority of observable cases occur in children under 12 months of age, but a potentially significant yet unknown amount of subclinical reinfection is likely to circulate unobserved throughout the wider population as well [Cane, 2001].

For simplicity it is typically assumed that observable disease is directly proportional to infection, or at least infectivity, where, for example, the transmission of many airborne respiratory infections are aided by the nature of their clinical symptoms (e.g. coughing and sneezing). In these cases it is common to include an unknown observation gain k (i.e. $y(t,a) = kI(t,a)$) that acts as a constant scalar between predicted infection and real data. For hRSV it is often assumed that susceptibility to disease decreases with prior experience of infection, whereby hospital data is considered as a proportion of all primary infection (see examples by Weber et al. [2001] and White et al. [2007]).

Further indeterminacy arises in age structured models when attempting to estimate heterogeneous transmission characteristics and basic reproduction from serological survey data [Anderson and May, 1991]. The problem derives from the dependency of R_0 on the potentially infectious contact patterns represented by the transmission function $\beta(t, a_s, a_i)$, whereby the rate of increase in seropositive individuals with age is indicative of the force of infection (i.e. rate that susceptibles become infected, see equation (2.36)), but does not provide information relating to which age classes the transmission of infection originates. This issue is addressed in the work by Farrington et al. [2001] where relationships between the contact patterns of different infections with similar routes of transmission are assumed thus

allowing further elicitation of information regarding $\beta(t, a_s, a_i)$. Alternatively, the work by Edmunds et al. [1997] documents the analysis of a questionnaire for the direct determination of adult contact patterns associated with the spread of airborne infections. However, estimates such as this are unlikely to be sensitive to many casual social interactions such as those in crowded public spaces. It should also be noted that the indeterminacy issue becomes more intractable if the dependency of individual susceptibility and infectivity is additionally considered with respect to age.

2.5 Conclusions

Mathematical models of epidemiological systems are developed in order to investigate potential responses to critical input conditions and to gain a better understanding of the underlying physical processes that characterise observed system behaviour. Population dynamics of infectious diseases are often explored through the use of lumped compartmental models, where complex host-pathogen interactions are generalised into common stages within the natural history of infection. It has been shown throughout this chapter that a wide range of epidemiological characteristics may be described and analysed within this framework, with varying levels of complexity and application.

In order for postulated model structures to accurately describe the behaviour of specific real world systems, they must be parameterised with respect to empirical measurements under a known set of experimental conditions. Numerous examples of epidemiological measures may be found throughout the literature, however, these are typically based on records of clinical disease or serological surveys and often provide only a very limited observation of the full system state. As a result, issues of indeterminacy frequently arise in epidemic modelling, leading to poor characterisation during data fitting. Formal methods to identify model indetermi-

nacy are an essential prerequisite to parameter estimation and future experimental design and are discussed in later chapters of this work.

Chapter 3

Models for Maternal & Early Childhood Immunisation

The models presented in this chapter have been developed to investigate the population level influences of maternally acquired immunity on epidemic systems with contrasting epidemiological characteristics and their potential response to perturbation from mass maternal immunisation. It is intended that this work encourage a more panoptic consideration of how prospective maternal and potentially conflicting childhood vaccines might be optimally implemented within different dynamic populations, and what the resulting impact of the intervention on broader system behaviour might be.

Models are derived to study the potential outcomes and consequences of maternally targeted intervention strategies, both in terms of their potential to reduce neonatal morbidity and mortality from infection, and their effects on the static, dynamic and seasonal characteristics of the system. The models are discussed in three main structural forms: homogeneous time and age domain ordinary differential equation (ODE) models (Sections 3.2 and 3.3.2), discrete age (continuous time) structured ODE models (Section 3.4.1) and decoupled continuous age-time partial

differential equation (PDE) models (Section 3.4.2), which are derived successively from an encompassing general model framework described in (Section 3.2).

3.1 Background Biology

The human immune system is an extremely complex collection of biological mechanisms that continually acts to protect the individual against infection from external pathogens capable of causing damage and disease to the body [Janeway and Travers, 2005]. Molecules that are found to induce a response in the immune system are called antigens (antibody generators) and comprise of either (non-self) foreign substances (such as bacteria, viruses and other microorganisms etc.) or (self) cells belonging to the individual. The success of the immune system relies heavily on its ability to distinguish between self and non-self elements; an abnormal breakdown in this process can often lead to various autoimmune type disorders where the immune system mounts an aberrant response on the individual's own cells and tissues. The system is generally divided into two staged components:

- **Innate immune system** - provides an immediate, but non-specific response to infection. This includes anatomical barriers such as the desquamation of epithelial surfaces, and mucosal secretions in the respiratory and gastrointestinal tracts.
- **Adaptive immune system** - antigen specific response that adapts to improve the recognition and removal of a particular pathogen, resulting in immunological memory.

The innate and adaptive components of the immune system are also both highly dependent on a combination of cell-mediated and humoral reactions to infection. The cell-mediated response involves the migration of white blood cells such as

macrophages and natural killer cells around the body, and the activation of antigen-specific cytotoxic T-lymphocytes (T-cells). In contrast, the humoral immune response emanates from the secretion of antibodies (immunoglobulin) into the blood and tissue fluids [Davies, 1997].

Antibodies (Ab) contribute to the immune function by binding to a specific antigen, either tagging it for removal by the complement system, or neutralising its ability to bind with target cells and cause infection. Antibodies also occur on the surface of B-cell lymphocytes forming a B-cell receptor (BCR). When activated by the presence of a corresponding antigen, these BCRs differentiate into either plasma cells that produce large quantities of specific free antibodies, or memory cells that survive for long periods of time and allow the system to respond more rapidly to repeat exposures.

3.1.1 Maternally Acquired Immunity

During early life the neonatal immune function is highly immature, naive to infection and largely deficient in its ability to protect the individual against circulating pathogens. Adaptive components of the immune system are yet to be primed through exposure to foreign antigens (which includes the absence of memory cells), inhibiting its ability to react with the rapid antibody production synonymous with a typical secondary immune response [Kemp and Campbell, 1996]. Newborns are therefore acutely dependent on the accumulated immunologic experience of the mother, which is conveyed in the specific form of immunoglobulin isotopes IgA and IgG [Zinkernagel, 2001].

The majority of maternal IgG transfer occurs during the final four weeks of pregnancy, where antibodies actively enter foetal circulation by means of a specific receptor-mediated mechanism via the placenta [Saji et al., 1999] and exceed ma-

ternal concentrations by a ratio of around 1.2:1 - 1.8:1 at full term [Pitcher-Wilmott et al., 1980; Sato et al., 1979]. The bulk of IgA is transferred after birth through breast feeding and remains predominantly within mucosal secretions in the digestive and respiratory tracts of the infant. Active components of the mother's immune system such as specific T-cells are unable to transfer protection to the infant due to differences between maternal (self) and foetal (non-self) tissue antigens, raising the possibility of an adverse response being mounted on the foetus.

Given that the bulk of transplacental maternal IgG is acquired so late in the gestation period, concentrations of maternal antibodies (MAb) in premature infants are considerably lower than that of full term infants [Costa-Carvalho et al., 1996], further compromising immunity and significantly increasing the risk of inimical infection. The work by Ballow et al. [1986] reports an average IgG concentration for 28 week gestation infants of around 250 mg dL^{-1} compared to 1500 mg dL^{-1} for full term infants.

Immunoglobulin proteins are also ultimately short lived and, following birth, neonatal concentrations of maternally acquired serum IgG decay exponentially with age. However, estimates for the rate of this clearance appear to vary enormously; half lives of between 12 and 100 days are reported in the literature (see Table I in [Sarvas et al., 1993]). Several hypotheses exist regarding these inconsistencies such as: measurement error, perhaps caused by damage to the IgG molecules from iodine-labelling in work such as that by Waldmann and Strober [1969]; misinterpretation of seroconversion due to infection [Ochola et al., 2009]; and variability in more physiological characteristics such as endogenous synthesis, concentration dependency of decay (due to saturatable recycling of antibodies through a finite number of FcRn receptors), or rapid growth of the infant (increasing apparent volume of distribution). At a population level, seroepidemiological surveys of common viral infections such as those by Cox et al. [1998] and Hacimustafaoglu et al. [2004] for hRSV, Williams et al. [1995] for measles and Nicoara et al. [1999] for MMR, have shown that most infants become seronegative within 6-9 months of age.

3.1.2 Maternal Immunisation

Despite the limited duration and inherently passive characteristics of MAb, the magnitude of their afforded protection against a number of common viral and bacterial diseases is frequently reported. Studies such as those by Ogilvie et al. [1981] and Hacimustafaoglu et al. [2004] for hRSV, and Puck et al. [1980] and Reuman et al. [1987] for influenza A have demonstrated a strong correlation between high cord antibody titres (a measure of serum antibody concentration (titre) taken from the umbilical cord) and a reduced risk of infection among neonates. Similarly, the administration of hRSV specific immunoglobulin prophylaxis to high-risk infants and young children has produced a notable decrease in hospitalisation and severity of disease [Dougherty and Meissner, 2000; Groothuis et al., 1993].

The implementation of a maternally targeted vaccine acts to augment these protective properties by inducing a complementary active immune response to immunisation in the mother at around 30 weeks gestation. The immediate intention is to raise maternally acquired serum IgG titres in newborns, hence providing passive supplementary protection during the first few months of life [Munoz and Englund, 2000]. Additional benefits and demerits of this form of intervention include:

Advantages:

- Pregnant women respond well to vaccination and antibodies (IgG) are readily transferred across the placenta.
- Intervention directly targets neonatal age classes, which are typically the most susceptible to infectious diseases and least responsive to vaccines.
- Pregnant women tend to be regularly accessible through existing health care infrastructure.
- Immunisation has the potential to protect both the infant and the mother.

Disadvantages:

- Protection is less effectively conveyed to preterm infants who are likely to be among those most requiring supplementary protection.
- Potentially limited efficacy in areas with high prevalence of infections such as HIV and malaria, which can suppress the immune system, diminish placental function and induce prematurity.
- High levels of MAb are likely to inhibit the immune response of young infants to active childhood vaccines and natural infection.
- Many women are reluctant to accept vaccination during pregnancy due to concern of associated risk to the foetus.

Maternal immunisation is of primary interest in cases where a significantly high incidence of disease occurs in particularly young age classes, before immune system maturation or the successful uptake of an appropriate childhood vaccine [van der Zeijst et al., 2007]. As a result, intervention strategies of this nature are particularly applicable in developing contexts where high birth rates and infant transmission skew the incidence age profile towards younger age groups, and neonatal mortality due to infection is high [Greenwood, 2003]. Mass maternal immunisation campaigns have already been successfully implemented in a number of developing regions to reduce young infant mortality due to tetanus [WHO, 2002], where the contribution of this infection to global neonatal mortality has subsequently been reduced from 14% in 1993 to around 5% in 2002 [Vandelaer et al., 2003].

Further candidate infections for prospective control by maternal immunisation include *Haemophilus influenzae* type b (Hib) [Englund and Glezen, 2003; Mulholland et al., 1996], pertussis (whooping cough) [Mooi and de Greeff, 2007], influenza [Englund, 2003; Sumaya and Gibbs, 1979; Zaman et al., 2008] and hRSV [Englund, 1994; Munoz et al., 2003] (for additional information see also the reviews by Munoz and Englund [2000], Englund et al. [1998] and Healy and Baker [2006]).

In cases where maternally acquired IgG has been shown to inhibit the infant response to vaccine, work such as that by Williams et al. [1995] and Nicoara et al. [1999] carefully target childhood immunisation at the peak age of susceptibility (nadir in seropositivity) where as much exposure to natural infection is avoided as possible, whilst also minimising ineffective interaction with maternally derived immunity. For example, with measles the (natural) average age at primary infection is around 5-6 years and vaccination is therefore not routinely administered until 12-23 months of age [Williams et al., 1995].

However, in more developing settings where transmission rates among pre-school children are often much higher, and with more virulent infections such as hRSV, selection of an optimal age for vaccination is more difficult, often requiring strategies that include multiple dosing. Studies such as those by Siegrist [2003] and Crowe [2001] suggest that immunisation induced MAb can also inhibit childhood targeted intervention, therefore increasing maternally derived immunity through maternal immunisation may prove detrimental to this challenge.

3.2 General MSIR Model Framework

The structure of the general model framework is based on that of an MSIR compartmental system, where the natural history of infection includes an additional state variable that corresponds to neonates and young infants protected by passive, maternally acquired immunity [Anderson and May, 1991]. It is intended that the complete model structure describe as much of our prior knowledge or hypotheses of the underlying biological processes as possible, including the following significant properties:

- **Neonatal MAb protection** - a degree of passively acquired (temporary) immune protection is afforded to newborn infants, depending on the mother's

prior experience of infection and immunisation.

- **Intervention** - implementation of maternal and young infant targeted immunisation invokes an active immune response in the recipient.
- **Age structure** - complete model must be supportive of age dependency in all parameters and state variables.
- **Transmission** - inclusive of separable mixing and varying susceptibility with respect to age, and periodic seasonal forcing.
- **Incomplete immunity** - a range of outcomes following infection encompassing complete/incomplete immunity and potentially altered secondary infection.

In reality, protective immunity $z \in [0,1]$ is a continuous property that tends to increase with experience of infection or vaccination, and decrease with respect to time since recovery. The work by White [2000] discusses the capture of these characteristics in a PDE model framework where time, age and immunity are all implemented as continuous independent variables. A possible, though highly intractable implementation of this approach to the MAb problem can be illustrated by the following expression for a subpopulation of newborns prior to natural infection or vaccination:

$$\begin{aligned}\frac{\partial S(t,a,z)}{\partial t}+\frac{\partial S(t,a,z)}{\partial a}-\frac{\partial \omega_M(z)S(t,a,z)}{\partial z} \;&=\\ \delta(a)\int_0^\infty \mu_b(a)N(a,z)da-\mu_d(a)S(t,a,z)&\\ -\big[\sigma(a,z)\lambda(t,a)+\vartheta(a,z)V(t,a)\big]S(t,a,z),&\end{aligned} \tag{3.1}$$

where

$$\lambda(t,a_s) \;=\; \int_0^\infty \beta(t,a_s,a_i)\int_0^1 \gamma(a_i,z)\; I(t,a_i,z)\; dz\; da_i. \tag{3.2}$$

The protective effects of MAb and physiological development against circulating infection are described by a reduced susceptibility parameter $\sigma(a, z)$, which is dependent on both age and passively acquired immunity. The subsequent attenuation of vaccine uptake (from a vaccination programme $V(t, a)$) is included through the function $\vartheta(a, z)$, and the waning of acquired immunity is governed by the parameter $\omega_M(z)$. The distribution of acquired protection at birth is governed by that of wider population immunity, $N(t, a, z)$, and the application of an age dependent fertility function $\mu_b(a)$, where the Dirac delta function, $\delta(a)$, ensures all newborns are born at age zero. The force of infection $\lambda(t, a)$ is representative of heterogeneous contact patterns determined by $\beta(t, a_s, a_i)$, an infectivity variable, $\gamma(a_i, z)$, and the corresponding distribution of the infective population $I(t, a_i, z)$.

The solution to each state variable of the resulting system is therefore a two-dimensional surface, characteristically an age serological profile, that is continuously evolving with respect to time. Rigorous validation or even numerical evaluation of such a system is found to be largely unmanageable and extremely computationally intensive [White, 2000]. Therefore in this work the continuous nature of immunity is discretised according to distinct (compartmentalised) events in the natural history of infection, i.e. maternally protected, susceptible, recovered etc., whereby fixed degrees of immunity are afforded to individuals depending on their current state. A number of other common assumptions are made in order to constrain the scope and complexity of the problems addressed in this work. These include:

- Constant population size and age distribution.
- No disease induced mortality.
- No vector or vertical routes of transmission.
- No latent incubation prior to becoming infectious.
- Maternally acquired immunity provides complete protection.

These assumptions are considered to be appropriate since many of the infectious agents currently being considered for maternal immunisation tend to evolve over relative short time frames, are largely non-fatal and are not contracted before birth or via non-human vectors. The inclusion of a latent incubation period prior to becoming infectious, and a partial immunity stage due to the progressive waning of MAb are natural extensions to the proposed model structure and are discussed in later chapters as a suggestion for future research.

The general model is therefore defined as a continuous age-time PDE type structure, which is extended from that of the SIR model (2.33)-(2.37) described in Section 2.3, to support the inclusion of MAb and epidemiological characteristics associated with incomplete immunity and intervention (discussed separately in Sections 3.3.1 and 3.3.2 respectively). The model is described by the following system of partial integro-differential equations:

$$\begin{aligned}
\frac{\partial M(t,a)}{\partial t} + \frac{\partial M(t,a)}{\partial a} &= -\big[\omega_M(a)+\mu_d(a)\big]M(t,a), && (3.3)\\
\frac{\partial S(t,a)}{\partial t} + \frac{\partial S(t,a)}{\partial a} &= \omega_M(a)M(t,a) - \big[\lambda(t,a)+\mu_d(a)\big]S(t,a), && (3.4)\\
\frac{\partial I(t,a)}{\partial t} + \frac{\partial I(t,a)}{\partial a} &= \lambda(t,a)S(t,a) - \big[v(a)+\mu_d(a)\big]I(t,a), && (3.5)\\
\frac{\partial R(t,a)}{\partial t} + \frac{\partial R(t,a)}{\partial a} &= v(a)I(t,a) - \mu_d(a)R(t,a), && (3.6)
\end{aligned}$$

where

$$\lambda(t,a_s) = \frac{1}{N(a_s)}\int_0^\infty \beta(t,a_s,a_i)I(t,a_i)\,da_i. \qquad (3.7)$$

The state variables $M(t,a)$, $S(t,a)$, $I(t,a)$ and $R(t,a)$ correspond to the distribution with age of subpopulations classified as protected by maternally acquired immunity, susceptible to circulating infection, currently infective and recovered at time t, respectively.

Age dependent functions for birth, $\mu_b(a)$, and mortality, $\mu_d(a)$, rates, average duration of infection, $v(a)^{-1}$, heterogeneous and potentially seasonal transmission, $\beta(t, a_s, a_i)$, and population age distribution, $N(a)$, are all congruent with those described in Section 2.3. However, the boundary conditions for $M(t, 0)$ and $S(t, 0)$ are subsequently amended in order to reflect the coupled dependency of maternally acquired protection on the levels of immunity in the adult population. The conditions are therefore given by:

$$M(t,0) = \int_0^\infty \mu_b(a) Ab^+(t,a)\, da, \qquad S(t,0) = \int_0^\infty \mu_b(a) Ab^-(t,a)\, da, \tag{3.8}$$

where the variables $Ab^+(t, a)$ and $Ab^-(t, a)$ correspond to subpopulations of individuals grouped as either seropositive or seronegative, depending on their current state of immunity. Given that $M(t, a)$ and $R(t, a)$ represent those protected by high levels of maternal and post-infection acquired antibody, it is intuitive that $Ab^+(t) = M(t) + R(t)$, where an appropriate age dependent fertility function, $\mu_b(a)$, prevents the birth of newborns to infants protected by MAb. It is therefore assumed that active immunity is acquired upon recovery from the infective state, whereby mothers 'currently infected' at the time of giving birth do not transfer protective levels of MAb to their offspring. This is a reasonable assumption to make since adult IgG levels are typically found to peak at around 20 to 30 days after the onset of clinical symptoms [Ogra, 2004]. Hence, the variables $S(t)$ and $I(t)$ are considered seronegative, where $Ab^-(t) = S(t) + I(t)$.

A series of reduced model structures can then be derived from successive simplifications of the general model, in order to aid analytical tractability of specific system attributes with respect to the problem statement:

- **Dynamics** - seasonal and other time dynamic characteristics of the system may be isolated by removing or compartmentalising age specific processes within the system.

- **Statics** - age profile characteristics may be studied without the complexities of time dependency by considering the system at a stable endemic equilibrium, and, if necessary, averaging across complete recurrent epidemic cycles.
- **Decoupling** - simplification through decoupling the dependency of passive neonatal protection on adult infection dynamics allows the inclusion of a more empirical model for the rate at which neonates lose maternally acquired protection.

3.3 Homogeneous MSIR Models

The most fundamental realisation of the general MSIR framework can be derived by neglecting the inclusion of age dependency in the model parameters and only considering the system behaviour with respect to either time or age. In this instance homogeneous and non-separable mixing is assumed regarding the transmission function $\beta(t)$, and other epidemiological characteristics such as susceptibility to infection are dependent entirely on immunological experience (i.e. history of infection). Physiological properties attributed to varying age are therefore excluded from the model.

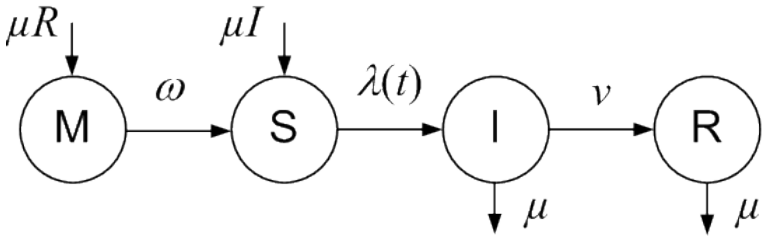

Figure 3.1: MSIR Compartmental Model

Integrating the system equations (3.3)-(3.6) with respect to age (i.e. finding the total number of individuals residing in each state of disease for time t):

$$\frac{dM(t)}{dt} = \mu_b \int_0^\infty \delta(a) Ab^+(t,a)\, da - \big(\omega_M + \mu_d\big) \int_0^\infty M(t,a)\, da, \tag{3.9}$$

$$\frac{dS(t)}{dt} = \mu_b \int_0^\infty \delta(a) Ab^-(t,a)\, da - \big(\lambda(t) + \mu_d\big) \int_0^\infty S(t,a)\, da, \tag{3.10}$$

$$\frac{dI(t)}{dt} = \lambda(t) \int_0^\infty S(t,a)\, da - \big(v + \mu_d\big) \int_0^\infty I(t,a)\, da, \tag{3.11}$$

$$\frac{dR(t)}{dt} = v \int_0^\infty I(t,a)\, da - \mu_d \int_0^\infty R(t,a)\, da, \tag{3.12}$$

where

$$\lambda(t) = \frac{\beta(t)}{N} \int_0^\infty I(t,a_i)\, da_i, \tag{3.13}$$

and the Dirac delta function, $\delta(a)$, terms replace the boundary conditions (3.8), yields a more concise, single domain, time dynamic ODE model analogous to that of a fundamental SIR given by (2.1)-(2.4) in Section 2.1. The fundamental MSIR, shown in Figure 3.1, is therefore described by the following set of ordinary differential equations:

$$\dot{M}(t) = \mu Ab^+(t) - \big[\omega_M + \mu\big] M(t), \qquad M(0) = M^0, \tag{3.14}$$

$$\dot{S}(t) = \mu Ab^-(t) + \omega_M M(t) - \frac{\beta(t)}{N} S(t) I(t) - \mu S(t), \qquad S(0) = S^0, \tag{3.15}$$

$$\dot{I}(t) = \frac{\beta(t)}{N} S(t) I(t) - (\mu + v) I(t), \qquad I(0) = I^0, \tag{3.16}$$

$$\dot{R}(t) = vI(t) - \mu R(t), \qquad R(0) = R^0, \tag{3.17}$$

where ω_M depicts the rate at which maternally protected newborns lose passive immunity through natural antibody clearance and become fully susceptible to infection.

Overall net birth and death rates are equal, i.e. $\mu_b = \mu_d = \mu$, hence a constant size population is maintained. As before, individuals are born either maternally protected or fully susceptible, at rates $\mu\, Ab^+(t)$ and $\mu\, Ab^-(t)$, respectively, depending on the previous infection experience of the mother. It should be noted that in

the general model (3.3)-(3.8) the inclusion of age dependent fertility prevents the unlikely event of babies born to maternally protected mothers. However, in the homogeneous model, where the fertility function, μ, is a constant, this becomes a consequential characteristic of the reduced system.

In the most simple case, where total net birth/death rate is μN and $Ab^+(t) = M(t) + R(t)$, the inflow of passively protected newborns from mothers with high levels of MAb is cancelled by neonatal mortality. Therefore if both fertility and mortality from the maternally protected population $M(t)$ are neglected, where the net birth/death rate becomes $\mu(N - M(t))$, the time domain model remains structurally equivalent.

Alternatively, if neonatal mortality is included and births from MAb protected mothers is removed, the seropositive/seronegative variables can be proportioned such that:

$$Ab^+(t) = \frac{R(t)}{N - M(t)}N \quad \text{and} \quad Ab^-(t) = \frac{S(t) + I(t)}{N - M(t)}N, \tag{3.18}$$

where $Ab^+(t) + Ab^-(t) = N$, hence maintaining balanced inflows ($\mu Ab^+(t) + \mu Ab^-(t)$) and outflows ($\mu N$), and a constant population size N.

Choice of input structure is therefore determined by the characteristics of the studied population; in developed countries it is found that infant mortality (under 1 year of age) is typically below 1%, making the neglection of $\mu M(t)$ a more reasonable description. However, in developing regions where death rates among young infants is often much higher, the proportioned fertility model may be more appropriate. In both cases the coupled nature of MAb dependence on adult immunity is preserved, however analytic analysis of the latter (inclusive of neonatal mortality) can become considerably more complex.

The acquisition of MAb serves to protect seropositive newborns for an average du-

ration given by ω_M^{-1}, whereby the average age at primary infection is dependent on both the force of infection and the number of infants born with passively acquired immunity. For an MSIR system residing at a fixed point endemic equilibrium, the average age at primary infection can be approximated by the expression:

$$A_v \approx \frac{Ab^+}{N}(\omega_M^{-1} + \lambda^{-1}) + \frac{Ab^-}{N}(\lambda^{-1}), \tag{3.19}$$

which is derived from a weighted average corresponding to the respective proportions of seropositive/seronegative newborns. The expression (3.19) is an approximation to the actual value predicted by this model as it does not account for the effects of mortality and the resulting (exponentially decaying) age distribution assumed by its structure. It can be seen that increased population immunity, due to a high force of infection, acts antagonistically against a low average age of contraction synonymous with high levels of exposure.

3.3.1 Incomplete Immunity

Candidate cases for maternal immunisation generally correspond to systems where there is a significant prevalence of infection among neonates in the first few months of life, close to the average duration of MAb. A particularly low average age at primary infection is likely to be driven by a high force of infection, suggesting either very high infant transmission or sub-optimal immunity and significant reinfection throughout the wider population. Intuitively, the corresponding influence of MAb over wider system dynamics is likely to crucially depend on the age distribution of population level infectivity, i.e. the relative contributions of primary (potentially influenced by MAb) and secondary (all subsequent) infection, in addition to the average age of primary challenge.

However, recalling the issues of indeterminacy with hRSV (see Section 2.4.1), it is

not always clear whether primary or subsequent reinfection dominate the behaviour of the system. It is known that a significant level of subclinical reinfection exists throughout the wider population [Falsey et al., 2006], but its likely contribution to the total force of infection (or that acting on the neonatal age group) is yet to be confidently established. As a result, two limiting hypotheses exist regarding the relationship between observed (disease) dynamics of hRSV and maternally acquired immunity:

- Neonatal MAb levels may be an insignificant consequence of dominant adult infection dynamics, whereby they provide protection to only a negligible proportion of the total population and are therefore unlikely to influence the system as a whole.
- Conversely, if the majority of secondary subclinical infection does not result in high infectivity and frequent antibody boosting occurs largely as a result of exposure to primary infected infants, then MAb may be a significant driving force in the availability/supply of susceptibles and therefore the time course of the infection.

The MSIRS2 model structure, shown by the connectivity diagram in Figure 3.2, has been derived in order to delineate the continuum of system characteristics between these two extremes and to examine the potential influence of MAb as the dominance of infectivity is varied within this domain. This approach is similar to that described by White et al. [2007], and Greenhalgh et al. [2000], who explore the consequences of altered secondary infection on the transmission dynamics and equilibrium characteristics of human and bovine RSV. The MSIRS2 model is also structurally similar to the more expansive MSEIRS4 model proposed in the work by Weber et al. [2001] (see Appendix A), where the objective was to include additional realism relating to processes of temporary and accumulating immunity consistent with observations from a number of longitudinal studies.

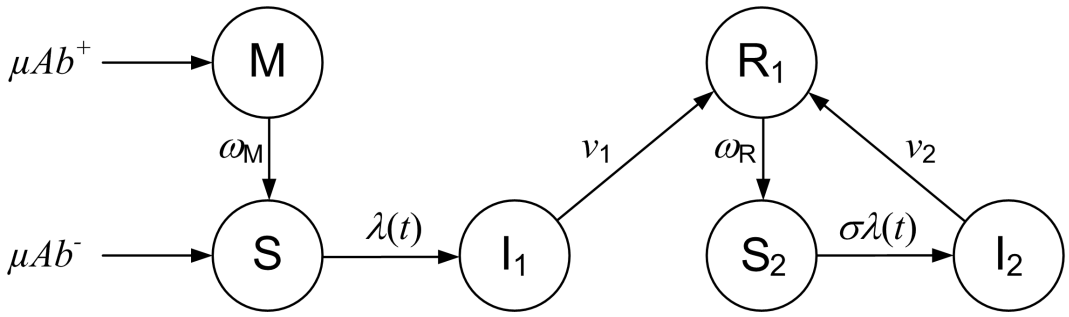

Figure 3.2: MSIRS2 Incomplete Immunity Model

In accordance with clinical observation [Falsey et al., 2006; Hacimustafaoglu et al., 2004], passive and actively acquired immunity are assumed to wane at different rates, where the average duration of protection is given by ω_M^{-1} and ω_R^{-1}, respectively. In an analogous manner to the work by Weber et al. [2001], maternally protected neonates lose immunity and become fully susceptible, $S_1(t)$, to circulating infection, whereas recently recovered individuals become only partially susceptible, $S_2(t)$, due to a degree of immunological memory. This subsequent reduction in the risk of infection is governed by the parameter $\sigma \in [0, 1]$, by means of a similar process to that of the SIRp example described in Section 2.1.4.

Secondary infection, $I_2(t)$, is assumed to be less severe than primary infection, $I_1(t)$ [Ogra, 2004], with a shorter duration $v_2^{-1} < v_1^{-1}$ and reduced infectivity (viral shedding) $\gamma \in [0, 1]$ [Hall et al., 1991]. Therefore the parameters σ and γ can be varied in order to govern the dominance of primary and repeat infectivity within the population. The model is defined by the following system of ordinary

differential equations:

$$\dot{M}(t) = \mu Ab^{+}(t) - \big[\omega_M + \mu\big]M(t), \qquad M(0) = M^0, \tag{3.20}$$

$$\dot{S}_1(t) = \mu Ab^{-}(t) + \omega_M M(t) - \big[\lambda(t) + \mu\big]S_1(t), \qquad S_1(0) = S_1^0, \tag{3.21}$$

$$\dot{I}_1(t) = \lambda(t)S_1(t) - \big[\mu + v_1\big]I_1(t), \qquad I_1(0) = I_1^0, \tag{3.22}$$

$$\dot{R}_1(t) = v_1 I_1(t) + v_2 I_2(t) - \big[\mu + \omega_R\big]R_1(t), \qquad R_1(0) = R_1^0, \tag{3.23}$$

$$\dot{S}_2(t) = \omega_R R_1(t) - \big[\mu + \sigma\lambda(t)\big]S_2(t), \qquad S_2(0) = S_2^0, \tag{3.24}$$

$$\dot{I}_2(t) = \sigma\lambda(t)S_2(t) - \big[\mu + v_2\big]I_2(t), \qquad I_2(0) = I_2^0, \tag{3.25}$$

where

$$\lambda(t) = \frac{\beta(t)}{N}\Big[I_1(t) + \gamma I_2(t)\Big]. \tag{3.26}$$

The seropositive variable $Ab^{+}(t) = M(t) + R_1(t)$ includes individuals who have recently recovered from an immunising infection and those protected by high levels of MAb. Individuals considered to be seronegative, where $Ab^{-}(t) = S_1(t) + I_1(t) + I_2(t) + S_2(t)$ (i.e. $N = Ab^{-}(t) + Ab^{+}(t)$), include those fully or partially susceptible and currently infective. It can also be noted that the incomplete immunity model is a generalisation of the fundamental MSIR, whereby setting $\omega_R = 0$, i.e. fully protective immunity from experience of infection no longer wanes with time, the model becomes equivalent to that given by (3.14)-(3.17).

3.3.2 Maternal Immunisation Models

In accordance with the biological description of the intervention in Section 3.1.2, mass maternal immunisation is applied to a proportion, P_m, of the total net birth rate, μN, whereby an additional influx of newborns from low immunity mothers, given by $\mu P_m Ab^{-}(t)$, are born maternally protected, $M(t)$, instead of fully suscep-

tible, $S_1(t)$ (see Figure 3.3). It is assumed that the mother's immune response to the vaccine is actively protective, i.e. the same as that for natural infection, hence the function $\mu\ P_m\ Ab^-(t)$ also corresponds to the net rate at which seronegative pregnant women are immunised and subsequently move into the protected state $R_1(t)$.

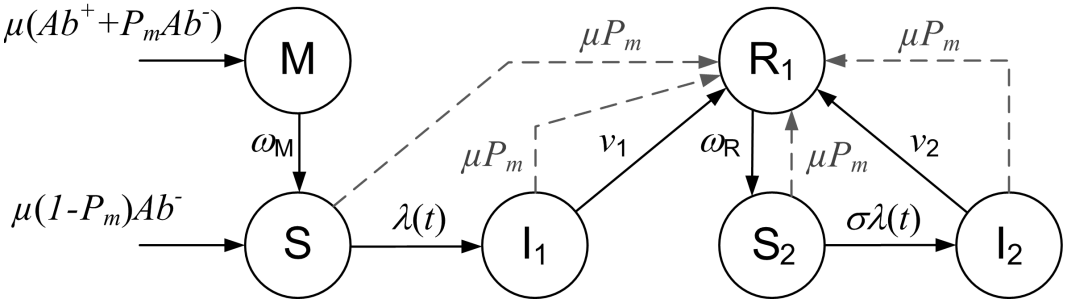

Figure 3.3: MSIRS2 Maternal Immunisation Model

However, a degree of ambiguity exists over the exact implementation of the active response in the model due to the difference in time at vaccine administration and duration of full term (around 30 and 37 weeks gestation respectively). To avoid the introduction of complex delay functions and gender structure, it is intuitive to assume that vaccination is actively applied at the time of birth and is instantly transferable to the newborn, although this is arguably a contradiction to the prior assumption that mothers who are infective at this time do not transfer any subsequent immunity to their offspring. Mathematically this discrepancy is only significant when considering the application of the vaccine to $I_{1,2}(t)$, where immunised infectives (in reality vaccinated several weeks before giving birth) should not have contracted the infection during that time. Given that the target population for the vaccine (i.e number of pregnant woman) is realistically a very small proportion of N, it is anticipated that this is a reasonable simplification to make. Therefore the following set of system equations can be extended from those given

in (3.20)-(3.25):

$$\dot{M}(t) = \mu\big[Ab^{+}(t)+P_m Ab^{-}(t)\big] - \big[\omega_M+\mu\big]M(t), \tag{3.27}$$

$$\dot{S}_1(t) = \mu(1-P_m)Ab^{-}(t) + \omega_M M(t) - \big[\lambda(t)+\mu(1+P_m)\big]S_1(t), \tag{3.28}$$

$$\dot{I}_1(t) = \lambda(t)S_1(t) - \big[v_1 + \mu(1+P_m)\big]I_1(t), \tag{3.29}$$

$$\dot{R}_1(t) = \mu P_m Ab^{-}(t) + v_1 I_1(t) + v_2 I_2(t) - \big[\omega_R+\mu\big]R_1(t), \tag{3.30}$$

$$\dot{S}_2(t) = \omega_R R_1(t) - \big[\sigma\lambda(t) + \mu(1+P_m)\big]S_2(t), \tag{3.31}$$

$$\dot{I}_2(t) = \sigma\lambda(t)S_2(t) - \big[v_2 + \mu(1+P_m)\big]I_2(t). \tag{3.32}$$

It is assumed that maternally immunised newborns incur only the same passive protection as those born to naturally immune mothers and that no extra immunity is afforded to those already seropositive. All infants protected by natural and vaccine induced MAb (except those who succumb to infant mortality) ultimately become fully susceptible to infection and do not acquire (active) lasting immunity until they have independently experienced primary infection.

3.3.3 Interacting Childhood Vaccination

Young infant targeted vaccination can be simplified to that of the birth targeted model described in Section 2.2. A proportion, P_v, of either all newborns, μN (if the vaccine does not immunologically interact with MAb), or only the offspring of low immunity mothers, $\mu Ab^{-}(t)$ (if MAb completely inhibits vaccine response), are born into a protected or partially protected state, bypassing primary infection. The degree of interaction between the two vaccines is governed by the parameter $\vartheta \in [0,1]$, whereby a proportion $(1-\vartheta)P_v$ of maternally protected newborns successfully respond to an administered childhood immunisation. The system can

then be described by the following set of differential equations:

$$\dot{M}(t) = \mu(1-(1-\vartheta)P_v)\big[Ab^+(t)+P_mAb^-(t)\big] - \big[\omega_M+\mu\big]M(t), \tag{3.33}$$

$$\dot{S}_1(t) = \mu(1-P_v)(1-P_m)Ab^-(t) + \omega_M M(t) - \big[\lambda(t)+\mu(1+P_m)\big]S_1(t), \tag{3.34}$$

$$\dot{I}_1(t) = \lambda(t)S_1(t) - \big[v_1 + \mu(1+P_m)\big]I_1(t), \tag{3.35}$$

$$\dot{R}_1(t) = V(t) + v_1I_1(t) + v_2I_2(t) - \big[\omega_R+\mu\big]R_1(t), \tag{3.36}$$

$$\dot{S}_2(t) = \omega_R R_1(t) - \big[\sigma\lambda(t) + \mu(1+P_m)\big]S_2(t), \tag{3.37}$$

$$\dot{I}_2(t) = \sigma\lambda(t)S_2(t) - \big[v_2 + \mu(1+P_m)\big]I_2(t), \tag{3.38}$$

where

$$\begin{aligned} V(t) = {} & \mu\,(1-\vartheta)\,P_v\big[Ab^+(t) + P_mAb^-(t)\big] \; + \\ & \mu\,P_v(1-P_m)Ab^-(t) \;\; + \;\; \mu\,P_mAb^-(t). \end{aligned} \tag{3.39}$$

A potential limitation of this model arises again from the omission of age structure, this time with respect to fertility. It can be seen that vaccinated newborns immediately contribute to the birth rate of maternally protected babies, where in reality the peak age of fertility is predominantly in early adulthood. This assumption may lead to an over estimation of the impact of active intervention on maternally acquired immunity, particularly in cases where the relative duration of active immunity is short.

3.3.4 Age Domain Models

If instead the reduced (non age-structured) general PDE model is considered at endemic equilibrium (steady state variables denoted by $\hat{X}$) and integrated with respect to time, for example over τ complete annual cycles (to find the average number of individuals residing in each state of disease for a given age a), then the

following system of age domain integro-differential equations can be derived:

$$\frac{dM(a)}{da} = \frac{\mu\delta(a)}{\tau}\int_0^\tau Ab^+(t,a)\,dt - \big(\omega_M+\mu\big)\frac{1}{\tau}\int_0^\tau M(t,a)\,dt, \tag{3.40}$$

$$\frac{dS(a)}{da} = \frac{\mu\delta(a)}{\tau}\int_0^\tau Ab^-(t,a)\,dt - \frac{1}{\tau}\int_0^\tau \big(\lambda(t)+\mu\big)S(t,a)\,dt, \tag{3.41}$$

$$\frac{dI(a)}{da} = \frac{1}{\tau}\int_0^\tau \lambda(t)S(t,a)\,dt - \big(v+\mu\big)\frac{1}{\tau}\int_0^\tau I(t,a)\,dt, \tag{3.42}$$

$$\frac{dR(a)}{da} = \frac{v}{\tau}\int_0^\tau I(t,a)\,dt - \frac{\mu}{\tau}\int_0^\tau R(t,a)\,dt, \tag{3.43}$$

where

$$\lambda(t) = \frac{\beta(t)}{N}\int_0^\infty I(t,a_i)\,da_i, \tag{3.44}$$

If the transmission function β does not vary with time, or if some seasonal average value is assumed, then the equations (3.40)-(3.44) reduce to a linear ODE model of the form:

$$\frac{dM(a)}{da} = -\big(\omega_M+\mu\big)M(a), \qquad M(0) = \mu A\hat{b}^+, \tag{3.45}$$

$$\frac{dS(a)}{da} = \omega_M M(a) - \big(\frac{\beta}{N}\hat{I}+\mu\big)S(a), \qquad S(0) = \mu A\hat{b}^-, \tag{3.46}$$

$$\frac{dI(a)}{da} = \frac{\beta}{N}\hat{I}S(a) - (\mu+v)I(a), \qquad I(0) = 0, \tag{3.47}$$

$$\frac{dR(a)}{da} = vI(a) - \mu R(a), \qquad R(0) = 0, \tag{3.48}$$

where the following analytic solutions may be found:

$$M(a) = \mu A\hat{b}^+ e^{-a(\mu+\omega_M)}, \tag{3.49}$$

$$S(a) = \frac{\mu e^{-a(\mu+\lambda)}\big(A\hat{b}^-(\lambda-\omega_M)+\omega_M A\hat{b}^+(e^{a(\lambda-\omega_M)}-1)\big)}{\lambda-\omega_M}. \tag{3.50}$$

However, if the transmission function $\beta(t)$ is explicitly dependent on time, then the incidence age profile is calculated to be of the form:

$$\frac{1}{\tau N}\int_0^{\tau}\beta(t)\,S(t,a_s)\int_0^{\infty}I(t,a_i)\,da_i\,dt, \tag{3.51}$$

whereby for seasonal systems there is inevitably some residual time dependency in the age profile, requiring the full PDE system to be solved.

3.3.5 Preliminary Model Analysis

In the following section a general steady state analysis is performed on a number of the non age-structured MSIR models discussed so far. The models are compared to the basic SIR framework described in Section 2.1, the vaccination models in Section 2.2 and to each other, in order to assess the relative implications of their structural forms.

Standard MSIR

The basic MSIR structure, given by equations (3.14)-(3.17), can be derived from the encompassing incomplete immunity model (3.20)-(3.25) by setting $\omega_R = 0$, i.e. an infinite duration of immunity following primary infection, and ensuring that the initial conditions $S_2^0, I_2^0 = 0$. Setting these differential equations equal to zero and through simple algebraic manipulation it can be shown that two equilibrium points exist, corresponding to either extinction (disease free) or endemic persistence of the invading pathogen. The disease free steady state, given by:

$$\hat{M} = 0, \qquad \hat{S} = N, \qquad \hat{I} = 0, \qquad \hat{R} = 0, \tag{3.52}$$

is equivalent to that of the basic SIR (2.8), and through an eigenvalue analysis of the resulting Jacobian matrix:

$$\lambda_1 = -\mu, \qquad \lambda_2 = -\omega_M, \qquad \lambda_3 = \beta-(\mu+v), \tag{3.53}$$

is also found to adhere to the same conditions for stability (i.e. the stability condition $R_0 < 1$ gives rise to an invasion threshold at $R_0 = 1$). The endemic susceptible population $\hat{S}$ is again found to be the same as that for a system without maternally acquired protection, as shown by the corresponding equilibrium expression:

$$\hat{M} = \frac{Nv\mu(\beta-(\mu+v))}{\beta(\mu\omega_M+v(\mu+\omega_M))}, \quad \hat{S} = \frac{N(\mu+v)}{\beta}, \quad \hat{I} = \frac{\omega_M}{v}\hat{M}, \quad \hat{R} = \frac{\omega_M}{\mu}\hat{M}, \tag{3.54}$$

implying that in an analogous manner to birth targeted vaccination, natural immunity attributed to MAb has no static influence over the number of susceptibles in a population already supporting an endemic infection. The endemic prevalence $\hat{I}$ and the proportion recovered $\hat{R}$ are however found to be dependent on ω_M, and subsequently differ from that of the basic SIR. Given that all parameters are positive and $R_0 > 1$, an increase in the duration of MAb (i.e. a decrease in ω_M) can only result in a greater proportion of the population residing in $\hat{M}$, and hence a smaller proportion currently infective or recovered.

This is an interesting result as it suggests that maternally acquired immunity has the capability to reduce population level infection despite the passivity of MAb (i.e. all maternally protected neonates ultimately become fully susceptible). It can be deduced that this reduction in prevalence is due to an additional proportion of the population being immune to circulating pathogens and the subsequent loss of infants who do not survive the background death rate before contracting an infection. However, from an eigenvalue analysis at the corresponding system equilibrium (3.53) it can be seen that there is no possible value of ω_M that will give rise to otherwise unconditional stability of the disease free steady state. This infers that there is no duration of MAb that can lead to eradication of the pathogen as

population immunity diminishes with reducing levels of infection.

The number of protected neonates is also strongly dependent on the nature of population net birth/mortality rates, where an increase in μ leads to a larger $\hat{M}$ and subsequently accentuates the resulting reduction in $\hat{I}$. This reiterates the hypothesis that MAb may be more influential in developing regions where there are likely to be higher birth and infant mortality rates, and additionally an age distribution skewed towards young infant age classes.

The approximate average age at primary infection predicted by the standard time domain MSIR model can be found explicitly in terms of its parameters by recalling equation (3.19) and substituting endemic steady state values from (3.54) (note also $\hat{\lambda} = \beta\hat{I}/N$):

$$A_v \;\approx\; \frac{\hat{M}(\mu+\omega_M)}{N\mu\,\omega_M} + \frac{Nv(v+\mu)}{\hat{M}\beta^2\omega_M} + \frac{\mu\,\omega_M + v(\mu+\omega_M)}{\beta\mu\,\omega_M}. \tag{3.55}$$

Taking the first derivative of this function with respect to ω_M^{-1}, and providing $[\beta, \omega_M, v, N, \mu] > 0, \quad R_0 > 1$, it can be shown that:

$$\frac{d\,A_v}{d\,\omega_M^{-1}} \;\geq\; 0, \tag{3.56}$$

implying that an increase in the duration of MAb can only result in an increase in the average age at primary infection.

It should be noted that a more detailed illustration of this characteristic may also be shown using the age domain realisation (3.45)-(3.48) described in Section 3.3.4. In this instance the analytic solution for $S(a)$, given by (3.50), is substituted into the general expression for the average age of infection given by (2.39).

MSIR with Maternal Immunisation

Setting the parameters ω_R, S_2^0 and I_2^0 equal to zero in equations (3.27)-(3.32), i.e. reducing the model to that of the basic MSIR (3.14)-(3.17) with maternal immunisation, the following disease free equilibrium can be found:

$$\hat{M} = \frac{2P_m\mu N}{\theta}, \qquad \hat{S} = \frac{N\omega_M}{\theta}, \qquad \hat{I} = 0, \qquad \hat{R} = \frac{P_m\omega_M N}{\theta}, \tag{3.57}$$

with common denominator,

$$\theta \; = \; \omega_M + P_m(2\mu+\omega_M).$$

It can be seen that the distribution of individuals throughout a naive, disease free population is governed by the parameters P_m, μ and ω_M, where $\hat{M} + \hat{S} + \hat{R} = N$. Increasing the amount of maternal immunisation, P_m, reduces the proportion of individuals susceptible to infection, and consequently increases the proportion of those both passively and actively protected. An interesting outcome of this analysis can be found in the numerators of the expressions for $\hat{M}$ and $\hat{R}$, where the relative contributions of neonatal and maternal immunity to the reduction in population susceptibility is seen to be dependent on the differential magnitudes of μ and ω_M. Inevitably the average duration of MAb is considerably less than life expectancy ($2\mu << \omega_M$), hence $\hat{M} << \hat{R}$, inferring that lifelong active immunisation is a considerably more effective population level intervention.

The disease free eigenvalues of the system are found to be expressed by the following parameter combinations:

$$\begin{aligned} \lambda_1 &= -\mu(P_m+1) - v_1 + \frac{\beta\omega_M}{P_m(2\mu+\omega_M)+\omega_M}, \\ \lambda_{2,3} &= -\frac{1}{2}\left(\mu(1+2P_m) + \omega_M \pm \sqrt{\mu^2(1-2P_m)^2 - 2\mu\omega_M + \omega_M^2}\right), \end{aligned} \tag{3.58}$$

where λ_1 indicates that increasing P_m subsequently alters the stability character-

istics of the disease free equilibrium (i.e. the effective reproduction number). In contrast to the standard MSIR model this suggests that it is in some cases theoretically possible to eradicate an infection through mass maternal immunisation. The condition for possible eradication is calculated in terms of the basic reproduction number (2.5) by substituting complete vaccination coverage $P_m = 1$ into λ_1, giving rise to the inequality:

$$R_0 \ < \ \frac{2(2\mu + v)(\mu + \omega_M)}{\mu + v}. \tag{3.59}$$

The second and third eigenvalues can be seen to become complex under certain parameterisations, leading to oscillatory behaviour. However, given that $P_m \in [0, 1]$ and $2\mu << \omega$ this is generally not the case.

The endemic equilibrium is found to be given by the following expressions:

$$\begin{aligned} \hat{M} &= \frac{\mu N\big[(P_m-1)v^2 + 2P_m\beta\mu + v\big(\beta + (P_m^2-1)\mu\big)\big]}{\beta\big[v(\mu+\omega_M) + \mu\big(\omega_M + P_m(2\mu + \omega_M)\big)\big]}, \\ \hat{S} &= \frac{N(\mu(P_m+1)+v)}{\beta}. \end{aligned} \tag{3.60}$$

The model predicts that the introduction of maternal immunisation, P_m, will result in an increase in the proportion of the population protected by MAb and a decrease in the prevalence of infection. In this instance, the average age at primary infection can be approximated by the following form:

$$A_v \ \approx \ \frac{\hat{M} + \hat{R} + P_m(\hat{S} + \hat{I})}{N}(\omega^{-1} + \lambda^{-1}) + \frac{(1-P_m)(\hat{S} + \hat{I})}{N}(\lambda^{-1}), \tag{3.61}$$

where the average age is seen to increase with greater levels of maternal immunisation.

MSIRS Temporary/Waning Immunity

The effects of temporary/waning immunity resulting from natural infection can be explored by setting $\sigma = 1$, $\gamma = 1$ and $v = v_1 = v_2$ in equations (3.20)-(3.26), whereby secondary infection characteristics are considered to be identical to that of primary infection. Susceptible and infective states can then be combined such that: $S(t) = S_1(t) + S_2(t)$ and $I(t) = I_1(t) + I_2(t)$, giving rise to a model structure analogous to that of the SIRS described in Section 2.1.4. The disease free steady state remains the same as that of the SIR and MSIR systems (3.52), and the resulting endemic equilibrium is given by:

$$\hat{M} = \mu N v\,\theta, \quad \hat{S} = \frac{N(\mu+v)}{\beta}, \quad \hat{I} = \omega_M N(\mu+\omega_R)\,\theta, \quad \hat{R} = \omega_M N v\,\theta, \qquad (3.62)$$

where

$$\theta = \frac{\beta - (\mu+v)}{\beta\big(\omega_M(\mu+\omega_R) + v(\mu+\omega_M)\big)}.$$

Comparing the expressions in (3.62) with those in (3.54) reiterates the result that waning of active immunity acts to raise endemic prevalence (force of infection) within a population through a reduction in the number of individuals currently protected from infection. Consequently the number of newborns protected by MAb is also reduced, thus through a combination of this and a higher force of infection, a short duration of immunity can significantly lower the average age at primary challenge.

3.4 Age Structured MSIR Models

It is the intention of this work to use a continuous PDE type age structured model (see the book by Anderson and May [1991]) to assess the impact of MAb on the distribution of primary infection incidence. This is attempted using the general

MSIR model (3.3)-(3.8) described in Section 3.2. However, models that include both time and age as continuous independent variables are inherently complex to rigorously analyse. Therefore an intermediate, discretised age structure is also proposed in order to ease analytical tractability.

3.4.1 Discrete Age Structure

In discrete age-structured models the key characteristics of heterogeneous mixing patterns are lumped together in distinct (homogeneously mixed) age classes with common epidemiological properties associated with infection [Farrington et al., 2001]. The age classes are divided according to known characteristics of transmission, such as higher transmissive contact rates of respiratory viruses among school aged children or of sexually transmitted infections among young adults. This approach also allows for a more realistic inclusion of birth and mortality functions and potentially the influence of physiological development on susceptibility and infectivity.

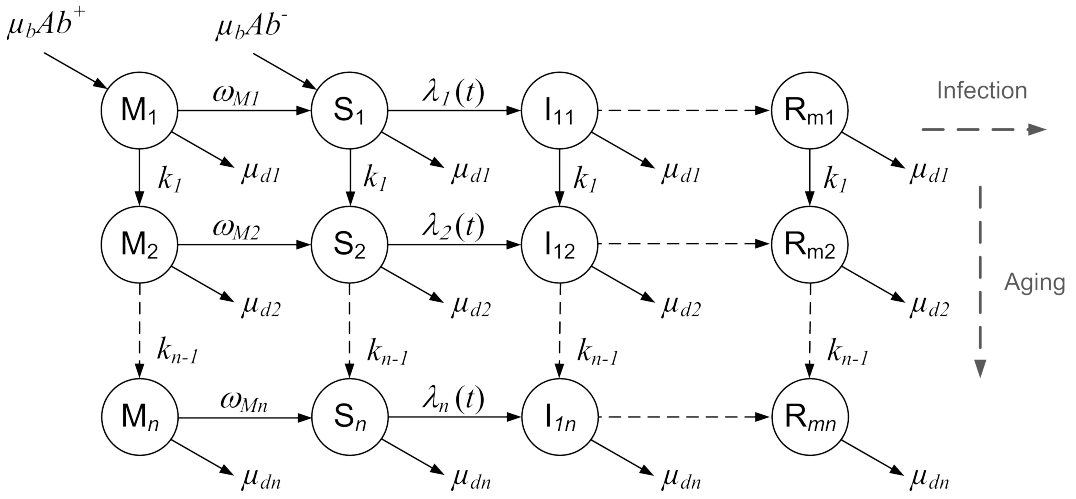

Figure 3.4: Discrete Age Model Structure

In this instance the transmission function $\beta(t)$ becomes an $n \times n$ matrix, often

referred to as a 'who acquires infection from who' matrix, that describes the transmissive interaction of individuals between n discretised age groups. Each element $\beta_{ij}(t)$ denotes the rate of transmission arising from contacts between susceptibles residing in age class i and infectives in age class j. The process of progressive ageing throughout the model structure is included by means of a linear coefficient decay parameter k_i (see Figure 3.4) that describes the rate at which individuals mature and leave a particular age class i, where k_i^{-1} corresponds to the age-span of the group.

The set of ordinary differential equations describing an MSIR type model with n discrete age classes can be expressed as follows:

$$\dot{M}_1(t) = U_{Ab^+}(t) - \big(\omega_{M1} + \mu_{d1} + k_1\big)M_1(t), \qquad M_1(0) = M_1^0, \quad (3.63)$$

$$\dot{S}_1(t) = U_{Ab^-}(t) + \omega_{M1}M_1(t) - \big(\lambda_1(t) + \mu_{d1} + k_1\big)S_1(t) \qquad S_1(0) = S_1^0, \quad (3.64)$$

$$\dot{I}_1(t) = \lambda_1(t)S_1(t) - \big(v_1 + \mu_{d1} + k_1\big)I_1(t), \qquad I_1(0) = I_1^0, \quad (3.65)$$

$$\dot{R}_1(t) = v_1 I_1(t) - \big(\mu_{d1} + k_1\big)R_1(t), \qquad R_1(0) = R_1^0, \quad (3.66)$$

- -

$$\dot{M}_i(t) = k_{i-1}M_{i-1}(t) - \big(\omega_{Mi} + \mu_{di} + k_i\big)M_i(t), \qquad M_i(0) = M_i^0, \quad (3.67)$$

$$\dot{S}_i(t) = k_{i-1}S_{i-1}(t) + \omega_{Mi}M_i(t) - \big(\lambda_i(t) + \mu_{di} + k_i\big)S_i(t) \qquad S_i(0) = S_i^0, \quad (3.68)$$

$$\dot{I}_i(t) = k_{i-1}I_{i-1}(t) + \lambda_i(t)S_i(t) - \big(v_i + \mu_{di} + k_i\big)I_i(t), \qquad I_i(0) = I_i^0, \quad (3.69)$$

$$\dot{R}_i(t) = k_{i-1}R_{i-1}(t) + v_i I_i(t) - \big(\mu_{di} + k_i\big)R_i(t), \qquad R_i(0) = R_i^0, \quad (3.70)$$

where

$$i = \{2, \ldots, n\}, \qquad k_n = 0, \qquad \lambda_i(t) = \sum_{j=1}^{n} \beta_{ij}(t)I_j(t).$$

In the general case all model parameters are allowed to vary with age, supporting heterogeneity in transmission, fertility and mortality. The population net birth

and death rates are balanced to ensure constant population size N and distribution $\{N_i, \ldots, N_n\}$ with respect to age:

$$\mu N \;=\; \sum_{i=1}^{n} \mu_{bi} N_i \;=\; \sum_{i=1}^{n} \mu_{di} N_i, \tag{3.71}$$

where the population sizes for each age class are found to be:

$$N_1 \;=\; \frac{\mu N}{\mu_{d1} + k_1}, \qquad N_i \;=\; \mu N \, \frac{\displaystyle\prod_{j=1}^{i-1} k_j}{\displaystyle\prod_{j=1}^{i} \left(\mu_{dj} + k_j\right)} \quad \text{for } \; i = \{2, \ldots, n\}. \tag{3.72}$$

The corresponding influxes for seropositive and seronegative newborns are then defined according to the number of individuals currently immune such that:

$$U_{Ab^+}(t) \;=\; \sum_{i=1}^{n} \mu_{bi} \big[M_i(t) + R_i(t) \big] \tag{3.73}$$

$$U_{Ab^-}(t) \;=\; \sum_{i=1}^{n} \mu_{bi} \big[S_i(t) + I_i(t) \big], \tag{3.74}$$

where individuals are born into the youngest age class.

Basic Reproduction Number

As discussed in Section 2.3.1 the average transmission function β_{ij} corresponds to an $n \times n$ matrix, where the basic reproduction number is subsequently defined as the average number of expected cases arising from a single typical infective introduction into an otherwise naive population. Recalling the expression for R_0 (2.5), and neglecting movement of infectives due to ageing, the basic reproductive growth in age class i emanating from a single infective individual residing in age

class j can be given by:

$$R_0 = \begin{pmatrix} \beta_{11}N_1D_1 & \beta_{12}N_1D_2 & \dots & \beta_{1n}N_1D_n \\ \beta_{21}N_2D_1 & \beta_{22}N_2D_2 & \dots & \beta_{2n}N_2D_n \\ \vdots & \vdots & \ddots & \vdots \\ \beta_{n1}N_nD_1 & \beta_{n2}N_nD_2 & \dots & \beta_{nn}N_nD_n \end{pmatrix}, \tag{3.75}$$

where $D_i = (\mu_{di} + v_i)^{-1}$ corresponds to the average duration an individual remains infective.

Unfortunately, the derivation of an appropriate, single value for R_0 that describes the invasion threshold and the initial growth rate for the whole system cannot be achieved through simple averaging of the individual components in equation (3.75). Following the method documented by Diekmann et al. [1990], the progression of an epidemic system may be considered in terms of generations, where each new generation, ϕ_{g+1}, is found by applying an $n \times n$ matrix reproduction function, K, to the current generation, ϕ_g. Each generation of infectives is represented by an n-dimension vector, ϕ, showing their distribution throughout the different age classes in the model:

$$\phi_g = K\phi_{g-1} = K^2\phi_{g-2} = \ldots = K^g\phi_0, \tag{3.76}$$

where in the early stages of an epidemic the reproductive function K can be assumed to be the matrix R_0 (3.75).

If, for example, $K = R_0$ is a 2×2 matrix (signifying a model structure with two discrete age classes), with two distinct real eigenvalues λ_1 and λ_2, and it is known that $\lambda_1 > 0$ is the dominant eigenvalue, i.e. $\lambda_1 > |\lambda_2|$, then $\psi^{(1)}$ and $\psi^{(2)}$ are corresponding eigenvectors from which any vector $x \in \mathbb{R}^2$ can be expressed as a linear combination:

$$x = c_1\psi^{(1)} + c_2\psi^{(2)}, \tag{3.77}$$

where

$$Kx = c_1\lambda_1\psi^{(1)} + c_2\lambda_2\psi^{(2)}, \tag{3.78}$$

and subsequently

$$K^g x \;=\; c_1\lambda_1^g\left[\psi^{(1)} + \frac{c_2}{c_1}\left(\frac{\lambda_2}{\lambda_1}\right)^g \psi^{(2)}\right]. \tag{3.79}$$

Given that $|\lambda_2/\lambda_1| < 1$ and provided $c_1 \neq 0$, then the second term in (3.79) will tend to zero as the number of generations $g \to \infty$, effectively reducing (3.79) to:

$$K^g x \;\sim\; c_1\lambda_1^g\psi^{(1)}. \tag{3.80}$$

The basic reproduction number for the overall system can therefore be quoted as the dominant eigenvalue λ_1, given that $\lambda_1 > 1$ results in exponential growth and $\lambda_1 < 1$ results in exponential decay, thus describing the invasion threshold for a completely susceptible population. It can also been noted that the influence of the initial condition is restricted to the value of c_1.

3.4.2 Continuous Age Structure

An alternative approach to modelling the effects of MAb on the average age profile of primary incidence is to consider a more empirical representation of the rate at which the neonatal population loses passively acquired immunity. The process is implemented as a simplification to the continuous immunity model (3.1)-(3.2), proposed in Section 3.2, where the acquisition of protective MAb is decoupled from wider adult infection/immunity dynamics. This may be appropriate for systems where high titres of disease specific neutralising antibodies are ubiquitous throughout the adult (child bearing) population and are relatively unaffected by 'childhood' epidemics or seasonality. The model is also extended from that of the continuous age-time SIR (2.33)-(2.37) discussed in Section 2.3 and defined by the

following set of equations:

$$\begin{aligned}
\frac{\partial M(t,a)}{\partial t} + \frac{\partial M(t,a)}{\partial a} &= -Q(t,a) - \mu_d(a)M(t,a), && (3.81)\\
\frac{\partial S(t,a)}{\partial t} + \frac{\partial S(t,a)}{\partial a} &= Q(t,a) - \big[\lambda(t,a) + \mu_d(a)\big]S(t,a), && (3.82)\\
\frac{\partial I(t,a)}{\partial t} + \frac{\partial I(t,a)}{\partial a} &= \lambda(t,a)S(t,a) - \big[v(a) + \mu_d(a)\big]I(t,a), && (3.83)\\
\frac{\partial R(t,a)}{\partial t} + \frac{\partial R(t,a)}{\partial a} &= v(a)I(t,a) - \mu_d(a)R(t,a), && (3.84)
\end{aligned}$$

where

$$\lambda(t,a_s) = \frac{1}{N}\int_0^\infty \beta(t,a_s,a_i)\; I(t,a_i)\; da_i. \qquad (3.85)$$

The boundary conditions (i.e. the number of newborns seropositive and seronegative) are both determined by $C(t, Ab)$; a function that describes the population cord log antibody titre distribution at a given point in time, and τ, a parameter representing a discrete cut-off threshold in Ab that distinguishes between complete immunity and full susceptibility. Although $C(t, Ab)$ includes some inherent dependency on time, the integral of this function with respect to Ab corresponds to the current net birth rate and is therefore considered to be constant. Hence:

$$M(t,0) = \int_\tau^\infty C(t,Ab)\; dAb, \quad S(t,0) = \int_0^\tau C(t,Ab)\; dAb, \quad I(t,0) = 0. \qquad (3.86)$$

Individual log antibody titres are assumed to decay linearly with respect to age [Ochola et al., 2009], where the average population decay rate is given by ω_M, and the rate at which maternally protected infants lose MAb and become fully susceptible to infection is modelled by the function $Q(t, a)$.

Neglecting infant mortality, if an instantaneous birth cohort (i.e. $a = t$ for all members) is born at t_0 and has a log antibody titre distribution $C(t_0, Ab)$, then at t_0, the rate at which individuals cross the immunity threshold and subsequently lose maternally acquired protection is given by $Q(0) = \omega_M C(t_0, \tau)$. For $a > 0$ this

rate becomes $Q(a) = \omega_M C(t_0, \omega_M a + \tau)$. Generalising this function beyond that of a single cohort and including infant mortality yields the expression:

$$Q(t,a) \;=\; \omega_M \; C(t-a, \omega_M a+\tau) \; e^{-\int_0^a \mu(\alpha) d\alpha}, \tag{3.87}$$

where all individuals of age a (born at time $t-a$) have antibody titres according to the same distribution $C(t-a, Ab)$.

The average duration of protection from MAb is evaluated as the average age of all individuals becoming susceptible at a given time t. In the general case this can be found in a similar manner to the average age of infection (2.39) from the following integral expression:

$$A_v(t) \;= \frac{\int_0^\infty a \, Q(t,a) \; da}{\int_0^\infty Q(t,a) da}. \tag{3.88}$$

In the more simple case where the effects of infant mortality are omitted from the model and $C(t, Ab)$ is assumed constant with respect to time, this value can be expressed more simply as:

$$A_v \;=\; \frac{(\bar{C} - \tau)}{\omega_M}, \tag{3.89}$$

where the average duration is dependent on the difference between the average cord antibody titre, $\bar{C}$, and the cut-off threshold for immunity τ, as well as the average individual MAb decay rate ω_M.

3.4.3 Maternal Immunisation

Maternal immunisation can be applied to the model (3.81)-(3.87) by means of a distorting function $V_M(Ab)$, which is applied to the initial cord antibody titre distribution $C(t, Ab)$. If the average MAb response (scalar increase in log Ab

titre) to the implemented vaccine is independent of the mother's initial antibody level, and $V_M(Ab)$ follows some random (Gaussian) distribution, then the resulting post-vaccine cord antibody function can be generated in the following manner:

$$C_v(t, Ab) = \int_0^{Ab} \frac{C(t, z)V_M(Ab/z)}{\bar{C}(t)} dz. \tag{3.90}$$

However, given that only a limited proportion, P_m, of pregnant women will successfully take up the vaccine, the actual resulting cord log antibody function is given by:

$$C_v(t, Ab) = (1 - P_m)C(t, Ab) + P_m \int_0^{Ab} \frac{C(t, z)V_M(Ab/z)}{\bar{C}(t)} dz. \tag{3.91}$$

If the administered vaccine does immunologically interact with a mother's response to prior experience of infection, then the potential efficacy of the vaccine may be impeded by an initially high antibody titre. At a population level, only those individuals who would not otherwise already be protected by high MAb would benefit from the immunisation. Neglecting any change in antibody titre between immunisation at 30 weeks gestation and birth, and assuming Ab titres corresponding to mother and foetus are equal, if a discrete threshold τ_m defines both immune protection and vaccine interaction in the adult population, then the function $V_M(Ab)$ is only applied to the region of $C(t, Ab)$ between 0 and τ_m. Therefore

$$C_v(t, Ab) = (1 - P_m)C(t, Ab) + P_m \int_0^{Ab} f(t, Ab, z) dz, \tag{3.92}$$

where

$$f(t, Ab, z) = \begin{cases} \dfrac{C(t, z)V_M(Ab/z)}{\bar{C}(t)} & \text{for} \quad z \leq \tau_m, \\ C(t, z) & \text{for} \quad z > \tau_m. \end{cases} \tag{3.93}$$

If A_T defines some point in age, then all individuals born with log antibody titres below $A_T\omega + \tau$ will become susceptible and at risk of contracting infection before they reach age A_T. One primary aim of maternal immunisation is then to minimise

the number of infants with cord titres below this target. However, if the vaccine is ineffective above the mother's antibody interaction threshold, τ_m, then assuming $\tau < \tau_m < A_T\omega + \tau$, there is a proportion of newborns who remain at risk from the infection and are unaided by the vaccine. This proportion may be described by the following integral expression:

$$\int_{\tau_m}^{A_T\omega+\tau} C(t, Ab)\, dAb. \tag{3.94}$$

In this instance good vaccine response is required in mothers with log antibody titres up to at least $\tau_m \geq A_T\omega + \tau$.

3.5 Nominal Parameter Values

Throughout the forthcoming work, realistic estimates of model parameters are required for numerical and qualitative analysis. Nominal values are not estimated from fitting the proposed model structures to empirical data, since it is initially unknown if particular parameters are sufficiently determined by the available input/output behaviour of the system. Alternatively, estimates are based on prior knowledge extracted from a number of clinical studies, epidemiological observations and the validation of alternative epidemic models presented in the literature. The following section is used to collate these results and to provide appropriate sets of initial parameter values corresponding to the ODE MSIR and MSIRS2 models presented in Sections 3.3 and 3.3.1. The parameterisation of models that incorporate age dependency is discussed for specific examples in Chapter 6.

The models are considered in the context of two contrasting viral infections, namely measles and human respiratory syncytial virus (hRSV). These pathogens are both members of the *Paramyxoviridae* virus family but show differing degrees of antigenic variability. The primary route of transmission is through respiratory secre-

tions by means of either inhalation of aerosol droplets or contact with contaminated fomites. It is likely that both infections may be subject to similar processes of temporal variation, although their resulting seasonality is markedly different. These pathogens are adopted as illustrative examples since they subsequently display contrasting interactions with the host immune system that complement the varying reinfection models presented throughout this chapter and have also been the subject of an extensive degree of study.

3.5.1 Measles

The foundation model structure described in this work is the fundamental MSIR model (3.14)-(3.17), which describes the evolution of pathogens that are seen to induce solid, lifelong immunity following infection. The epidemiology of measles is traditionally considered in this manner, where clinical disease is generally only observed among primary cases [Hawker et al., 2005]. However, the boosting and waning of adult antibody titres has been observed in studies such as that by Huiss et al. [1997] and Pedersen et al. [1989], which raises the possibility of persistent subclinical reinfection throughout the recovered/vaccinated population [Damien et al., 1998; Glass and Grenfell, 2004]. Although measles is unlikely to be a future candidate for mass maternal immunisation, the potential interaction of MAb with infant vaccine response, and relations between passively acquired antibodies in neonates and population wide immunity are of ongoing interest [Gans et al., 1998; Pabst et al., 1992; Siegrist, 2003].

The infection is widely reported to have an average duration of infectivity, v^{-1}, of approximately 5 days (i.e. $v = 73\,\mathrm{yr}^{-1}$) [Hawker et al., 2005; Schenzle, 1984], and a basic reproduction number, R_0, of around 18 within the UK [Anderson and May, 1991]. Assuming a constant birth/mortality rate coefficient, $\mu = 0.014\,\mathrm{yr}^{-1}$ [White et al., 2007] (corresponding to an average life expectancy of 71.4 years), the average

Table 3.1: Initial estimated values for MSIR model parameters corresponding to pre-vaccine measles in the UK.

Parameter	Description	Value	Source
μ	UK net birthrate coefficient	$0.014\,\mathrm{yr}^{-1}$	[White et al., 2007]
N	UK population size	5.7×10^{7}	[White et al., 2007]
β_0	Annual average transmission rate	$1314\,\mathrm{yr}^{-1}$	[Anderson and May, 1991]
β_1	Seasonal variation in transmission	0.046	[Keeling and Grenfell, 2002]
ϕ	Annual epidemic timing	0.019	[Fine and Clarkson, 1982]
υ	Rate of recovery	$73\,\mathrm{yr}^{-1}$	[Hawker et al., 2005]
ω_M	Waning MAb rate coefficient	$4\,\mathrm{yr}^{-1}$	[Nicoara et al., 1999]

transmission rate, β_0, may be calculated from (2.5) to be approximately $1314\,\mathrm{yr}^{-1}$. Although the duration of maternally acquired immunity does not appear to have been estimated explicitly, typical values of around 2-4 months ($\omega_M = 4\,\mathrm{yr}^{-1}$) have been suggested in a number of sources (such as those by Nicoara et al. [1999] and Williams et al. [1995]). Table 3.1 provides a complete set of nominal parameter values for the homogeneous MSIR model derived in Section 3.3.

3.5.2 Respiratory Syncytial Virus

Human respiratory syncytial virus is one of the leading world wide causes of severe respiratory tract infection among neonate and young infant age classes [Ogra, 2004]. The disease results in hospitalisation rates of 1-3% in infants under 12 months of age, with a peak at 2-3 months and a mortality rate of 1-3% among those admitted [Munoz et al., 2003]. Age serological surveys such as those described in the work by Cox et al. [1998] suggest an overall force of infection, λ, in the region of $0.84\,\mathrm{yr}^{-1}$, where the majority of infants have immunological experience by 3 years of age [White et al., 2007].

In contrast to the measles virus, hRSV is found to display significant antigenic variability [Cane, 2001], leading to frequent reinfection throughout the wider pop-

Table 3.2: Fixed nominal MSIRS2 model parameter values corresponding to hRSV infection in the UK.

Parameter	Description	Value	Source
μ	UK net birthrate coefficient	$0.014\,\mathrm{yr}^{-1}$	[White et al., 2007]
N	UK population size	5.7×10^{7}	[White et al., 2007]
λ	Average force of infection	$0.84\,\mathrm{yr}^{-1}$	[Cox et al., 1998]
v_1	Primary infection recovery rate	$40.56\,\mathrm{yr}^{-1}$	[White et al., 2005]
v_2	Secondary infection recovery rate	$107.35\,\mathrm{yr}^{-1}$	[Hall et al., 1991]
ω_M	Waning MAb rate coefficient	$4\,\mathrm{yr}^{-1}$	[Hacimustafaoglu et al., 2004]

ulation [Weber et al., 2001]. As a result, the infection is more appropriately described by the MSIRS2 model defined in Section 3.3.1. Adult infection is typically less severe than that of young children [Falsey and Walsh, 2000]. However, it is not known whether this is primarily the result of accumulating immunological experience or some aspect of physiological development [White et al., 2005]. Documented estimates for the duration of viral shedding are found to vary between $6.7-10.1$ days for infants (corresponding to values of v_1 equal to $54.48\,\mathrm{yr}^{-1}$ [Hall et al., 1976], $40.56\,\mathrm{yr}^{-1}$ [White et al., 2007] and $36\,\mathrm{yr}^{-1}$ [Weber et al., 2001]), and $3.0-4.4$ days for adults (corresponding to values of v_2 equal to $121.67-91.25\,\mathrm{yr}^{-1}$ [Falsey and Walsh, 2000], $107.35\,\mathrm{yr}^{-1}$ [Hall et al., 1991] and $82.95\,\mathrm{yr}^{-1}$ [Lee et al., 2004]).

The average duration of maternally acquired immunity is reported to be around 1.23-3.75 months (corresponding to values of ω_M equal to $9.73\,\mathrm{yr}^{-1}$ [Brandenburg et al., 1997], $3.67\,\mathrm{yr}^{-1}$ [Cox et al., 1998] and $3.20\,\mathrm{yr}^{-1}$ [Ochola et al., 2009]). A representative midrange value of $4\,\mathrm{yr}^{-1}$ (average duration of 3 months) is chosen since it also corresponds with the observations reported by Hacimustafaoglu et al. [2004] for hRSV and Nicoara et al. [1999] for measles mumps and rubella.

As previously discussed, the contributions of primary and secondary hRSV transmission to the overall force of infection remains largely unclear. Nominal values for the duration of secondary immunity are found to be between $6.67-24$ months

Table 3.3: Varying nominal MSIRS2 model parameter values corresponding to hRSV infection in the UK.

Parameter	Description	A	B	C	D
β_0	Average transmission rate	$2490\,\mathrm{yr}^{-1}$	$2490\,\mathrm{yr}^{-1}$	$152\,\mathrm{yr}^{-1}$	$486\,\mathrm{yr}^{-1}$
β_1	Seasonal variation in transmission	0.15	0.15	0.21	–
ϕ	Annual epidemic timing	0.51	0.51	0.11	–
σ	Susceptibility to secondary infection	0	1	1	0.5
γ	Infectivity of secondary infection	0	0	1	0.6
ω_R	Waning immunity rate coefficient	$0\,\mathrm{yr}^{-1}$	$1.8\,\mathrm{yr}^{-1}$	$1.8\,\mathrm{yr}^{-1}$	$0.67\,\mathrm{yr}^{-1}$

(corresponding to values of ω_R equal to $1.8\,\mathrm{yr}^{-1}$ [Weber et al., 2001], $1.0-0.5\,\mathrm{yr}^{-1}$ [Falsey et al., 2006] and $0.51\,\mathrm{yr}^{-1}$ [White et al., 2005]). However, altered secondary infection parameters, i.e. proportionally reduced susceptibility, σ, and infectivity, γ, are inherently more difficult to estimate, particularly from clinical studies. In this instance, these parameters are varied within their valid ranges in order to emulate the continuum of possible reinfection characteristics described by the model. The average transmission parameter, β, is set such that the average force of infection, λ, remains constant. Sets of nominal estimates for fixed and varied MSIRS2 model parameter values are given by Tables 3.2 and 3.3, respectively, for hRSV in the UK.

Parameter sets A and B correspond to cases where the overall force of infection is dominated by primary infectivity. Set A gives rise to a realisation equivalent to that of the fundamental MSIR model (3.14)-(3.15), where high levels of maternal antibodies are sustained through solid and lifelong immunity acquired following primary infection. In contrast, parameter set B corresponds to a situation where wider population immunity dynamics are dependent on exposure to primary infection among infants, but do not contribute to overall transmission. Parameter sets C and D correspond to cases where secondary infectivity is considered equivalent to primary infection and partially reduced, respectively.

3.6 Conclusions

A series of MSIR framework models have been presented that aim to address questions regarding the population level influence of maternally acquired immunity and the potential outcomes of mass maternal immunisation. The models have been derived through successive simplifications of an encompassing general PDE model structure in order to address specific aspects of the problem statement for systems with contrasting epidemiological characteristics. Sets of initial parameter estimates have also been collated from the literature corresponding to two common viral diseases that provide suitable illustrative examples during forthcoming numerical analysis of the models.

Chapter 4

Structural Identifiability & Indistinguishability Analysis

The problems of structural identifiability and indistinguishability (see the work by Bellman and Åström [1970] and Godfrey and DiStefano III [1987]) are purely theoretical concepts that aim to address the question of uniqueness in the determination of unknown model parameters and the inference of system structure from known input-output behaviour of a real system. These analyses are an essential, yet often overlooked, prerequisite to experiment design and parameter estimation [Evans et al., 2002]. They are particularly relevant in disciplines such as epidemiology where there is often a significantly limited observation of the full system state.

In model indistinguishability, the objective is to determine whether or not a series of competing model structures that represent alternative descriptions of some underlying physical process can be parametrised in such a way as to yield identical input/output behaviour. If two prospective models are found to be structurally indistinguishable then it is hence not possible, without the use of additional knowledge of the real system, to determine which structure best corresponds to the col-

lected data. This analysis is of particular importance when there is a degree of uncertainty in the elemental function of the real system.

The concept of structural identifiability (a special case of indistinguishability where competing models have the same structure) describes the problem of whether or not the unknown parameters of a single postulated model can be uniquely determined from perfect, noise free and continuous experimental data. Global identifiability indicates that a given parameter (or model structure, should all parameters be globally identifiable) is uniquely determinable from the considered observation. Should a model structure prove to be unidentifiable, whereby a number of different parametrisations exist that give rise to identical measurable behaviour of the system, parameter values estimated from fitting to real data should be treated with extreme caution.

Application to Epidemic Systems

The application of identifiability/indistinguishability techniques to identifying problems of indeterminacy can provide cogent advocation for the more rigorous validation of epidemic models used in the assessment of decisions regarding large scale public health policy. However, the illustrated use of these methods are relatively sparse in the literature and generally not common practice among the epidemiological community. In reality, the identifiability problem is arguably reduced through the substitution of 'known' parameter values, such as population size, N, and the duration of infection, v^{-1}, into the model prior to fitting. However, clear estimation of these attributes is often difficult to obtain, for example defining geographical bounds around a population supporting an unubiquitous infection, or measuring the exact duration of viral shedding, and do not necessarily scale consistently between individual and population level characteristics.

The work by White et al. [2001] describes the use of a structural identifiability

analysis in the validation of a multispecies model for the spread of major and minor pathogens causing mastitis in dairy cattle. Despite the size and complexity of the model, it was found that all model parameters were uniquely determinable from the available data. However, in this case a very comprehensive longitudinal data set was available for the study, effectively allowing for simultaneous observation of all four state variables. In contrast, the work by Evans et al. [2004, 2005] considers, respectively, an identifiability analysis of the seasonally forced general SIR model (2.1)-(2.4), (2.14), and an indistinguishability analysis of an SIR model (2.1)-(2.4) and an SIRS model (2.15)-(2.4) with temporary/waning immunity. The output structure is limited to a more common prevalence observation with an unknown scaling factor, and in both cases the models were found to be unidentifiable/indistinguishable.

It is the objective of this chapter to broaden the application of these techniques to epidemic models that include characteristics of incomplete immunity and birth targeted vaccination, as described in Sections 2.1 and 2.2, and to some of the fundamental MSIR model structures derived in Section 3.3.

4.1 Formal Definitions

In order to provide a more formal definition of structural identifiability the following standard form for uncontrolled nonlinear systems is assumed:

$$\Sigma(p) \quad \begin{cases} \dot{x}(t,p) &= f(x(t,p),p), \\ y(t,p) &= h(x(t,p),p), \\ x(0,p) &= x^0(p), \end{cases} \tag{4.1}$$

where $x(t,p) \in \mathbb{R}^n_{\geq 0}$ and $y(t,p) \in \mathbb{R}^m_{\geq 0}$ denote the state and output vectors respectively; $p \in \Omega$ (an open subset of $\mathbb{R}^q_{>0}$ denoting all feasible parameter vectors)

corresponds to a constant parameter vector, and for all $p \in \Omega$, $f(\cdot, p)$ and $h(\cdot, p)$ are analytic on $\mathbb{R}^n_{\geq 0}$.

Definition 1. Two particular parameter vectors $p, \tilde{p} \in \Omega$ are said to be *indistinguishable* ($\tilde{p} \sim p$) if they give rise to identical outputs, i.e. $y(t, p) = y(t, \tilde{p})$ for all $t \geq 0$. Hence it is impossible to distinguish between p and $\tilde{p}$ from an ideal noise free observation via the output.

Definition 2. For generic $p \in \Omega$, the i^{th} parameter p_i is said to be *globally identifiable* if $\tilde{p} \sim p$ and $\tilde{p} \in \Omega$ imply that $\tilde{p}_i = p_i$, and *locally (non-uniquely) identifiable* if there exists some open neighbourhood $\mathcal{N}(p) \subset \Omega$ ($\mathcal{N}(p) \neq \Omega$) such that $\tilde{p} \sim p$ for $\tilde{p} \in \mathcal{N}$ implies that $\tilde{p}_i = p_i$. If p_i is shown not to be at least locally identifiable then it is said to be *unidentifiable*.

Definition 3. A model conforming to (4.1) is said to be *structurally globally identifiable* if all parameters p_i are globally identifiable, and *structurally locally identifiable* if any non-globally identifiable parameters are locally identifiable. If any parameters are found to be unidentifiable then the model is *unidentifiable*.

For structural indistinguishability, a competing model structure analogous to that of (4.1) is also defined in standard form:

$$\tilde{\Sigma}(\tilde{p}) \quad \begin{cases} \dot{\tilde{x}}(t, \tilde{p}) &= \tilde{f}(\tilde{x}(t, \tilde{p}), \tilde{p}), \\ \tilde{y}(t, \tilde{p}) &= \tilde{h}(\tilde{x}(t, \tilde{p}), \tilde{p}), \\ \tilde{x}(0, \tilde{p}) &= \tilde{x}^0(\tilde{p}), \end{cases} \tag{4.2}$$

where $\tilde{x}(t, \tilde{p}) \in \mathbb{R}^{\tilde{n}}_{\geq 0}$ and $\tilde{p} \in \tilde{\Omega}$ (an open subset of $\mathbb{R}^{\tilde{q}}_{>0}$) correspond to state and parameter vectors respectively, outputs from both competing models $y(t, p), \tilde{y}(t, \tilde{p}) \in \mathbb{R}^m_{\geq 0}$, and for all $\tilde{p} \in \tilde{\Omega}$, $\tilde{f}(\cdot, \tilde{p})$ and $\tilde{h}(\cdot, \tilde{p})$ are analytic on $\mathbb{R}^{\tilde{n}}_{\geq 0}$.

Definition 4. The competing systems $\Sigma(p)$ and $\tilde{\Sigma}(\tilde{p})$, where $p \in \Omega$ and $\tilde{p} \in \tilde{\Omega}$, are said to be *output indistinguishable* ($\Sigma(p) \sim \tilde{\Sigma}(\tilde{p})$) if they give rise to identical outputs, i.e. $y(t,p) = \tilde{y}(t,\tilde{p})$ for all $t \geq 0$. Hence it is impossible to distinguish between $\Sigma(p)$ and $\tilde{\Sigma}(\tilde{p})$ from an ideal noise free observation.

Definition 5. The models Σ and $\tilde{\Sigma}$ are said to be *structurally indistinguishable* ($\Sigma \sim \tilde{\Sigma}$) if for generic $p \in \Omega$ there exists a $\tilde{p} \in \tilde{\Omega}$ such that $\Sigma(p) \sim \tilde{\Sigma}(\tilde{p})$; and for generic $\tilde{p} \in \tilde{\Omega}$ there exists a $p \in \Omega$ such that $\Sigma(p) \sim \tilde{\Sigma}(\tilde{p})$.

4.2 Identifiability Methods for Nonlinear Systems

Since the early 1970's, an extensive base of literature has accumulated regarding the issue of identifiability in compartmental systems, for examples see the review by Cobelli and DiStefano III [1980], the relevant chapter in Jacquez [1996] and the book by Godfrey [1983], as well as the papers by Godfrey and Chapman [1990], Godfrey et al. [1994] and Chappell et al. [1990]. Epidemic models such as those characterised in this work tend to be uncontrolled (free or autonomous) and inherently nonlinear due to the explicit dependency of infection incidence ($\beta S(t)I(t)/N$) on both the susceptible and infective state variables of the system. However, despite the additional complexity in analysis over linear systems (see the book by Walter [1982]), the problem of structural identifiability can still be approached with a number of well documented methods (for a brief review on general techniques for nonlinear identifiability see the paper by Boubaker and Fourati [2004]).

4.2.1 Taylor Series Expansion Approach

The work by Godfrey and Fitch [1984] describes the use of a Taylor series expansion method on a number of examples in pharmacokinetics. This technique was first utilised by Pohjanpalo [1978] and is also equally applicable to time varying and nonlinear systems. The output functions corresponding to two competing parametrisations, $y(t,p)$ and $y(t,\tilde{p})$, are expanded as a Taylor series about a known point in time (usually at an initial condition i.e. $t = 0^+$) in the following manner:

$$y(t,p) \;=\; y(0,p) \;+\; \dot{y}(0,p)t \;+\; \ddot{y}(0,p)\frac{t^2}{2!} \;+\ldots+\; y^{(k)}(0,p)\frac{t^k}{k!} \;+\ldots, \qquad (4.3)$$

where $$y^{(k)}(0,p) = \left.\frac{d^k y}{dt^k}\right|_{t=0} \qquad \text{for} \qquad k = 1,2,3,\ldots .$$

The resulting infinite series of successive derivatives, $y^{(k)}(0,p)$, are theoretically measurable and unique for a particular output expansion. Therefore, if two competing parametrisations are indistinguishable (i.e. yield identical output trajectories) and hence the considered model structure is unidentifiable, they must have an identical series of Taylor coefficients. It follows, that in order to perform an analysis, the Taylor series coefficients for the two parametrisations are found, compared, and algebraically solved to generate a set of conditions for $\tilde{p}$ that give rise to identical output behaviour [Godfrey and DiStefano III, 1987].

For linear systems it can be shown through the use of the Cayley-Hamilton theorem that a maximum of $2n-1$ independent equations (Taylor coefficients) are required to yield a result (i.e. no further information gained from considering later coefficients) [Vajda, 1984]. However, for a single output nonlinear system with rational polynomial transfer coefficients, the upper bound is found to be $n+q+1$ [Margaria et al., 2001]. In this instance, the full number of coefficients defined by the upper bound must be evaluated in order to guarantee that further computation does not elicit a reduced result and hence prove a model unidentifiable.

Consequently, particularly in nonlinear cases, the Taylor series method is more practically appropriate for proving models that are globally identifiable.

In the case of the basic SIR model, where $n = 2$ and $p = (\mu, N, \beta, v, k, S^0, I^0)$, i.e. $q = 7$, a total of 10 Taylor coefficients would need to be evaluated given that the model is shown to be unidentifiable. Implementing this method using a symbolic manipulation package such as MATHEMATICA (version 7.0.0) [Wolfram, 1999] or MAPLE (version 13.0) [Heal et al., 1998], it is found that a maximum of only 3 or 4 coefficients are realistically tractable.

4.2.2 Differential Algebra

The application of differential algebra [Ritt, 1950] techniques to identifiability problems in nonlinear systems has been presented by a number of authors, see the work by Ljung and Glad [1994], Saccomani et al. [2003], Margaria et al. [2004] and Yates et al. [2009]. These methods rely on differential algebraic manipulation to redefine the set of equations that describe a given system into relations that contain only terms corresponding to the system parameters (p), known inputs (u) and outputs (y), and their successive derivatives ($u^{(k)}$, $y^{(k)}$).

The system equations are used as generators for a radical differential ideal, that is a set of all differential polynomials formed by successive addition, multiplication and differentiation of the system polynomial equations:

$$\begin{aligned} \dot{x}(t,p) &- f(x(t,p),p), \\ y(t,p) &- h(x(t,p),p). \end{aligned} \tag{4.4}$$

This ideal is decomposed and ranked according to a set of criteria that aims to eliminate the unknown state variables, $x(t,p)$. The process is performed by means of a computational algorithm (typically Ritt's algorithm [Ritt, 1950] or the Rosen-

feld Gröbner algorithm [Boulier et al., 2009]), in order to generate either a reduced set of differential polynomials (known as a characteristic set), or an input-output map, $g(y, u, p)$, that can be used to determine the identifiability of p.

If it can be shown that the polynomial functions relating to indistinguishable parameterisations, $p, \tilde{p} \in \Omega$, given by:

$$g(y, \ldots, y^{(k)}, u, \ldots, u^{(k)}, p) \; - \; g(y, \ldots, y^{(k)}, u, \ldots, u^{(k)}, \tilde{p}) \; = \; 0, \qquad (4.5)$$

are identically zero, i.e. have linearly independent monomials, then their coefficients can be equated and solved in order to find relationships between p and $\tilde{p}$ with respect to the identifiability problem (see Definition 2).

The method is most commonly implemented in either of two software modules: DAISY [Bellu et al., 2007] and DiffAlg [Hubert, 2005], that are run in the algebraic manipulation packages: REDUCE [Hearn, 1995] and MAPLE [Heal et al., 1998], respectively.

4.2.3 Nonlinear State Transformation

State transformation based methods result in the generation of a set of all possible models that conform to the same structural properties determined by the postulated model, and have identical input-output behaviour. Linear methods (see the texts by Godfrey [1983], Godfrey and DiStefano III [1987] and Jacquez [1996]) are based on the use of a similarity transformation (in this case an invertible linear map T) of minimal (i.e. controllable and observable) systems represented in standard vector matrix form:

$$\begin{aligned} \dot{x}(t) &= Ax(t) + Bu(t), \qquad x(0) = x^0, \\ y(t) &= Cx(t). \end{aligned} \qquad (4.6)$$

The transformation, T, therefore relates all equivalent models (i.e. with identical eigenvalues and input/output kinetics), described by $\tilde{A}$, $\tilde{B}$ and $\tilde{C}$, to the original model such that:

$$\begin{aligned} \tilde{A} &= TAT^{-1}, \\ \tilde{B} &= TB, \\ \tilde{C} &= CT^{-1}. \end{aligned} \tag{4.7}$$

The analysis then reduces to utilising constraints imposed by known physical properties of the original postulated model on the elements of A, B and C, and the preceding matrix relationships, to determine the unknown elements of T. If T can be shown to be unique, i.e. the only solution to (4.7) is $T = I_n$, then the system is found to be structurally globally identifiable. If there are a finite (distinct) set of possible T then the system is locally identifiable, and an infinite number of solutions for T implies that the system is unidentifiable.

A common generalisation of this method is the exhaustive modelling approach, whereby the structure or connectivity (characterised by zero and non-zero elements) of the original system is not imposed on the set of equivalent systems. In this instance, the analysis is extended to include all competing model structures within a defined framework and yields results associated with the problem of structural indistinguishability.

The similarity transformation approach has subsequently been extended to nonlinear systems by a number of authors including Vajda et al. [1989] through the use of various forms of nonlinear mapping. The following technique, presented by Evans et al. [2002], utilises the existence of an infinitely differentiable map, $\phi(x)$, that connects the state trajectories corresponding to indistinguishable parameter vectors, $p \sim \tilde{p}$, such that:

$$\phi(x(t, \tilde{p})) = x(t, p). \tag{4.8}$$

The Lie derivative of $h \in C^{\infty}(M(p))$ along the vector field f is the smooth function

given by:

$$L_f h(x) = \frac{\partial h}{\partial x}(x) f(x). \tag{4.9}$$

Let $f^p = f(\cdot, p)$ and, for some $1 \leq l \leq m$, $h_l^p(\cdot) = h_l(\cdot, p)$. For any n smooth functions $u_1(x,p), \ldots, u_n(x,p)$ of the form $h_j(x,p)$, for some j, or $L_{f^p}^r h_l^p(x)$ (where L^r denotes successive Lie derivatives), for some l and r, a function H can be defined by

$$H(x,p) = (u_1(x,p), \ldots, u_n(x,p))^T, \tag{4.10}$$

where for a particular $p \in \Omega$, H_p denotes the vector field $H(\cdot, p)$. The system (4.1) can be shown to satisfy the Observability Rank Criterion (ORC) [Hermann and Krener, 1977] at the initial condition $x^0(p)$ if a function H, of the form (4.10), exists such that the Jacobian matrix of H_p, evaluated at $x^0(p)$, is nonsingular.

Theorem 6. *[Evans et al., 2002] For the system (4.1), suppose that there exists a suitable function H for which the ORC is satisfied at the initial condition for a particular parameter vector $p \in \Omega$, then $\tilde{p} \in \Omega$ is indistinguishable, $\tilde{p} \sim p$, provided a $\tau > 0$, an open neighbourhood $V_{\tilde{p}}$ of $x^0(\tilde{p})$ and a smooth mapping $\phi : V_{\tilde{p}} \to \phi(V_{\tilde{p}})$ exist, such that*

$$H_p(\phi(x)) = H_{\tilde{p}}(x), \tag{4.11}$$

for all $x \in V_{\tilde{p}}$, and

$$\begin{aligned} \phi(x^0(\tilde{p})) &= x^0(p), & (4.12)\\ f(\phi(x(t,\tilde{p})), p) &= \frac{\partial \phi}{\partial x}(x(t,\tilde{p})) f(x(t,\tilde{p}), \tilde{p}), & (4.13)\\ h(\phi(x(t,\tilde{p})), p) &= h(x(t,\tilde{p}), \tilde{p}), & (4.14) \end{aligned}$$

for all $t \in [0, \tau)$ with $x(t,\tilde{p}) \in V_{\tilde{p}}$, where $x(t,\tilde{p})$ is the solution of the system for parameter vector $\tilde{p}$.

Full proof of Theorem 6 can be found in the work by Evans et al. [2002].

For analysis, provided the system is found to meet the observability rank criterion,

a smooth mapping, $\phi(x)$, is generated according to (4.11), such that (4.14) is also satisfied, i.e. the first m smooth functions $u_1(x,p)\dots u_m(x,p)$ are chosen to correspond to the m dimensional output function, $y(t,p)$, and $u_{m+1}(x,p)\dots u_n(x,p)$ are their successive Lie derivatives. In a similar manner to the linear method, the conditions defined by (4.12) and (4.13) are then used to establish the unknown elements of $\phi(x)$ and elicit any relations between indistinguishable parameter vectors. The intention is to show that $\phi(x) = I_n$, whereby the system is found to be structurally globally identifiable.

4.3 Structural Identifiability Analysis of SIR Framework Models

It has previously been shown by Evans et al. [2005] that a general SIR model (2.1)-(2.2) with a prevalence observation of infection is unidentifiable given that the parameters k, N, S^0 and I^0 (hence β/N) are not uniquely determined by the output. This indicates that it is inappropriate to use this model and output structure to estimate the proportion of contacts between infective and susceptible individuals that result in infection, β/N, without additional knowledge of parameter values within the model.

However, this analysis also shows that the individual parameters μ, v and β are uniquely determined by the output and hence globally identifiable. Therefore, the model structure can be used to uniquely determine the basic reproduction number, R_0 (2.5), and hence from (2.23) also the proportion of vaccination coverage required to eradicate the infection and provide herd immunity against future epidemics.

The following section explores the results of a structural identifiability analysis applied to other fundamental SIR framework models that include epidemiological

characteristics associated with suboptimal immunity and birth targeted vaccination. The objective is to find out how processes of reinfection through antigenic diversity and the implementation of simple public health intervention might affect the unique determinability of system characteristics from empirical data.

Methods of Analysis

Although a large number of publications suggest that the differential algebra approach is mathematically rigorous, the exact implementation used in either of the two available software modules is not easily examinable by the user. Therefore the analysis in this work is worked and presented using the nonlinear state transformation approach. This allows for more detailed examination of working, and more manual manipulation of the computing process to aid in the inference of results for otherwise intractable problems. The method is also more intuitively extended to the general problem of structural indistinguishability.

The state transformation method is implemented in MATHEMATICA version 7.0.0; for completeness, all results are also compared to those obtained from DAISY version 1.5 (using REDUCE version 3.8) and the DiffAlg differential algebra package within MAPLE version 13. All analyses are computed on a standard desktop machine with a Pentium D CPU 3.4GHz and 1Gb of RAM.

4.3.1 SIR With Birth Targeted Vaccination

The first model structure to be analysed is that of a general SIR with simple birth targeted vaccination, as shown in Figure 2.6. The model is reduced to a two state problem given that $R(t) = N - S(t) - I(t)$, and expressed in the general form shown in (4.1):

$$\begin{aligned} f(x(t,p),p) &= \begin{pmatrix} \mu N(1-P_v)-\beta S(t,p)I(t,p)/N-\mu S(t,p) \\ \beta S(t,p)I(t,p)/N-(\mu+v)I(t,p) \end{pmatrix}, \\ h(x(t,p),p) &= kI(t,p), \\ x^0(p) &= \begin{pmatrix} S^0 & I^0 \end{pmatrix}^T, \end{aligned} \tag{4.15}$$

where $x(t,p) = (S(t,p), I(t,p))^T$; the output structure, $kI(t,p)$, corresponds to a prevalence type observation (with unknown gain k) of the infection; S^0 and I^0 are the respective initial conditions for the susceptible and infective states; and $p = (\mu, N, P_v, \beta, v, k, S^0, I^0)^T$ is a vector of the unknown model parameters (assumed to be indistinguishable from $\tilde{p} = (\tilde{\mu}, \tilde{N}, \tilde{P_v}, \tilde{\beta}, \tilde{v}, \tilde{k}, \tilde{S^0}, \tilde{I^0})^T$).

The first step of the analysis is to ensure that the system is observable, in accordance with the observability rank criterion detailed by Hermann and Krener [1977], at $x^0(p)$. Let the vector field $H_p(x) = (u_1(x,p),\ u_2(x,p))^T$, where

$$\begin{aligned} u_1(x,p) &= h^p(x) &&= kI, \\ u_2(x,p) &= L_{f^p} u_1^p(x) &&= kI\big[\beta S/N - (\mu+v)\big]. \end{aligned} \tag{4.16}$$

It can be seen that the ORC is satisfied given that the Jacobian matrix of $H_p(x)$,

$$\begin{pmatrix} 0 & k \\ k\beta I/N & k\big[\beta S/N - (\mu+v)\big] \end{pmatrix}, \tag{4.17}$$

has full rank for any $p \in \Omega$ and for all $x \in W = \{x \in \mathbb{R}^n : x \neq 0\}$. Given that $x(t,p) \in W$ for all $t \geq 0$ it can be seen from Theorem 6 that if the parameter vectors $p, \tilde{p} \in \Omega$ are indistinguishable $\tilde{p} \sim p$, the open neighbourhood $V_{\tilde{p}}$ of $x^0(\tilde{p})$ exists and the smooth mapping ϕ is a diffeomorphism on $V_{\tilde{p}}$ onto its range [Evans et al., 2005].

The diffeomorphism, $\phi = H_p^{-1} \circ H_{\tilde{p}} = (\phi_1,\ \phi_2)^T$, can then be generated according to (4.11), such that:

$$\phi(x) \ = \ \left(\frac{N(\tilde{N}\big[\mu + v - (\tilde{\mu} + \tilde{v})\big] + \tilde{\beta} S)}{\tilde{N}\beta}, \ \ \frac{\tilde{k} I}{k} \right)^T, \tag{4.18}$$

where $x = (S, I)^T$. Since $u_1(x, p)$ is chosen to correspond to the output function, $h^p(x)$, it can be seen that $\phi(x)$ automatically satisfies (4.14) from Theorem 6 as well as (4.11).

In order to satisfy (4.13) it is necessary that:

$$f(\phi(x(t,\tilde{p})), p) = \begin{pmatrix} \mu N(1-P_v) - \beta\, \phi_1\, \phi_2 / N - \mu\, \phi_1 \\ \phi_2(\beta\, \phi_1 / N - (\mu + v)) \end{pmatrix} =$$

$$\frac{\partial \phi}{\partial x}(x(t,\tilde{p})) f(x(t,\tilde{p}),\tilde{p}) = \begin{pmatrix} (N\tilde{\beta}/\tilde{N}\beta)(\tilde{\mu}\tilde{N}(1-\tilde{P}_v) - \tilde{\beta} S I / \tilde{N} - \tilde{\mu} S) \\ (\tilde{k}/k) I(\tilde{\beta} S / \tilde{N} - (\tilde{\mu} + \tilde{v})) \end{pmatrix}. \tag{4.19}$$

Note: for presentation, certain functions in the right hand side of (4.19) have been abbreviated, for example $\phi_1 = \phi_1(x(t,\tilde{p}))$ and $S = S(t,\tilde{p})$.

Subsequently the second row of (4.19) is also automatically equal and the resulting expression from the first component can be rearranged into the following multivariate polynomial form:

$$q_1 + q_2 S(t,\tilde{p}) + q_3 I(t,\tilde{p}) + q_4 S(t,\tilde{p}) I(t,\tilde{p}) \ = \ 0, \tag{4.20}$$

where

$$q_1 = \frac{N\big[\mu\big(\tilde{\mu} + \tilde{v} - (v + \mu) + \beta(1 - P_v)\big) - \tilde{\beta}\tilde{\mu}(1 - \tilde{P}_v)\big]}{\beta}, \quad q_2 = \frac{N\tilde{\beta}(\tilde{\mu} - \mu)}{\tilde{N}\beta},$$
$$q_3 = \frac{\tilde{k}(\tilde{\mu} + \tilde{v} - (\mu + v))}{k}, \qquad q_4 = \frac{\tilde{\beta}(-\tilde{k}\tilde{N}\beta + kN\tilde{\beta})}{k\tilde{N}^2\beta}. \tag{4.21}$$

In order to obtain general conditions from this expression, it is necessary to ensure that (4.20) is identically zero, i.e. the resulting monomials, $M_i(t)$ for $i = 1, \ldots, r$, are linearly independent. In many cases this stage can prove to be an entirely non-trivial task [Bearup et al., 2010]. However, for this specific example, linear independence can be successfully shown through computation of the Wronski determinant:

$$W_D(M_1(t), \ldots, M_r(t)) \;=\; \left| \begin{pmatrix} M_1(t) & M_2(t) & \ldots & M_r(t) \\ M_1(t)^{(1)} & M_2(t)^{(1)} & \ldots & M_r(t)^{(1)} \\ \vdots & \vdots & \ddots & \vdots \\ M_1(t)^{(r-1)} & M_2(t)^{(r-1)} & \ldots & M_r(t)^{(r-1)} \end{pmatrix} \right|, \quad (4.22)$$

where $M_1(t) = 1, \quad M_2(t) = S(t, \tilde{p}), \quad M_3(t) = I(t, \tilde{p}), \quad M_4(t) = S(t, \tilde{p})I(t, \tilde{p})$, and $M_i(t)^{(j)}$ denotes the j^{th} derivative of $M_i(t)$ with respect to t. If it can be shown that W_D is non-zero for any time point t on some open interval, then the solutions to the multivariate polynomial are linearly independent (see the work of Krusemeyer [1988] and the text by Kreyszig [2006]).

Consequently, the only solution to (4.20) is $q_1 = q_2 = q_3 = q_4 = 0$, whereby each of the four monomial coefficients, $q_i = 0$ for $i = 1, \ldots, 4$ can then be solved along with (4.12) to give all possible conditions for $\tilde{p} \sim p$:

$$\begin{aligned} \big\{ \tilde{\mu} = \mu, \quad \tilde{v} = v, \quad \tilde{\beta}(1 - \tilde{P}_v) = \beta(1 - P_v), \\ \tilde{k}\tilde{S}^0 = kS^0, \quad \tilde{k}\tilde{I}^0 = kI^0, \quad \frac{\tilde{k}\tilde{N}}{\tilde{\beta}} = \frac{kN}{\beta} \big\}. \end{aligned} \quad (4.23)$$

Therefore, in this case, the state transformation is found to be an invertible diagonal linear map of the form:

$$\phi(x) \;=\; \frac{\tilde{k}}{k} \begin{pmatrix} S \\ I \end{pmatrix}, \quad (4.24)$$

which is same as that for the unvaccinated SIR, as shown by Evans et al. [2005].

The results show that the parameters μ and v are still globally identifiable, however, the effective coverage of the applied vaccination, P_v, cannot be uniquely determined from the output. Further to this, the transmission parameter, β, and hence the basic reproduction number, R_0 (2.5), are no longer uniquely identifiable following the implementation of a vaccination campaign where $P_v > 0$. It should also be noted that only direct knowledge of either β, P_v, or k and N will result in a structurally globally identifiable system, whereby all other parameters can be uniquely determined.

4.3.2 SIRS Temporary/Waning Immunity

The SIRS model (2.15)-(2.4), shown in Figure 2.4, is reduced and expressed in the form given by (4.1), in a similar manner to the previous example, where the output structure $y(t,p) = kI(t,p)$, initial conditions are given by S^0 and I^0, and unknown parameter vector $p = (\mu, N, \omega_R, \beta, v, k, S^0, I^0)^T$ (assumed indistinguishable from $\tilde{p} = (\tilde{\mu}, \tilde{N}, \tilde{\omega}_R, \tilde{\beta}, \tilde{v}, \tilde{k}, \tilde{S^0}, \tilde{I^0})^T$). It is found that the first stages of the analysis regarding verification of the ORC and the generation of ϕ are the same as for the SIR and SIR with vaccination models discussed in Section 4.3.1. In this instance, the smooth mapping, ϕ, given by (4.18), can also be seen to automatically satisfy conditions (4.11) and (4.14) of Theorem 6 for the SIRS model. However, in order to satisfy (4.13) it is necessary that:

$$\begin{pmatrix} \mu N - \beta\,\phi_1\,\phi_2/N - \mu\,\phi_1 + \omega_R(N - \phi_1 - \phi_2) \\ \phi_2(\beta\,\phi_1 - (\mu + v)) \end{pmatrix} = \begin{pmatrix} (N\tilde{\beta}/\tilde{N}\beta)(\tilde{\mu}\tilde{N} - \tilde{\beta}SI/\tilde{N} - \tilde{\mu}S + \tilde{\omega}_R(\tilde{N} - S - I)) \\ (\tilde{k}/k)I(\tilde{\beta}S - \tilde{N}(\tilde{\mu} + \tilde{v})) \end{pmatrix}. \tag{4.25}$$

Solving (4.25) along with (4.12) yields the following set of necessary and sufficient conditions for $\tilde{p} \sim p$:

$$\begin{aligned}\big\{\tilde{v} = v, \quad \tilde{\mu} - \tilde{\beta} = \mu - \beta, \quad \tilde{\omega}_R + \tilde{\mu} = \omega_R + \mu, \\ \frac{\tilde{\beta}\tilde{S^0}}{\tilde{N}} + \tilde{\omega}_R = \frac{\beta S^0}{N} + \omega_R, \quad \tilde{k}\tilde{I^0} = kI^0, \quad \frac{\tilde{k}\tilde{N}}{\tilde{\beta}} = \frac{kN}{\beta}\big\}.\end{aligned} \tag{4.26}$$

The smooth mapping function can subsequently be reduced to:

$$\phi(x) \;=\; \left(\frac{N(\tilde{\omega}_R - \omega_R)}{\beta} + \frac{\tilde{k}S}{k}, \quad \frac{\tilde{k}I}{k}\right)^T, \tag{4.27}$$

whereby only the recovery rate coefficient, v, is found to be globally identifiable (except also the combinations $\mu - \beta$, $\omega_R + \beta$ and $\omega_R + \mu$). The consequence of this outcome is that neither parameters associated with R_0 or the duration of immunity can be uniquely determined from the model output. This implies that it is impossible to determine what level of vaccine coverage would be required to eradicate an infection of this type (2.28), or even if such an outcome were even possible (2.27).

Following the addition of birth targeted vaccination, the structural identifiability results are given by:

$$\begin{aligned}\big\{\tilde{v} = v, \quad \tilde{\mu}+\tilde{\omega}_R = \mu+\omega_R, \quad \frac{\tilde{k}\tilde{N}}{\tilde{\beta}} = \frac{kN}{\beta}, \quad \frac{\tilde{\beta}\tilde{S^0}}{\tilde{N}}+\tilde{\omega}_R = \frac{\beta S^0}{N}+\omega_R, \\ \tilde{k}\tilde{I^0} = kI^0, \quad \tilde{\mu}\tilde{\beta}\tilde{P}_v+(\tilde{\mu}-\tilde{\beta})(\tilde{\mu}+\tilde{\omega}_R) = \mu\beta P_v+(\mu-\beta)(\mu+\omega_R)\big\},\end{aligned} \tag{4.28}$$

where the smooth map, $\phi(x)$, remains the same as (4.27). It can subsequently be seen that even with prior knowledge of the parameter combination $(\mu-\beta)$, perhaps from pre-vaccination model fitting, the vaccine efficacy parameter P_v cannot be globally identified from prevalence data. It should be noted that a minimum of three parameters are required to be known in order for the model to be structurally

globally identifiable.

4.3.3 SIR with Partial Immunity

Analysis of the partial immunity model, shown in Figure 2.5, is performed by first expressing the model equations given by (2.19)-(2.4) in the general form for a nonlinear two-state system:

$$\begin{aligned} f(x(t,p),p) &= \begin{pmatrix} \mu N - \beta S(t,p) I(t,p)/N - \mu S(t,p) \\ \Big[\beta\Big(S(t,p)+\sigma\big[N-S(t,p)-I(t,p)\big]\Big)/N-(\mu+v)\Big] I(t,p) \end{pmatrix}, \\ h(x(t,p),p) &= kI(t,p), \\ x^0(p) &= \begin{pmatrix} S^0 & I^0 \end{pmatrix}^T, \end{aligned} \tag{4.29}$$

and then generating the vector field, $H_p(x) = (u_1(x,p),\ u_2(x,p))^T$, through successive Lie derivatives of the output function, $h(x(t,p),p)$, such that:

$$\begin{aligned} u_1(x,p) &= h^p(x) &&= kI, \\ u_2(x,p) &= L_{f^p} u_1^p(x) &&= kI\big[\big(S+\sigma(N-S-I)\big)\beta/N-(\mu+v)\big]. \end{aligned} \tag{4.30}$$

The ORC is satisfied given that the Jacobian matrix of $H_p(x)$, given by:

$$\begin{pmatrix} 0 & k \\ k\beta I(1-\sigma)/N & k((\beta(S(1-\sigma)-2\sigma I)-N(\mu+v-\beta\sigma)))/N \end{pmatrix}, \tag{4.31}$$

has full rank for all $p \in \Omega$ and for all $x \in W = \{x \in \mathbb{R}^n : x \neq 0\}$, provided that $\sigma \in [0,1)$, i.e. $\sigma \neq 1$. It can be noted that the ORC is not met for $\sigma = 1$ because this eventuality corresponds to a reduction of the SIRp model structure into a single state SIS model. Analysis of the SIS incomplete immunity model would therefore require consideration of only a single smooth function $u_1(x,p) = kI$.

Solving (4.11) of Theorem 6 for $\phi = (\phi_1,\ \phi_2)^T$ yields the following smooth map:

$$\phi(x) = \left(\frac{\theta}{k\tilde{N}\beta(\sigma-1)},\quad \frac{\tilde{k}I}{k}\right)^T, \tag{4.32}$$

where

$$\theta = kN\Big(\tilde{N}\big[\tilde{\mu}+\tilde{v}-(\mu+v)+\beta\sigma-\tilde{\beta}\tilde{\sigma}\big]+\tilde{\beta}(\tilde{\sigma}-1)S\Big)+\Big(kN\tilde{\beta}\tilde{\sigma}-\tilde{k}\tilde{N}\beta\sigma\Big)I,$$

which additionally satisfies condition (4.14).

Further satisfying equations (4.13) and (4.12) completes the structural identifiability analysis for an SIR with partial immunity, in which the following relations between p and $\tilde{p}$ are found:

$$\big\{\tilde{\beta}=\beta,\ \ \tilde{\mu}=\mu,\ \ \tilde{v}=v,\ \ \tilde{\sigma}=\sigma,\ \ \tilde{k}\tilde{S^0}=kS^0,\ \ \tilde{k}\tilde{I^0}=kI^0,\ \ \tilde{k}\tilde{N}=kN\big\}. \tag{4.33}$$

Similar to the general SIR result, the smooth mapping $\phi(x)$ can be reduced to (4.24), and the model parameters associated with the basic reproduction number (i.e. β, μ, and v) are found to be globally identifiable. In addition, it can be noted that the reduced susceptibility parameter, σ, is also uniquely determined by the prevalence output structure. These results indicate that the possibility of eradication with 100% vaccination coverage (2.29), and the effective proportion of the population required to be immunised (2.31), are both uniquely determined by the model output.

Upon inclusion of a birth targeted vaccination programme, the identifiability conditions for the model are found to be:

$$\begin{aligned}\big\{\tilde{\mu}=\mu,\quad \tilde{\sigma}=\sigma,\quad \tilde{v}-\tilde{\beta}\tilde{\sigma}=v-\beta\sigma,\quad \tilde{k}\tilde{S^0}=kS^0,\\ \tilde{k}\tilde{I^0}=kI^0,\quad \tilde{\beta}(\tilde{P_v}-1)=\beta(P_v-1),\quad \frac{\tilde{k}\tilde{N}}{\tilde{\beta}}=\frac{kN}{\beta}\big\},\end{aligned} \tag{4.34}$$

where $\phi(x)$ is again reducible to that of (4.24), and the actual proportion of vaccine coverage, P_v, cannot be uniquely determined by the observation. The transmission parameter, β, recovery rate parameter, v, and hence the basic reproduction number, R_0, become unidentifiable once the intervention has been applied. However, it should also be noted that σ and μ both remain globally identifiable, and that if either v, β or kN are known, i.e. from fitting to pre-vaccination data, then R_0 and P_v can be uniquely identified.

4.4 Structural Identifiability Analysis of MSIR Framework Models

The homogeneous time domain MSIR model (3.14)-(3.17), shown in Figure 3.1, is analysed in order to ascertain whether the model structure suggests that neonatal immunity due to maternally acquired antibody has an analytic influence on the observable behaviour of the system, and consequently if the parameter ω_M is globally identifiable.

The model is considered with a prevalence output structure and defined as a three state problem given that a closed, constant size population is assumed:

$$\begin{aligned} f(x(t,p),p) &= \begin{pmatrix} \mu\big[N-M(t,p)-S(t,p)-I(t,p)\big] - \omega_M M(t,p) \\ \mu I(t,p) + \omega_M M(t,p) - \beta S(t,p) I(t,p)/N \\ \beta S(t,p) I(t,p)/N - (\mu+v) I(t,p) \end{pmatrix}, \\ h(x(t,p),p) &= kI(t,p), \\ x^0(p) &= \begin{pmatrix} M^0 & S^0 & I^0 \end{pmatrix}^T, \end{aligned} \tag{4.35}$$

where the state vector, $x(t,p) = (M(t,p), S(t,p), I(t,p))^T$; M^0, S^0 and I^0 are the initial conditions for the maternally protected, susceptible and infective states

respectively; and $p = (\mu, \omega_M, N, \beta, v, k, M^0, S^0, I^0)^T$ is an unknown parameter vector (assumed to be indistinguishable from $\tilde{p} = (\tilde{\mu}, \tilde{\omega}_M, \tilde{N}, \tilde{\beta}, \tilde{v}, \tilde{k}, \tilde{M^0}, \tilde{S^0}, \tilde{I^0})^T$).

The function, $H_p(x) = (u_1(x,p),\ u_2(x,p),\ u_3(x,p))^T$, is found from successive Lie derivatives of the output according to (4.10), and corresponds to the following smooth functions:

$$\begin{aligned} u_1(x,p) &= h^p(x) &&= kI, \\ u_2(x,p) &= L_{f^p} u_1^p(x) &&= kI\Big[\beta S/N - (\mu+v)\Big], \\ u_3(x,p) &= L_{f^p} u_2^p(x) &&= kI\Big[\big(\beta S/N - (\mu+v)\big)^2 + \beta\big(\omega_M M - \beta SI/N + \mu I\big)/N\Big]. \end{aligned} \tag{4.36}$$

The Jacobian matrix of $H_p(x)$ is given by:

$$\begin{pmatrix} 0 & 0 & k \\ 0 & \dfrac{k\beta I}{N} & k\left(\dfrac{\beta S}{N} - (\mu+v)\right) \\ \dfrac{\omega_M k\beta I}{N} & \dfrac{kI\beta\big[\beta(2S-I)/N - 2(v+\mu)\big]}{N} & \dfrac{k\,\theta}{N} \end{pmatrix}, \tag{4.37}$$

where

$$\theta \;=\; \beta^2 S(S-2I)/N + N(v+\mu)^2 + \beta(\omega_M M - 2S(v+\mu) + 2\mu I),$$

which is again found to be non-singular for all $p \in \Omega$ and $x \in W = \{x \in \mathbb{R}^n : x \neq 0\}$, thus satisfying the observability rank criterion.

A smooth mapping, of the form $\phi = (\phi_1,\ \phi_2,\ \phi_3)^T$, is then generated according to Theorem 6 (4.11):

$$\phi(x) = \left(\frac{\theta}{k\omega_M \tilde{N}\beta},\ \frac{N\big(\tilde{N}\big[\mu+v-(\tilde{\mu}+\tilde{v})\big] + \tilde{\beta}S\big)}{\tilde{N}\beta},\ \frac{\tilde{k}I}{k}\right)^T, \tag{4.38}$$

where

$$\theta \;=\; k\tilde{\omega}_M N\tilde{\beta}M + \Big(\tilde{k}\tilde{N}\beta(v-\tilde{v}-\mu) + kN\tilde{\beta}\mu + \tilde{\beta}(\tilde{k}\beta - kN\tilde{\beta}/\tilde{N})S\Big)I,$$

and $x = (M, S, I)^T$, which automatically satisfies both (4.11) and (4.14).

In order to satisfy condition (4.13) it is necessary that:

$$\begin{pmatrix} \mu(N-\phi_1-\phi_2-\phi_3) - \omega_M\phi_1 \\ \omega_M\phi_1 + (\mu - \beta\phi_2/N)\phi_3 \\ \phi_3[\beta\phi_2/N - (v+\mu)] \end{pmatrix} = \begin{pmatrix} [\tilde{\mu}(\tilde{N}-M-S-I) - \tilde{\omega}_M M]\,\theta \\ (\tilde{\beta}N/\beta\tilde{N})(\tilde{\mu}I + \tilde{\omega}_M M - \tilde{\beta}SI/\tilde{N}) \\ (\tilde{k}/k)I[\tilde{\beta}S/\tilde{N} - (\tilde{v}+\tilde{\mu})] \end{pmatrix}, \quad (4.39)$$

where

$$\theta \;=\; \frac{\tilde{k}\beta\big[(S+I)\tilde{\beta} + \tilde{N}(v-\tilde{v}-\tilde{\mu})\big] + kN\tilde{\beta}\big(\tilde{\omega}_M - \big[(S+I)\tilde{\beta}\big]/\tilde{N} + \tilde{\mu}\big)}{k\omega_M\tilde{N}\beta}.$$

It can subsequently be seen, from substitution of (4.38) into (4.39), that the second and third rows are automatically equal. The resulting expression from the first component of (4.39) can then be rearranged into the form:

$$\begin{aligned} q_1 + q_2 M(t,\tilde{p}) + q_3 S(t,\tilde{p}) + q_4 I(t,\tilde{p}) + q_5 M(t,\tilde{p})S(t,\tilde{p}) + \\ q_6 M(t,\tilde{p})I(t,\tilde{p}) + q_7 S(t,\tilde{p})I(t,\tilde{p}) + q_8 S(t,\tilde{p})^2 + q_9 I(t,\tilde{p})^2 = 0, \end{aligned} \quad (4.40)$$

Linear independence of this expression is shown by considering the following factorisation of a general second order multivariate polynomial:

$$\begin{aligned} \Big(z_1 + z_2 M(t,\tilde{p}) + z_3 S(t,\tilde{p}) + z_4 I(t,\tilde{p})\Big) \\ \Big(z_5 + z_6 M(t,\tilde{p}) + z_7 S(t,\tilde{p}) + z_8 I(t,\tilde{p})\Big) = 0. \end{aligned} \quad (4.41)$$

where computing the Wronski determinant of either factors in (4.41) shows that $z_i = 0$ for either $i = 1, \ldots, 4$ or $i = 5, \ldots, 8$, for all t. Therefore, through expanding (4.41) and comparing equated coefficients from (4.40), the only solution to (4.40) is $q_i = 0$ for $i = 1, \ldots, 9$. These coefficients can then be solved along with (4.12) to give all possible conditions for $\tilde{p} \sim p$:

$$\Big\{\tilde{\omega}_M = \omega_M,\ \ \tilde{\mu} = \mu,\ \ \tilde{\beta} = \beta,\ \ \tilde{v} = v,$$
$$\tilde{k}\tilde{N} = kN,\ \ \tilde{k}\tilde{M}^0 = kM^0,\ \ \tilde{k}\tilde{S}^0 = kS^0,\ \ \tilde{k}\tilde{I}^0 = kI^0\Big\},$$

or

$$\Big\{\tilde{\omega}_M = \mu,\ \ \tilde{\mu} = \omega_M,\ \ \tilde{v} = v,\ \ \tilde{\beta}+\tilde{\omega}_M = \beta+\omega_M,\ \ \frac{\tilde{k}\tilde{N}}{\tilde{\beta}} = \frac{kN}{\beta},$$
$$\tilde{k}\tilde{M}^0\tilde{\omega}_M = kM^0\omega_M,\ \ \tilde{S}^0\frac{\tilde{\beta}}{\tilde{N}}+\tilde{\omega}_M = S^0\frac{\beta}{N}+\omega_M,\ \ \tilde{k}\tilde{I}^0 = kI^0\Big\}. \tag{4.42}$$

It can be seen from the analysis that the system is unidentifiable, i.e. there are an infinite number of combinations for values for k and N that give rise to the same observable system behaviour. However, if either k or N are known then the system becomes locally identifiable given that only two possible parameterisations exist. In addition, it can be noted that provided the parameters ω_M and μ are in practice clearly distinguishable from their magnitude (i.e. duration of immunity from MAb is significantly less than average life expectancy), or any of the unidentifiable parameters are known (in addition to k or N), the model becomes structurally globally identifiable. In this instance the duration of MAb protection has at least an analytically unique influence on the output of the system.

4.4.1 MSIR Models with Incomplete Immunity & Vaccination

Extending the analysis to further variations of the MSIR model yields a series of results indicating how the addition of secondary infection and basic public health intervention might impact identifiability issues within the model framework.

MSIRS with Temporary/Waning Immunity

An MSIRS model structure with temporary/waning immunity can be derived from the full incomplete immunity system by setting $\sigma = 1$, $\gamma = 1$ and $v_1 = v_2 = v$ in equations (3.20)-(3.26), where for simplification secondary infection characteristics are considered to be identical to that of primary infection. Susceptible and infective states can then be combined such that $S(t) = S_1(t) + S_2(t)$ and $I(t) = I_1(t) + I_2(t)$, giving rise to a model structure analogous to that of the SIRS analysed in Section 4.3.2.

The analysis is performed in order to establish whether the temporary immunity parameter, ω_R, is uniquely determinable from a typical prevalence output structure, and to establish if the process of repeat infection through antigenic evolution has an impact on the identifiability of other characteristic parameters within the model. The procedure follows the same methodology as previous examples and yields the following set of conditions for indistinguishable parameterisations $\tilde{p} \sim p$:

$$\Big\{\tilde{\omega}_M = \omega_M,\ \ \tilde{\mu} = \mu,\ \ \tilde{\beta} = \beta,\ \ \tilde{v} = v,\ \ \tilde{\omega}_R = \omega_R,$$
$$\tilde{k}\tilde{N} = kN,\ \ \tilde{k}\tilde{M}^0 = kM^0,\ \ \tilde{k}\tilde{S}^0 = kS^0,\ \ \tilde{k}\tilde{I}^0 = kI^0\Big\},$$

or

$$\Big\{\tilde{\omega}_M = \mu+\omega_R,\quad \tilde{\mu} = \omega_M-\omega_R,\quad \tilde{v} = v,\quad \tilde{\omega}_R = \omega_R,\quad \tilde{\beta}+\tilde{\omega}_M = \beta+\omega_M,$$
$$\frac{\tilde{k}\tilde{N}}{\tilde{\beta}} = \frac{kN}{\beta},\ \ \frac{\tilde{k}\tilde{M}^0}{\tilde{\mu}} = \frac{kM^0}{\mu},\ \ \tilde{S}^0\frac{\tilde{\beta}}{\tilde{N}}+\tilde{\omega}_M = S^0\frac{\beta}{N}+\omega_M,\ \ \tilde{k}\tilde{I}^0 = kI^0\Big\}. \tag{4.43}$$

These conditions reveal that the model is unidentifiable, however, similarily to the MSIR (4.42), two distinct sets of solutions exist. Interestingly, unlike for the SIRS results (4.26), the addition of a maternally protected state variable forces the temporary immunity parameter, ω_R, to become globally identifiable. If either

of the parameters μ, β or ω_M are known, then the two solutions become equal and the basic reproduction number, R_0, is then uniquely determined by the output.

MSIR with Maternal & Birth Targeted Immunisation

The implications of both maternal and childhood (birth targeted) vaccine intervention are examined through analysis of the interacting immunisation model presented in Section 3.3.3. The system equations are reduced by neglecting secondary infection, i.e. considering only (3.33)-(3.35), and presented as a three state problem assuming a constant population size:

$$\begin{aligned} f(x(t,p),p) &= \begin{pmatrix} \mu\big[1-(1-\vartheta)P_v\big]\big[Ab^+(t,p)+P_m Ab^-(t,p)\big] - \omega_M M(t,p) \\ \mu(1-P_m)(1-P_v)Ab^-(t,p) + \omega_M M(t,p) \\ \qquad\qquad - \beta S(t,p)I(t,p)/N - \big[\mu(1+P_m)\big]S(t,p) \\ \beta S(t,p)I(t,p)/N - \big[v+\mu(1+P_m)\big]I(t,p) \end{pmatrix}, \\ h(x(t,p),p) &= kI(t,p), \\ x^0(p) &= \begin{pmatrix} M^0 & S^0 & I^0 \end{pmatrix}^T. \end{aligned} \tag{4.44}$$

Inflows $Ab^+(t,p) = N - M(t,p) - S(t,p) - I(t,p)$ and $Ab^-(t,p) = S(t,p) + I(t,p)$, describe the birth rates of seropositive and seronegative newborns respectively. Varying combinations of the two interventions and their potential interaction are evoked through choice of the parameters P_m, P_v and ϑ.

For a birth targeted only intervention, with a vaccine that does not induce an active immune response in the presence of protective MAb, $P_m = 0$ and $\vartheta = 1$. In this instance a full identifiability analysis yields the following set of conditions:

$$\Big\{\tilde{\omega}_M = \omega_M,\ \ \tilde{\mu} = \mu,\ \ \tilde{\beta} = \beta,\ \ \tilde{v} = v,\ \ \tilde{P}_v = P_v,$$
$$\tilde{k}\tilde{N} = kN,\ \ \tilde{k}\tilde{M}^0 = kM^0,\ \ \tilde{k}\tilde{S}^0 = kS^0,\ \ \tilde{k}\tilde{I}^0 = kI^0\Big\},$$

or

$$\Big\{\tilde{\omega}_M = \mu,\ \ \tilde{\mu} = \omega_M,\quad \tilde{v} = v,\quad \tilde{\mu}\tilde{P}_v = \mu P_v,\quad \frac{\tilde{k}\tilde{N}}{\tilde{\beta}} = \frac{kN}{\beta},$$
$$\tilde{\beta}+\tilde{\omega}_M(1+\tilde{P}_v) = \beta+\omega_M(1+P_v),\quad \tilde{S}^0\frac{\tilde{\beta}}{\tilde{N}}+\tilde{\omega}_M = S^0\frac{\beta}{N}+\omega_M,$$
$$\tilde{k}\tilde{\omega}_M\Big(\tilde{M}^0 + \frac{\tilde{\mu}\tilde{N}\tilde{P}_v}{\tilde{\beta}}\Big) = k\omega_M\Big(M^0 + \frac{\mu N P_v}{\beta}\Big),\quad \tilde{k}\tilde{I}^0 = kI^0\Big\}. \tag{4.45}$$

Unlike the SIR model (see conditions in (4.23)), the implementation of birth targeted vaccination to the MSIR system with maternally acquired immunity does not have a further detrimental effect on structural identifiability. Additional knowledge of only μ, ω_M or β, is required for P_v to become uniquely determined by the output. In addition, if either k or N are also known, then the model becomes structurally globally identifiable.

Similar sets of conditions are found for the non-interacting vaccine system, where $P_m = 0$ and $\vartheta = 0$, and for the maternal immunisation only system, where $P_v = 0$. The first local solutions are equivalent to that of the interacting system shown in (4.45) and marginally more complex parameter combinations for β and M^0 exist in the second solution. However, the conditions for unique determination of all individual parameters and for global identifiability of the model are found to be the same.

4.4.2 Age Domain Model Analysis

As discussed in Section 2.4, population-level epidemiological measures of infectious disease can, in principle, be recorded with respect to both time and age. A struc-

tural identifiability analysis of age domain model variants is therefore required to establish whether key parameters within the model are uniquely determined by corresponding age dependent outputs, or if a combination of both age and time domain observations might improve system identifiability.

An age domain variant of the fundamental (homogeneous) MSIR model structure (3.14)-(3.17) can be derived according to Section 3.3.4, see equations (3.45)-(3.45). The system is considered to be at a constant endemic steady state with respect to time, and is expressed in the following standard form:

$$\begin{aligned} f(x(a,p),p) &= \begin{pmatrix} -\omega_M M(a,p) \\ \omega_M M(a,p) - (\lambda+\mu)S(a,p) \\ \lambda S(a,p) - (v+\mu)I(a,p) \end{pmatrix}, \\ h(x(a,p),p) &= kI(a,p), \\ x^0(p) &= \begin{pmatrix} \mu\, A\hat{b}^+ & \mu\, A\hat{b}^- & 0 \end{pmatrix}^T. \end{aligned} \tag{4.46}$$

The force of infection is therefore given by, $\lambda = \beta\hat{I}/N$, where $\hat{I}$ is the endemic steady state level of infection (3.54). The recovered/immune state variable, $R(a,p)$, is omitted from the set of system equations given that it does not influence any previous states in the natural history of infection and is hence not observable from a prevalence or incidence output. It should also be noted that if an observation of incidence is considered, then the model is further reduced to only the maternally protected and susceptible state variables, $M(a,p)$ and $S(a,p)$. In this instance, the infective state variable, $I(a,p)$, is also no longer observable via the output structure, since homogeneous transmission does not permit age dependency within the force of infection, i.e. $\hat{I} = \int_0^\infty \hat{I}(a,p)\, da$ is a constant. In addition, the recovery parameter, v, cannot be estimated unless algebraic expressions for the force of infection and endemic steady states are substituted into the model.

Provided that constant (annual average) values are taken for λ, i.e. the infective

population is not included within the force of infection as an age dependent state variable, the model (4.46) is found to be linear. In this instance, a state transformation based structural identifiability analysis may be implemented, where $\phi(x)$ is an invertible linear map of the form:

$$\phi(x) \;=\; \begin{pmatrix} t_{11} & t_{12} & t_{13} \\ t_{21} & t_{22} & t_{23} \\ t_{31} & t_{32} & t_{33} \end{pmatrix} \begin{pmatrix} M \\ S \\ I \end{pmatrix}. \tag{4.47}$$

Using condition (4.14) of Theorem 6:

$$\begin{aligned} h(\phi(x(a,\tilde{p})),p) \;&=\; k\Big(t_{31}M(a,p) + t_{32}S(a,p) + t_{33}I(a,p)\Big) \\ &=\; h(x(a,\tilde{p}),\tilde{p}) \;=\; \tilde{k}I(a,p), \end{aligned} \tag{4.48}$$

from which it is seen that $t_{31} = 0$, $t_{32} = 0$ (given that all parameters, specifically k and $\tilde{k}$, must be positive), and $t_{33} = \tilde{k}/k$.

Further satisfying (4.12) and (4.13) yields:

$$\phi(x) \;=\; \left(\frac{\tilde{k}\,\tilde{\omega}_M\,\tilde{\lambda}\,M}{k\,\omega_M} + t_{12}S + t_{13}I, \quad \frac{\tilde{k}\big(\big[v{+}\mu{-}(\tilde{v}{+}\tilde{\mu})\big]I{+}\tilde{\lambda}S\big)}{k\lambda}, \quad \frac{\tilde{k}I}{k}\right)^T, \tag{4.49}$$

where

$$t_{12} \;=\; 0, \quad \frac{\tilde{k}\big(\tilde{\omega}_M - (\tilde{v}{+}\tilde{\mu})\big)}{k\lambda(\tilde{v}{+}\tilde{\mu})}, \qquad \text{and} \qquad t_{13} \;=\; 0, \quad \frac{\tilde{k}(\tilde{v}{-}\tilde{\lambda})(v{+}\mu{-}\tilde{\omega}_M)}{k\lambda(\tilde{v}{+}\tilde{\mu})}. \tag{4.50}$$

The mapping gives rise to six local sets of solutions for $\tilde{p} \sim p$, comprising of various combinations of ω_M, μ, λ and v. It is subsequently found that all model parameters are unidentifiable, and a minimum of at least three out of the four inter-compartmental flow coefficients and either k or N are required to be known for the system to be structurally globally identifiable.

Substituting steady state expressions for $A\hat{b}^{+} = \hat{R}$, $A\hat{b}^{-} = \hat{S} + \hat{I}$ and $\hat{\lambda} = \beta\hat{I}/N$ from (3.54) is seen to further impede the identifiability of p (including the transmission parameter β) for an age domain prevalence output structure. However, if the resulting conditions for $\tilde{p} \sim p$ from analysis of an age domain MSIR are combined with those of the time domain equivalent model (4.42), the following conditions are obtained:

$$\Big\{\tilde{\omega}_M = \omega_M,\ \ \tilde{\mu} = \mu,\ \ \tilde{\beta} = \beta,\ \ \tilde{v} = v, \\ \tilde{k}\tilde{N} = kN,\ \ \tilde{k}\tilde{M}^0 = kM^0,\ \ \tilde{k}\tilde{S}^0 = kS^0,\ \ \tilde{k}\tilde{I}^0 = kI^0\Big\}, \tag{4.51}$$

where only k or N are required for the system to be globally structurally identifiable. Since (4.51) is a subset of (4.42), this suggests that despite the model parameters appearing to be poorly defined by age domain observations of infection prevalence, additional information could be elicited if also combined with equivalent time domain measurements of the same system.

4.5 A Cautionary Note

In all worked examples presented in this chapter, the analysed model structures have been reduced to either a two or three state system through the omission of the 'recovered' state variable, $R(t, p)$. This simplification is possible provided there is a constant population size, N, and was initially performed in an effort to minimise algebraic computation. However, it has since transpired that this model reduction is in fact a necessary step in order to attain full identifiability results for compartmental epidemic models.

Considering the SIRS example described in Section 4.3.2, a complete identifiability

analysis yields the following set of conditions for $\tilde{p} \sim p$:

$$\big\{\tilde{v} = v, \quad \tilde{\mu} - \tilde{\beta} = \mu - \beta, \quad \tilde{\omega}_R + \tilde{\beta} = \omega_R + \beta,$$
$$\frac{\tilde{\beta}\tilde{S}^0}{\tilde{N}} + \tilde{\omega}_R = \frac{\beta S^0}{N} + \omega_R, \quad \tilde{k}\tilde{I}^0 = kI^0, \quad \frac{\tilde{k}\tilde{N}}{\tilde{\beta}} = \frac{kN}{\beta}\big\}.$$

Implementing the analysis using the unreduced system equations:

$$\begin{aligned} f(x(t,p),p) &= \begin{pmatrix} \mu N + \omega_R R(t,p) - \beta S(t,p) I(t,p)/N - \mu S(t,p) \\ \beta S(t,p) I(t,p)/N - (\mu + v) I(t,p) \\ v I(t,p) - (\omega_R + \mu) R(t,p) \end{pmatrix}, \\ h(x(t,p),p) &= kI(t,p), \\ x^0(p) &= \begin{pmatrix} S^0 & I^0 & R^0 \end{pmatrix}^T, \end{aligned} \tag{4.52}$$

where $x(t,p) = (S(t,p), I(t,p), R(t,p))^T$, is a state vector, and S^0, I^0 and R^0 are the initial conditions for the susceptible, infective and recovered states respectively, an alternative (incorrect) result can be found:

$$\big\{\tilde{v} = v, \quad \tilde{\mu} = \mu, \quad \tilde{\beta} = \beta, \quad \tilde{\omega}_R = \omega_R,$$
$$\tilde{k}\tilde{N} = kN, \quad \tilde{k}\tilde{S}^0 = kS^0, \quad \tilde{k}\tilde{I}^0 = kI^0, \quad \tilde{k}\tilde{R}^0 = kR^0\big\}.$$

In this case the parameters μ, β and ω_R are incorrectly claimed to be globally identifiable, where in the full result it can be seen that they are non-uniquely determined within larger parameter combinations.

The discrepancy between the two analyses occurs due to a lack of linear independence in the resulting multivariate polynomials that arise from condition (4.13) of Theorem 6. This can be shown by considering the additional system equation:

$$N = S(t,p) + I(t,p) + R(t,p), \tag{4.53}$$

which is inherently included within the reduced two state model, but remains

undefined in the full three state model. Analysis of the latter model description (4.52) ultimately leads to the evaluation of the following multivariate expression:

$$q_1 + q_2 S(t, \tilde{p}) + q_3 I(t, \tilde{p}) + q_4 R(t, \tilde{p}) \; = \; 0, \tag{4.54}$$

where the monomial coefficients are subsequently solved in order to elicit relations between indistinguishable parameter vectors p and $\tilde{p}$. It is required that the resulting equation (4.54) be identically equal to zero. However, in this instance, it can be seen that $q_1 = q_2 = q_3 = q_4 = 0$ is not a unique solution, since, from equation (4.53), the solution $q_1 = N, \;\; q_2 = q_3 = q_4 = -1$ also satisfies (4.54). Therefore, if all state variables are to be included, the expression given by (4.53) must be stated additionally within the defining set of system equations.

This example emphasises the importance of checking for linear independence during structural identifiability analyses and provides an interesting illustration of how incorrect results may be obtained if this is not satisfactorily fulfilled.

4.6 Indistinguishability in Epidemic Modelling

The significance of indistinguishability analyses in the area of compartmental epidemic modelling is illustrated as a worked example by Evans et al. [2004]. It is shown that from purely prevalence data, it is not possible to structurally distinguish between a simple SIR model with solid lifelong immunity (2.1)-(2.4) and an SIRS model with temporary/waning immunity (2.15)-(2.4). The consequence of this result is that from perfect, noise free and continuous output data it is not possible to determine which postulated model structure best describes the observed behaviour of the real system, and hence make inferences about the underlying

biological processes at work (i.e. whether or not immunity wanes over time since infection). More crucially, depending on which of the two competing model structures are assumed, there are two possible sets for estimated values of the basic reproduction number, R_0, and thereby the proportion of the population required to be successfully vaccinated in order to achieve eradication and herd immunity.

Given that the SIR model can be considered as a submodel of the SIRS model, where the waning immunity parameter, ω_R, equals zero, the results of this analysis can also be extracted from those of an identifiability analysis applied to an SIRS model, as derived in Section 4.3.2. Setting $\omega_R = 0$ in (4.26), hence reducing model $\Sigma(p)$ (4.1) to that of a fundamental SIR model (2.1)-(2.4), yields an equivalent set of algebraic relations between p and $\tilde{p}$ to those found by Evans et al. [2004], corresponding to structurally indistinguishable systems ($\Sigma(p) \sim \tilde{\Sigma}(\tilde{p})$):

$$\Big\{\tilde{v} = v, \quad \tilde{\mu} - \tilde{\beta} = \mu - \beta, \quad \tilde{\omega}_R + \tilde{\mu} = \mu, \\ \frac{\tilde{\beta}\tilde{S}^0}{\tilde{N}} + \tilde{\omega}_R = \frac{\beta S^0}{N}, \quad \tilde{k}\tilde{I}^0 = kI^0, \quad \frac{\tilde{k}\tilde{N}}{\tilde{\beta}} = \frac{kN}{\beta}\Big\}. \tag{4.55}$$

In the case of the MSIR/MSIRS models it can be seen from (4.43) that the waning immunity parameter is globally identifiable, therefore setting either ω_R or $\tilde{\omega}_R$ to zero invalidates both sets of conditions, inferring that the two models are structurally distinguishable. The same result can be deduced for a general SIR and an SIR with partial immunity, where again the former can be considered as a submodel of the latter, and the distinguishing parameter σ is found to be globally identifiable (see the conditions given by (4.33)).

Interestingly, further consideration of the results given by (4.23), indicates that from a prevalence type output, it is not possible to distinguish between a general

SIR and one with birth targeted vaccination, provided:

$$\{\tilde{\mu} = \mu, \quad \tilde{v} = v, \quad \tilde{\beta}(1 - \tilde{P}_v) = \beta, \\ \tilde{k}\tilde{S}^0 = kS^0, \quad \tilde{k}\tilde{I}^0 = kI^0, \quad \frac{\tilde{k}\tilde{N}}{\tilde{\beta}} = \frac{kN}{\beta}\}. \tag{4.56}$$

It should be noted that for competing systems where neither model can be considered as a submodel of the other, for example SIR framework models with either temporary or partial immunity, the constraints (4.11)-(4.14) of Theroem 6 are extended according to Evans et al. [2004].

4.7 Conclusions & Discussion

The key results of this chapter arise from the application of structural identifiability/indistinguishability analyses to fundamental SIR and MSIR framework models, incorporating various processes of sub-optimal immunity and immunisation. It has been found that the actual vaccination coverage, P_v, achieved after employing a birth targeted immunisation campaign on any of the discussed SIR framework models, cannot be uniquely determined from ideal prevalence data. The addition of vaccination also serves to force important parameters associated with the natural basic reproduction number and the re-infection threshold to be unidentifiable. This outcome may prove important given that the proportion of vaccinees that successfully take an administered vaccine and acquire sufficient protection is often very difficult to measure directly, and this work suggests that the discussed vaccination models are not appropriate for estimating this effective coverage. It is also shown, in the case of the SIRS model, that it is not possible to uniquely determine the potential success of even an ideal birth targeted vaccination programme with respect to eradication of the infectious agent.

It should be noted that in both the SIR and SIRp cases, if R_0 (specifically β)

or the combination kN is known, perhaps from fitting the unvaccinated model to pre-vaccination prevalence data, then P_v can be uniquely identified. However, estimates from pre-intervention data are only appropriate if the parameters β, k and N can be confidently considered to have remained constant over the period of time corresponding to pre- and post-vaccination. Confidence in the consistency of these parameters is limited given the variable nature of population sizes and the observation gain (notification bias), and the dependency of infection transmission on changing social and environmental trends. The consequence of this is that assuming the selected model structure remains appropriate for the system, it cannot be uniquely determined whether an applied vaccination programme has failed due to an increase in R_0 or from an inadequate P_v. It is suggested that these results may have direct relevance to the current problem of post-vaccine measles persistence in the UK.

Application of these techniques to both time and age domain MSIR framework models has suggested that parameters are analytically better defined by time series observations than by those recorded with respect to age. However, in all presented time domain examples, the parameter ω_M, corresponding to waning protection from MAb, has been found to be locally identifiable, where two distinct sets of solutions exist. If a physical distinction between estimated values for ω_M and the birth/mortality rate coefficient, μ, can be made, or the conditions can be combined with those relating to an age domain analysis, the results are reduced to a single set of conditions where many important parameters associated with epidemiological characteristics and intervention become globally identifiable.

Although the models considered in this work are very basic, and would not be the primary basis for a national public health intervention, extended models with greater depth of realism and additional complexity are unlikely to reduce the identifiability problem given increasing degrees of freedom and continued limitations on the observation of the system. In all the examples presented, the parameters N and k are found to be unidentifiable, indicating that either the observation gain

or the population size must be known in order to obtain qualitative estimates of infection from fitting to prevalence type data.

All worked examples have been presented using the nonlinear state transformation method detailed in Section 4.2.3, and verified using either the DAISY or DiffAlg implementations of the differential algebra approach (see Section 4.2.2). Performance differences between the two techniques appear to be minimal, hence, there were no examples of models that could be successfully analysed by one technique and not the other. Unfortunately, the inclusion of further model complexity arising from epidemiological characteristics such as altered secondary infections, age dependency, and alternative observations such as incidence and serology, require a computational capacity in excess of that available during this work using either of the two methods. The DAISY software module is potentially more suitable for the casual user looking to obtain quick results, however, the algebraic manipulation package, REDUCE, although freely available, is unfortunately no longer supported by its developers.

Chapter 5

Formal Sensitivity Analysis

The theoretical techniques for structural identifiability and indistinguishability discussed in Chapter 4 have provided analytic results regarding indeterminacy issues in compartmental epidemic modelling. However, these methods do not provide any indication of how well globally identifiable parameters might be determined by a chosen output structure. There is subsequently no guarantee that estimation of these parameter values will be robust in the presence of experimental error. Such aspects of uncertainty and model indeterminacy in the inverse problem are typically addressed by the strongly related concepts of sensitivity, numerical identifiability and experimental design [Banks et al., 2007].

In contrast to structural identifiability techniques, sensitivity based methods are concerned with the quantitative responses of models to the perturbation of inputs and parameters, or some variation in structure, connectivity and submodels [Nestorov, 1999]. In a validation sense these techniques give an indication of confidence in the estimation of a particular model parameter from a given set of experimental input/output data. In analysis, they also provide an insight into the potential influence of specific physical processes over the observable behaviour

of the system. Sensitivity techniques are therefore often used as the basis for methods concerned with model reduction and experimental design [Banks and Cintrón-Arias, 2010].

Parameters that are found to have an insignificant influence on the observable behaviour of the system may be omitted from a postulated model structure in order to reduce excessive computation and aid tractable analysis (for examples see the work by Fink et al. [2007, 2008], Degenring et al. [2004], and Smets et al. [2002]). Conversely, output structures and sampling intervals that prove to be highly sensitive with respect to certain parameters of interest may be prioritised in the design of future experiments, thereby maximising the amount of information gained from fitting to data (see the work by Kappel et al. [2009], and Ogungbenro et al. [2009]).

It is the objective of the work in this chapter to explore the implementation of formal sensitivity methods to compare a number of prospective age and time domain output structures, corresponding to observations of infection and serology, with respect to the MSIR model framework proposed in Chapter 3. The intention is then to establish how well parameters associated with maternally acquired immunity might be determined by various observations of the real system and also to consider the potential influence of these processes on various aspects of system behaviour. The analysis is performed according to the work by Vajda et al. [1985] on models residing at endemic equilibrium. Analytic results are derived for systems without seasonal forcing and numerical results obtained for those that include annual variation with time.

5.1 Methods & Application

In describing the derivation of parametric sensitivities we consider the standard nonlinear system:

$$\Sigma(p) \;=\; \begin{cases} \dot{x}(t,p) &=& f(x(t,p),p), \\ y(t,p) &=& h(x(t,p),p), \\ x(0,p) &=& x^0(p), \end{cases} \tag{5.1}$$

where $x(t,p)$ is an n-dimensional vector of state variables and $y(t,p)$ denotes an m-dimensional output. It should be noted that both $x(t,p)$ and $y(t,p)$ may be defined as functions of either time, t, or age, a.

For a given function of time (or age), $y(t,p)$, which is also a differentiable function of some parameter vector $p = (p_1, p_2, ..., p_q)^T$, the point or local sensitivities indicate the rate of change of $y(t,p)$ with respect to p, evaluated at some nominal point in parameter space, p_0 [Jacquez, 1996]. In this case, the sensitivity functions correspond to partial derivatives of the form:

$$S_i(t,p) \;=\; \frac{\partial y(t,p)}{\partial p_i}, \tag{5.2}$$

which are considered as gradients about p_0 in a q-dimensional parameter space, given as a function of time.

In simple examples it may be possible to evaluate sensitivity derivatives analytically from tractable solutions of the system equations, thus allowing general results to be obtained. However, in most cases, increasing model complexity inhibits the direct calculation of these functions and a numerical approach must be adopted instead. In this instance, parametric sensitivity is estimated from manual manipulation (perturbation) of the individual model parameters and observation of the resulting deviation in the output (see the book by Tomović [1963]). Subsequently,

this approach yields only a local analysis about the point p_0, whereby an initial estimate for a nominal set of parameters values is required prior to evaluation. This may prove problematic in cases where there are high levels of uncertainty in our prior knowledge of the system.

The generalisation of local analyses over wider regions of parameter space has been attempted through a number of statistical techniques using Monte Carlo simulation [Archer et al., 1997; Kleijnen, 1997]. However, numerical based global evaluation of non-monotonic systems remains a challenging task since adjacent sample points in p may only coincidently yield similar behaviour of $y(t, p)$. Computation also becomes increasingly intensive with larger numbers of parameters.

5.1.1 Formal Derivation

The sum of squares deviation of an output function, $y(t, p)$, from some nominal point, $y(t, p_0)$, due to a variation Δp in p, can be expressed in the form:

$$Q(p) \;=\; \sum_{j=1}^{r} [y(t_j, p) - y(t_j, p_0)]^2, \tag{5.3}$$

for the selected time points $\{t_1,\ t_2,\ ...,\ t_r\}$. The function $Q(p)$ is an analytic function of p, which has a Taylor series expansion about the point p_0 given by,

$$Q(p) \approx Q(p_0) + (\Delta p)^T G(p_0) + \frac{1}{2}(\Delta p)^T H(p_0)\Delta p, \tag{5.4}$$

where the variation Δp is sufficiently small such that terms of $O(\|\Delta p\|^3)$ can be considered negligible. Since p_0 is assumed to minimise $Q(p)$, the gradient vector, $G(p_0)$, defined by $[G]_i = \partial Q/\partial p_i$, and the term $Q(p_0)$ are both equal to zero. Therefore, the expression given by (5.4) can be further reduced to:

$$Q(p) \approx \frac{1}{2}(\Delta p)^T H(p_0)\Delta p, \tag{5.5}$$

where $[H]_{ij} = \partial^2 Q/\partial p_i \partial p_j$ is the Hessian matrix of Q (matrix of second derivatives with respect to p). The q by r sensitivity matrix, S, where $2S^TS \approx H$, can then be constructed according to the selected time points $\{t_1, t_2, ..., t_r\}$ in the following manner:

$$S = \begin{pmatrix} \frac{\partial\, y(t_1,p)}{\partial\, p_1} & \cdots & \frac{\partial\, y(t_1,p)}{\partial\, p_q} \\ \vdots & \ddots & \vdots \\ \frac{\partial\, y(t_r,p)}{\partial\, p_1} & \cdots & \frac{\partial\, y(t_r,p)}{\partial\, p_q} \end{pmatrix}. \tag{5.6}$$

hence allowing (5.5) to be rewritten as:

$$Q(p) \approx (\Delta p)^T S^T S \Delta p. \tag{5.7}$$

Alternatively, following the work of Vajda et al. [1985], a normalised parameter vector, α, where $\alpha_i = \ln p_i$ for $i = 1, 2, \ldots, q$, may be defined. The resulting normalised sum of squares deviation of the output function $y(t, \alpha)$, from a nominal point, $y(t, \alpha_0)$, to a change $\Delta\alpha$ in α, can then be expressed by:

$$Q(\alpha) = \sum_{j=1}^{r} \left[\frac{y(t_j,\alpha) - y(t_j,\alpha_0)}{y(t_j,\alpha_0)}\right]^2, \tag{5.8}$$

hence replacing the response equation in (5.8). This results in the generation of a normalised sensitivity matrix of the form:

$$S = \begin{pmatrix} \frac{\partial\, \ln y(t_1,p)}{\partial\, \ln p_1} & \cdots & \frac{\partial\, \ln y(t_1,p)}{\partial\, \ln p_q} \\ \vdots & \ddots & \vdots \\ \frac{\partial\, \ln y(t_r,p)}{\partial\, \ln p_1} & \cdots & \frac{\partial\, \ln y(t_r,p)}{\partial\, \ln p_q} \end{pmatrix}. \tag{5.9}$$

In cases where analytic solutions to (5.1) are not practically obtainable, the partial derivatives of the sensitivity matrix are calculated numerically using either finite

differencing [Chapra and Canale, 2002] or direct differential methods [Rabitz et al., 1983]. The latter of these techniques involves solving an augmented system of equations derived by differentiating $h(x(t,p),p)$ in (5.1) with respect to p and switching the order of differentiation:

$$\frac{dS(t,p)}{dt} = \frac{\partial h(x(t,p),p)}{\partial x} S(t,p) + \frac{\partial h(x(t,p),p)}{\partial p}. \tag{5.10}$$

The state variables, $S_i(t,p)$, corresponding to the sensitivity derivatives given by (5.2), are then found using a suitable ODE integrator such as `ode15s` in MATLAB. The other derivative components in (5.10) can be calculated using automatic differentiation methods based on repeated application of the chain rule. These can be implemented using additional MATLAB modules such as `myAD` [Fink, 2006] or `MAD` [Forth and Ketzscher, 2004].

5.1.2 Numerical Identifiability & Model Reduction

Since sensitivity analyses are largely concerned with assessing the relationships between model output structure and parameter values, there are strong parallels with the problems of structural identifiability discussed in Chapter 4. Given that an observable change in output, $\Delta y(t,p)$, is governed by the sensitivity matrix, S, identifiability can be assessed numerically by considering whether or not the expression $\Delta y(t,p) = S\,\Delta p$ can be solved uniquely for a particular Δp [Batzel et al., 2009].

Definition 7. For a nominal parametrisation $p_0 \in \Omega$, a model, $\Sigma(p)$, is said to be *sensitivity identifiable* if the sensitivity matrix, S, has full rank, or equivalently if and only if the matrix S^TS is non-singular (i.e. $\left|S^TS\right| \neq 0$). If S is shown not to

have full rank then the model is found to be *unidentifiable* at the point p_0 [Batzel et al., 2009].

It should be emphasised that sensitivity identifiability applies only to a single, nominal point in parameter space and is therefore not indicative of global identifiability. The analysis is also not strictly an *a priori* technique since it requires an initial estimation of the model parameters to be made before evaluation.

Additional analysis of the sensitivity matrix can be performed through either QR factorisation with column pivoting, as in the work by Fink et al. [2007], and Banks and Cintrón-Arias [2010], or a principal component analysis (PCA), according to Vajda et al. [1985], Curtis and Sweetenham [1987], and Degenring et al. [2004]. These techniques allow the ranking of varied model parameters with respect to their relative importance, for the purpose of model reduction through subset selection.

A PCA can be implemented by means of an eigenvalue-eigenvector decomposition of the matrix $S^TS = U\Lambda U^T$, where S is typically the normalised sensitivity matrix given by (5.9), such that U denotes the matrix of normalised eigenvectors, u_i, for $i = 1, 2, \ldots, m$, and Λ corresponds to a diagonal matrix of eigenvalues, λ_i. The normalised response function, $Q(\alpha) \approx (\Delta\alpha)^T S^T S \Delta\alpha$, can then be redefined in terms of the principal components $\Psi = U^T\alpha$,

$$Q(\Psi) \;=\; \sum_{i=1}^{m} \lambda_i \left\|\Delta\Psi_i\right\|^2, \tag{5.11}$$

given that $\Delta\Psi_i = u_i^T\Delta\alpha = (u_{i,1}\Delta\alpha_1 + \ldots + u_{i,m}\Delta\alpha_m)$. Consequently, the function Q is most sensitive to changes in α along the principal axis corresponding to the largest eigenvalue and is least sensitive to changes in α along the principal axis corresponding to the smallest eigenvalue.

If λ_i is not small, hence the corresponding principal component is a significant one,

a small value for a particular $\|u_{i,j}\|$ indicates that the corresponding parameter α_i contributes little to the component. It is suggested by Vajda et al. [1985] that any element of u_i with magnitude less than 0.2 can be excluded from consideration. The justification is that they contribute less than 4% to the sum of squares of relative changes in $y(t, \alpha)$ as the parameters vary in the direction of the principal component.

5.2 Static Sensitivity Analysis of Time Domain MSIR Models

The objective of this work is to explore the results of a formal sensitivity analysis applied to a series of fundamental MSIR framework models, as described in Sections 3.3 and 3.4. The outcome of a structural identifiability analysis (see the results from Section 4.4) has shown that the parameter ω_M is at least analytically significant to the output of these systems. However, it does not provide any quantitative indication of the magnitude of this influence.

It is intended that the analyses in this chapter illustrate how the processes of reinfection, age structure and the implementation of simple public health intervention conveyed by these models might affect the sensitivity/determinability of characteristics associated with protective MAb. In the following section a sensitivity analysis is initially performed on time domain MSIR type models residing at endemic equilibrium, without the inclusion of seasonal forcing.

5.2.1 Fundamental MSIR Model

The homogeneous, time domain MSIR model is defined by the differential equations (3.14)-(3.17), and shown as a connectivity diagram in Figure 3.1. Provided that the basic reproduction number, $R_0 > 1$, it is found in Section 3.3.5 that the system has the following stable endemic fixed point equilibrium:

$$\hat{M} = \frac{Nv\mu(\beta-(\mu+v))}{\beta(\mu\omega_M+v(\mu+\omega_M))}, \quad \hat{S} = \frac{N(\mu+v)}{\beta}, \quad \hat{I} = \frac{\omega_M}{v}\hat{M}, \quad \hat{R} = \frac{\omega_M}{\mu}\hat{M}. \tag{5.12}$$

Sensitivity functions corresponding to the various epidemiological observations described in Section 2.4 can then be found algebraically about this equilibrium by taking partial derivatives according to (5.2).

For a time domain prevalence observation, where $y(t,p) = I(t,p)$, the magnitude and normalised sensitivities of the output equilibrium point, $\hat{y}(p) = \hat{I}$, with respect to the MAb parameter ω_M, are found, respectively, to be given by:

$$\frac{\partial\,\hat{y}(p)}{\partial\,\omega_M} = \frac{Nv\mu^2(\beta-(\mu+v))}{\beta(\mu\omega_M+v(\mu+\omega_M))^2}, \qquad \frac{\partial\,\ln\hat{y}(p)}{\partial\,\ln\omega_M} = \frac{\mu v}{\mu\omega_M+v(\mu+\omega_M)}. \tag{5.13}$$

Alternatively, for an incidence observation, where $\hat{y}(p) = \beta\hat{S}\hat{I}/N$, given that $\hat{S}$ is not a function of ω_M, the normalised sensitivity function is identical to that of a prevalence output and the absolute (non-normalised) sensitivity function is simply scaled by a factor of $\beta\hat{S}/N = \mu + v$.

Finally, if the output structure corresponds to a serological type observation, where $\hat{y}(p) = N - \hat{S} - \hat{I}$, since again $\hat{S}$ is not a function of ω_M, the non-normalised sensitivity function is the same as for $\hat{y}(p) = -\hat{I}$ (prevalence). The normalised sensitivity function is then found to be of the form:

$$\frac{\partial\,\ln\hat{y}(p)}{\partial\,\ln\omega_M} = \frac{-\mu^2\omega_M}{(\mu+\omega_M)(\mu v+\omega_M(\mu+v))}. \tag{5.14}$$

If, as in many SIR type infections, $v >> \mu$ (i.e. duration of infection is considerably less than average life expectancy), then the following parameter combination, which is a scaling between the magnitude of the normalised prevalence and serological sensitivity functions, adheres to the inequality:

$$\frac{\mu\omega_M}{v(\mu+\omega_M)} < 1. \tag{5.15}$$

Therefore, the magnitude of the normalised sensitivity values for prevalence and incidence observations will be greater than that of a serological type observation by a factor approximately equal to v/μ.

It can also be seen that the normalised sensitivity functions for all three observation types are only dependent on the parameters μ, v and ω_M; hence they are independent of the population size, N, and, more interestingly, the transmission parameter, β. Furthermore, if $v >> \mu$, it is shown, by dividing the second expression in (5.13) through by v, that the normalised sensitivity functions for incidence and prevalence type outputs have only a negligible dependence on the rate of recovery.

Substituting typical values of $v = 73\,\mathrm{yr}^{-1}$ (average duration of 5 days) and $\mu = 0.010$, 0.014 and $0.028\,\mathrm{yr}^{-1}$ (life expectancy of 100, 71 and 36 years respectively) from the set of nominal parameter values for measles (see Table 3.1), the normalised sensitivity function for an incidence or prevalence type observation can be plotted against varying ω_M (see Figure 5.1). Near identical relations are also found for the more complicated case where neonatal mortality is included in the model (see the proportional input structure described by (3.18)).

Subsequently, it can be seen that higher birth/mortality rates (i.e. lower life expectancy) and a higher duration of maternal immunity (i.e. lower ω_M) give rise to a heightened sensitivity to ω_M. This is because the influence of maternally

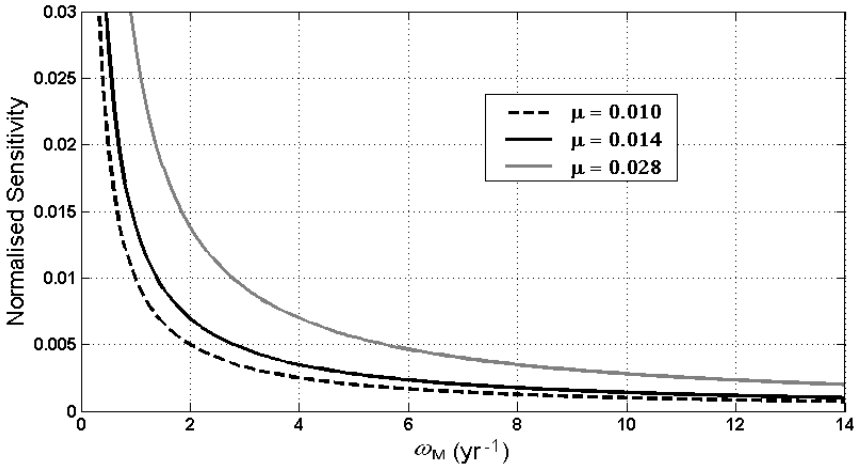

Figure 5.1: Static normalised sensitivity functions corresponding to an incidence or prevalence type observation of a fundamental MSIR system at endemic equilibrium; computed for varying ω_M and discrete values of μ.

Table 5.1: Normalised sensitivity values for all MSIR model parameters evaluated at nominal values corresponding to pre-vaccine measles in the UK.

Parameter	μ	N	β	v	ω_M
Prevalence	0.9963	1.0000	0.0588	-1.0586	0.0035
Incidence	0.9965	1.0000	0.0588	-0.0588	0.0035
Serological	-0.0020	1.0000	0.0588	-0.0586	-6.7×10^{-7}

acquired immunity on overall infection levels occurs due to a reduction in the susceptible proportion of the population. The influence is therefore dependent on the density age profile of the population as a whole, which is governed in the heterogeneous case by an age dependent mortality function.

For completeness, Table 5.1 contains the normalised sensitivities with respect to all system parameters in the MSIR model structure, corresponding to each of the three considered outputs. The values are calculated similarly to those presented for ω_M, i.e. in the second part of (5.13) and (5.14), and are evaluated at the nominal values for pre-vaccine measles in the UK given in Table 3.1.

It can be seen that ω_M is clearly the least sensitive parameter in the model for all three observation types. In addition, it also appears that the model as a whole

is least well determined by a serological-type output structure, with respect to parameter sensitivity.

5.2.2 MSIR Models with Incomplete Immunity

Epidemic systems that include processes of reinfection through antigenic variability have the potential to support considerably higher levels of endemic infection, and consequently a significantly lower average age at primary challenge. The steady state analysis is therefore applied to MSIR framework models with various forms of incomplete immunity, in order to explore how these processes might impact output sensitivity with respect to characteristics associated with MAb.

MSIRS with Temporary/Waning Immunity

A basic MSIRS model structure with temporary/waning immunity can be derived from the full incomplete immunity system described in Section 3.3.1. This is achieved by setting altered secondary infection parameters, $\sigma = 1$, $\gamma = 1$ and $v_1 = v_2 = v$ in equations (3.20)-(3.26), and then combining primary/secondary state variables such that $S(t) = S_1(t) + S_2(t)$ and $I(t) = I_1(t) + I_2(t)$.

Steady state solutions to the this system at endemic equilibrium, are given by (3.62), where an observation corresponding to the prevalence of infection is subsequently found to be of the form:

$$\hat{y}(p) \;=\; \frac{\omega_M N\big(\omega_R + \mu\big)\big(\beta - (\mu{+}v)\big)}{\beta\big(\omega_M(\mu{+}\omega_R) + v(\mu{+}\omega_M)\big)}. \tag{5.16}$$

The solution for an incidence output may also be deduced by simply multiplying (5.16) by a factor of $(\mu + v)$. In this instance, the normalised sensitivities for inci-

dence and prevalence output structures, derived with respect to ω_M using equation (5.6), are both found to be given by,

$$\frac{\partial \ln \hat{y}(p)}{\partial \ln \omega_M} = \frac{\mu v}{\omega_M(\mu+\omega_R) + v(\mu+\omega_M)}. \tag{5.17}$$

Similarly to the fundamental MSIR model, it can be seen that the function is only dependent on the parameters μ, v, ω_M and ω_R, and hence not on either the population size, N, or the transmission parameter, β. Comparing these expressions with those of the MSIR (complete lifelong immunity i.e. $\omega_R = 0$) in equation (5.13), it can be seen that provided $\omega_R > 0$, the normalised sensitivity of $\hat{y}(p)$ with respect to ω_M is always lower for the SIRS system.

Nominal values of $v = 73\,\mathrm{yr}^{-1}$ (average duration of 5 days), $\mu = 0.014\,\mathrm{yr}^{-1}$ (life expectancy of 71 years) and $\omega_M = 2$, 4 and $12\,\mathrm{yr}^{-1}$ (protective duration of 6, 3 and 1 months respectively), are substituted for comparison with Section 5.2.1, where the normalised sensitivity functions for an incidence or prevalence observation of an MSIRS can be plotted against ω_R (see Figure 5.2).

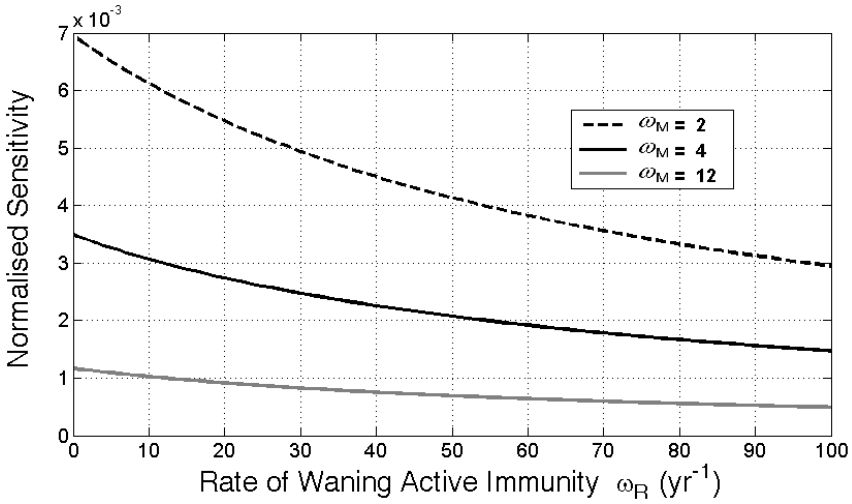

Figure 5.2: Normalised sensitivity functions for an incidence or prevalence observation of a MSIRS system with waning/temporary immunity; computed at endemic equilibrium, for varying ω_R and discrete values of ω_M.

Alternatively the model may be parametrised with nominal values corresponding

to hRSV (Tables 3.2 and 3.3(C)), an infectious disease more commonly observed to display secondary infection in hosts. However, it has already been noted that the normalised sensitivity function (5.17) is not dependent on transmission, β, and has only a negligible dependence on v. Therefore, if the infection is considered within the UK (i.e. maintaining population parameters μ and N), the relations shown in Figure 5.2 are found to be the same for both nominal parametrisations.

MSIRS2 with Incomplete Immunity & Secondary Infection

An immediate limitation of the simple MSIRS model is the amalgamated representation of both primary and secondary (repeat) infection as a single state variable. In order to distinguish the sensitivity of ω_M with respect to primary and secondary cases, the full MSIRS2 incomplete immunity model (3.20)-(3.26) described in Section 3.3.1 is analysed accordingly.

Nominal values are substituted for hRSV (Table 3.2), where demographic parameters such as birth/mortality rates, $\mu = 0.014\ \text{yr}^{-1}$, and population size, $N = 5.7 \times 10^7$, remain the same as in previous examples for infection in the UK. Disease specific parameters such as the rate of recovery from primary and secondary infection, $v_1 = 40.56\ \text{yr}^{-1}$ and $v_2 = 107.35\ \text{yr}^{-1}$ respectively (average durations of 9 and 3.4 days), loss of protection from MAb, $\omega_M = 2\text{yr}^{-1}$ (protective duration of 6 months), and the force of infection $\hat{\lambda} = 0.84$ (average age at primary infection of around 14.2 months) are fixed throughout the analysis.

Additional model parameters that do not appear to be as well defined in the literature, such as ω_R (loss of active immunity), σ (partial immunity factor) and γ (reduced infectivity factor) are varied across their valid ranges. In this instance, ω_R is varied between 0 and $\infty\,\text{yr}^{-1}$, and the proportions σ and γ are varied within the interval, $[0, 1]$, where it should be noted that the extreme values of 0 and 1 effectively alter the structure of the model. The unknown transmission parameter,

β, is continuously adjusted in order to maintain a constant force of infection, $\hat{\lambda} = 0.84$. Subsequently, changes in the three varied parameters (ω_R, σ and γ) generate a shift in the dominance of primary and secondary cases with respect to overall population infectivity.

The resulting normalised sensitivity functions corresponding to changes in ω_M are illustrated in Figures 5.3 and 5.4, for fixed values of $\gamma = 0.6$ (proportional infectivity of secondary cases) and $\omega_R = 0.67\,\mathrm{yr}^{-1}$ (average duration of active immunity of 18 months) respectively.

If the secondary infectivity parameter, γ, is fixed, then the normalised sensitivities for ω_M can be calculated with respect to varying ω_R (rate that actively protected individuals lose immunity and become partially susceptible) for a range of $\sigma \in [0, 1]$ (proportional degree of partial susceptibility).

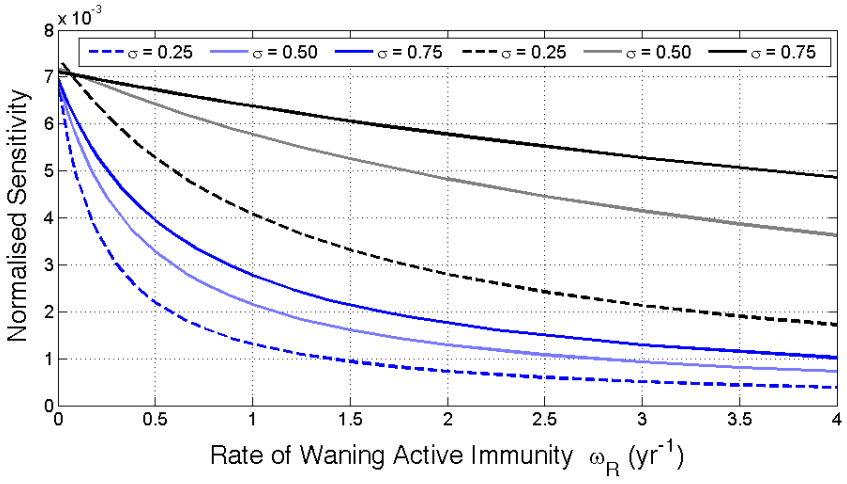

Figure 5.3: MSIRS2 model endemic equilibrium normalised sensitivity functions for ω_M corresponding to primary (blue) and secondary (black) prevalence/incidence of infection. Computed with nominal values for hRSV and $\omega_M = 2\,\mathrm{yr}^{-1}$, for varying ω_R and contrasting values of σ.

These relations are shown in Figure 5.3, where it can be seen that the processes of temporary/waning and partial immunity have contrasting effects on the normalised sensitivity of ω_M. An increase in ω_R (i.e. shortening the duration of

active immunity) causes a significant reduction in the sensitivity of both primary and secondary infection, see also the SIRS model results in Figure 5.2. However, an increase in σ (i.e. a decrease in partial protection afforded by experience of infection) gives rise to an increase in sensitivity of ω_M. This is likely to occur due to the corresponding effects of these processes on transferable MAb in the wider population. An increase in ω_R has the direct effect of reducing the average period of time that potentially child bearing individuals experience protective levels of antibody. Conversely, an increase in σ acts to increase the rate of reinfection, which subsequently leads to greater levels of population immunity.

Alternatively, for fixed $\omega_R = 0.67\ \mathrm{yr}^{-1}$ (average duration of active immunity of 18 months), the sensitivity relations corresponding to varying $\sigma \in [0, 1]$ and $\gamma \in [0, 1]$, are evaluated and shown in Figure 5.4. It can be seen from the results that the normalised sensitivity of ω_M is a monotonically increasing function with respect to both σ and γ. However, for observations of primary infection, the change in sensitivity due to varying γ is extremely small (note that all plot lines corresponding to primary infection are overlaid in Figure 5.4).

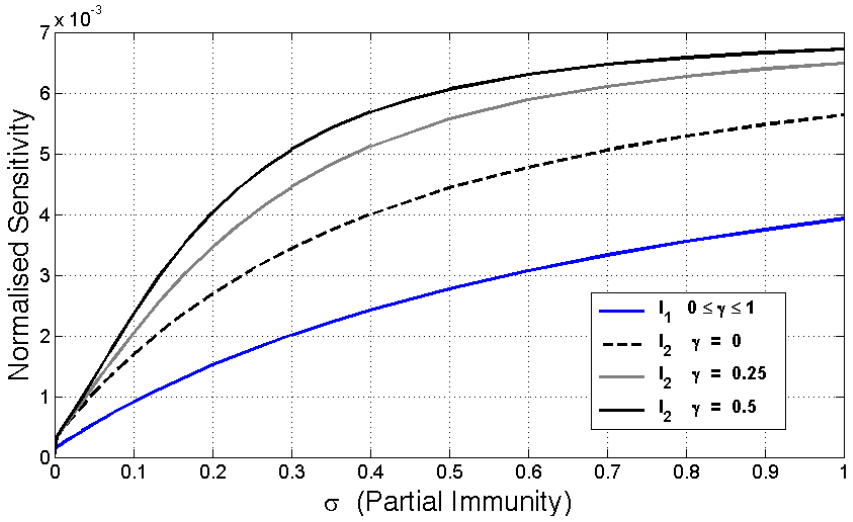

Figure 5.4: Steady state normalised sensitivity profiles to ω_M for a MSIRS2 model with a prevalence/incidence output and nominal values for hRSV. Plots correspond to primary (blue) and secondary (black) infection, for varying σ and discrete values of γ.

In all analysed examples, the normalised sensitivity of ω_M is considerably lower for observations of primary infection than for secondary infection. This may seem contrary to the intuitive assumption that maternally acquired immunity has, at least in the age domain, a greater, more direct degree of interaction with primary challenge. However, in the absence of age related heterogeneity, influence over population-wide infection levels arise purely from the proportional removal of potential infectives. In this instance, baseline fluctuations in primary transmission are often amplified through the reinfection process leading to a greater normalised change in secondary cases.

5.3 Static Sensitivity Analysis of Age Domain MSIR Models

At a fixed point (non-seasonally forced) endemic equilibrium, observations of infection and serology are static with respect to time, but still vary with respect to age. The following section describes a static sensitivity analysis applied to a set of equivalent (non-heterogeneous) age domain MSIR models (as derived in Section 3.3.4), in order to establish parameter sensitivity with respect to age. Homogeneous age domain models of this type are linear in form, where output solutions and corresponding sensitivity relations can be found analytically using symbolic manipulation software such as MATHEMATICA [Wolfram, 1999] or MAPLE [Heal et al., 1998].

5.3.1 Fundamental (Homogeneous) MSIR

Recalling from Section 3.3.4, for a non-seasonally forced MSIR system, residing at a fixed point endemic equilibrium (in time), a linear, purely age dependent system of equations can be derived (3.40)-(3.44) with the following analytic solution for an incidence observation:

$$y(a,p) \;=\; \frac{\hat{\lambda}\mu e^{-a(\mu+\hat{\lambda})}\left[A\hat{b}^{-}(\hat{\lambda}+\mu-\omega_M)+\omega_M A\hat{b}^{+}(e^{a(\hat{\lambda}+\mu-\omega_M)}-1)\right]}{\hat{\lambda}+\mu-\omega_M}. \qquad (5.18)$$

The seropositive and seronegative populations are assumed to be $A\hat{b}^{+} = \hat{R}$ and $A\hat{b}^{-} = \hat{S}+\hat{I}$ respectively, where the processes of neonatal fertility and mortality (i.e. from state $M(a)$) are removed according to the discussion on proportional birth rates in Section 3.3. The average force of infection is given by $\hat{\lambda} = \beta\hat{I}/N$, and steady state variables by the expressions in (5.12). Sensitivity functions are found symbolically according to (5.2), for all three observation types, through partial differentiation of the appropriate output solutions (i.e. (5.18) for incidence) with respect to p. In this instance, sensitivity functions are found to be age dependent and, algebraically, considerably more complex than those of the static time domain examples in Section 5.2.

The normalised sensitivity expressions for ω_M are evaluated at the nominal parameter values corresponding to pre-vaccine measles in the UK (Table 3.1), and displayed in Figure 5.5 with a prevalence output age profile. Figures 5.6 and 5.7 then illustrate how the three sensitivity curves change with varying basic reproduction number ($R_0 = 8$ and $R_0 = 80$), and rate of loss of maternally protected neonates ($\omega_M = 1$ and $\omega_M = 12$), respectively.

It can be seen from comparing the relations in Figure 5.6 and Figure 5.5, that an increase in infectivity (subsequently lowering the average age at primary in-

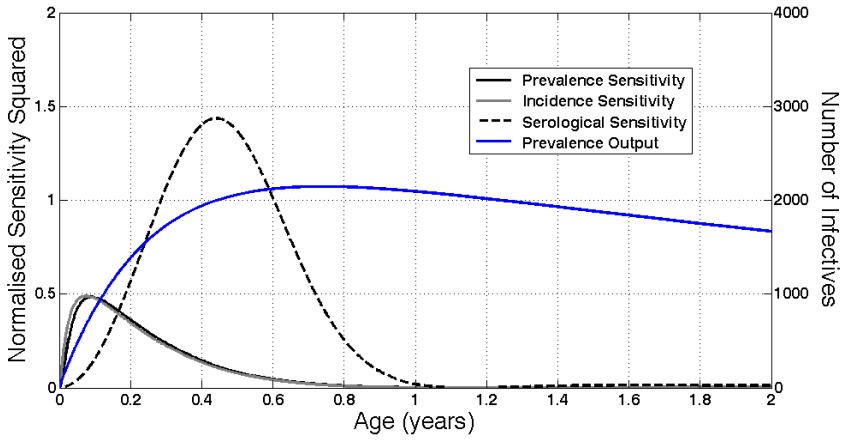

Figure 5.5: Age profile normalised sensitivity functions for incidence, prevalence and serological outputs of a fundamental MSIR system at endemic equilibrium. Sensitivities are evaluated with respect to ω_M at nominal parameter values for pre-vaccine measles in the UK (i.e. $R_0 = 18$).

fection) reduces the peak age of sensitivity for all three observation types, but has contrasting effects on their magnitude. For low values of R_0, peak sensitivity for the serological observation is notably larger than that of prevalence and incidence. However, while the latter two output sensitivities increase with higher R_0, serological sensitivity is found to decrease.

Variation in the sensitivity curves between different values of ω_M are elicited from comparison of the plots in Figures 5.5 and 5.7. The results show that the peak sensitivity for a serological observation varies considerably more than that of the prevalence and incidence outputs, which remain relatively unchanged at around 0.7. The age at peak sensitivity appears to decrease for all observations with increasing ω_M, which corresponds accordingly to a decrease in the average duration of acquired protection, ω_M^{-1}.

In all five examples there are no noticeable differences between the sensitivity characteristics of incidence and prevalence outputs. However, it does appear that the peak sensitivity for a serological type observation occurs consistently later in age. This result may prove to be significant in cases where there are limitations

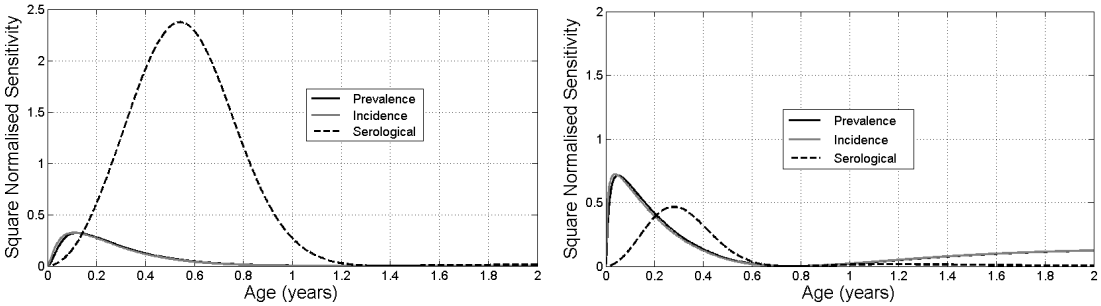

(a) Sensitivity Profiles for $R_0 = 8$ (b) Sensitivity Profiles for $R_0 = 80$

Figure 5.6: Prevalence, incidence and serological output normalised sensitivity functions corresponding to changes in ω_M, for contrasting values of basic reproduction. Results computed at time domain endemic equilibrium with nominal parameter values for pre-vaccine measles in the UK.

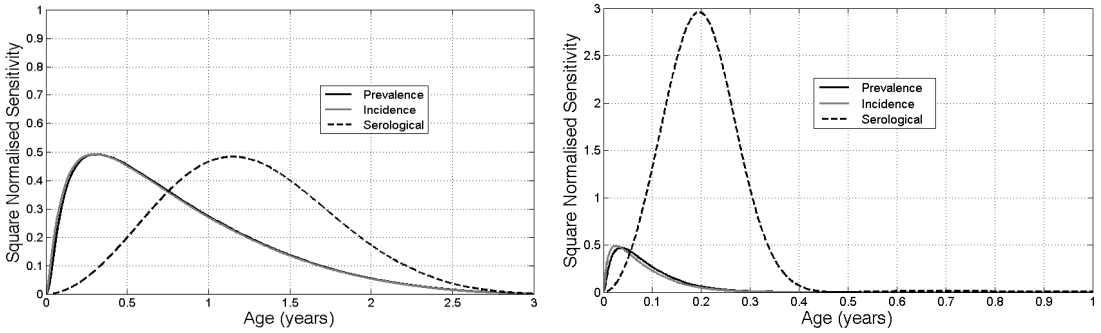

(a) Sensitivity Profiles for $\omega_M = 1$ (b) Sensitivity Profiles for $\omega_M = 12$

Figure 5.7: Age profile normalised sensitivity functions for ω_M, evaluated at endemic equilibrium with nominal values for pre-vaccine measles in the UK and at contrasting values for ω_M.

on the observation of clinical disease or on the collection of serological samples in very young infants.

In addition to peak values in sensitivity, it should also be noted that there are key points in age for all output types where the sensitivity of ω_M is equal to zero. Interestingly, the peak age of sensitivity (0.075 and 0.45 years for incidence or prevalence and serological outputs respectively, where $R_0 = 18$ and $\omega_M = 4$) appears well below both the average age at primary infection (calculated in this case to be 3.97 years) and the peak age of infection (0.75 years, see Figure 5.5). It should also be noted that in all cases, peak normalised sensitivities are found to

be significantly greater than those recorded for the static time domain examples in Section 5.2.1.

5.3.2 MSIRS with Temporary/Waning Immunity

Following the derivation of the linear age domain MSIR in Section 3.3.4, a purely age dependent system of equations can also be derived for an MSIRS model with temporary waning immunity. This is performed with the inclusion of an additional intercompartmental flow representing the process of recovered individuals losing active immunity and becoming fully susceptible to infection. Normalised sensitivity functions are again found symbolically from analytical solutions of the three observation types according to (5.2). The resulting expressions are found to be considerably more complex than those of the fundamental MSIR (5.18) since the state variable solutions for $S(a)$ and $I(a)$ become additionally dependent on $R(a)$ and hence also on $I(a)$.

For comparison with the MSIR model results shown in Figure 5.5, normalised sensitivity functions for the MSIRS model (see Figure 5.8) are evaluated at nominal parameter values taken from Table 3.1, where the waning active immunity parameter, ω_R, is set to 0.5, 1.8 and $4\,\mathrm{yr}^{-1}$ (protective duration of 24, 6.67 and 3 months, respectively).

The profiles in Figure 5.8 show that the initial peak in normalised sensitivity for prevalence or incidence observations are largely unaffected by variations in the rate that recovered individuals lose actively acquired immunity. However, for lower values of ω_R (i.e. longer durations of active immunity) a secondary, more variable, sensitivity peak occurs at around 9-10 months of age. Interestingly, this region

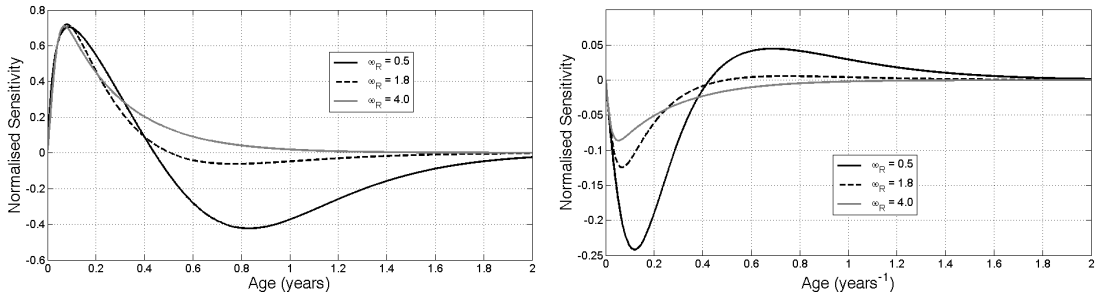

(a) Sensitivity for Incidence/Prevalence (b) Sensitivity for Serological Observation

Figure 5.8: Normalised sensitivity curves to changes in ω_M, for an age domain incidence/prevalence and serological observations of a MSIRS system; evaluated at endemic equilibrium, for various values of ω_R.

of sensitivity becomes negative in magnitude indicating a positive relationship between infection prevalence (infective state variable $I(a)$) and the duration of maternally acquired immunity, ω_M^{-1}, (i.e. a greater duration of protection from MAb acts to increase infection levels at certain ages).

In contrast to prevalence/incidence outputs, normalised sensitivity functions corresponding to serological type outputs are much more variable with respect to changes in ω_R. Shorter durations of actively acquired immunity (i.e. increasing ω_R) give rise to considerably lower sensitivity to changes in ω_M, see also Figure 5.5 where $\omega_R = 0$.

5.4 Dynamic Sensitivity Analysis of Seasonally Forced Models

As discussed in Section 2.1.3, many common infections such as measles, mumps and rubella (MMR), influenza and hRSV tend to display large (seasonal) recurrent epidemics at endemic equilibrium rather than settling to a constant level of transmission. This limit cycle behaviour is captured by time series data of prevalence, incidence or serology (see Figure 2.3) and often used for the estimation of epidemic

model parameters through data fitting (for examples see the work by Weber et al. [2001], White et al. [2007], and White et al. [2005]).

The following section aims to address the question of parameter sensitivity for characteristics associated with MAb in this context, through the dynamic analysis of MSIR framework models that include temporal variation. Since there are no convenient analytic solutions to the MSIR framework models when system parameters are allowed to vary dynamically with time, the analysis must resort to numerical methods, as outlined in Section 5.1.

5.4.1 Fundamental MSIR Model with Seasonal Forcing

Temporal variation of the transmission function is included in the homogeneous MSIR model (3.14)-(3.17) as a simple sinusoidal function of time of the form:

$$\beta(t) = \beta_0\big(1 + \beta_1 \cos\big[2\pi(t - \phi)\big]\big), \tag{5.19}$$

where β_1 defines the magnitude of the annual variation and ϕ corresponds to the phase (annual timing). Nominal parameter values are again substituted for pre-vaccine measles in the UK (Table 3.1), where additionally, $\beta_1 = 0.046$ and $\phi = 0.019$.

In order to perform a dynamic sensitivity analysis on the seasonally forced MSIR, an augmented system of differential equations are derived according to (5.10). In this instance, the dependent variables correspond to the dynamic sensitivity functions described by (5.2). The system of sensitivity equations are then solved numerically, for each of three output structures, using the `ode15s` ODE integrator, and the `myAD` automatic differentiation module [Fink, 2006] in MATLAB version

R2009b. The computation is performed on an RM desktop machine with a Pentium D 3.4GHz CPU and 1Gb of RAM, using a maximum step size of 0.001 years.

Prior to analysis, the simulation is run for a suitable period of settling time (i.e. 250 years) in order to allow the system solutions to converge satisfactorily close to their endemic limit cycle. The normalised sensitivity matrix, given by (5.6), is then generated for all 7 model parameters (i.e. $p = (\mu, N, \beta_0, \beta_1, \phi, v, \omega_M)^T$), with sample points taken at uniform time intervals of 0.01 years, for ten complete annual cycles. Figures 5.9 and 5.10 show the resulting deviation in the sum of squares function, $Q(\alpha)$, to a unit change in $\ln \omega_M$, i.e. normalised sensitivity squared, for incidence or prevalence and serological outputs respectively.

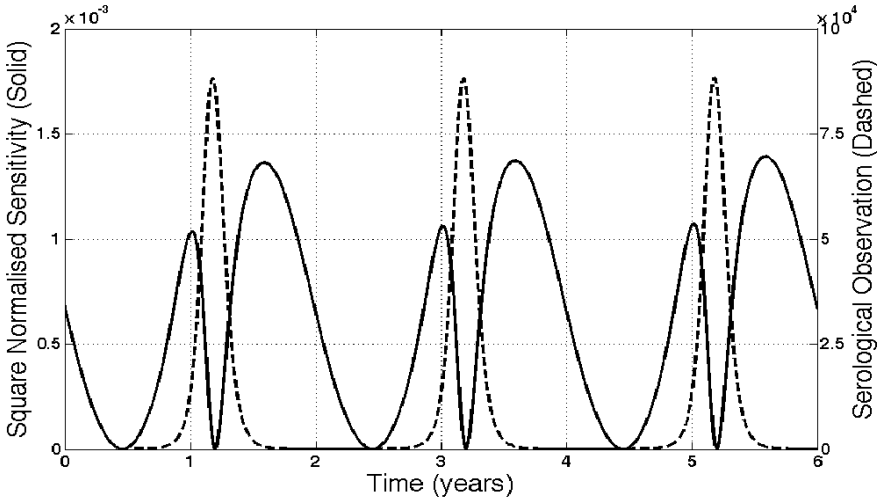

Figure 5.9: Sum of squares deviation to a unit change in $\ln \omega_M$ (normalised sensitivity squared), for an MSIR model with seasonal forcing and a prevalence or incidence output; evaluated with nominal parameter values for measles in the UK.

The system is seen to exhibit biennial epidemic behaviour in accordance with documented observations of pre-vaccine measles in the UK [Keeling and Grenfell, 2002], where the normalised sensitivity of ω_M is found also to be periodic with a time period of 2 years. Near identical results were obtained for both prevalence and incidence observations, with normalised sensitivity to ω_M varying between -0.037 and 0.032 throughout the biennial cycle. In contrast, the normalised sensitivity for

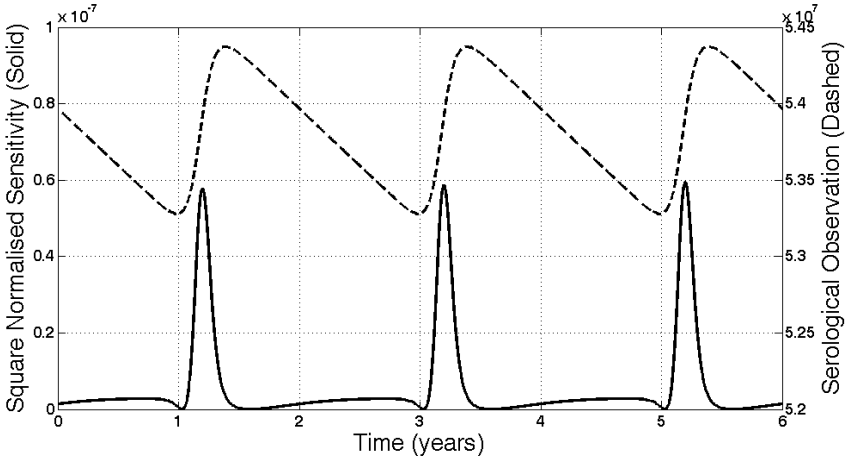

Figure 5.10: Sum of squares deviation to a unit change in $\ln \omega_M$ (normalised sensitivity squared), for a seasonally forced MSIR model with a serological type output structure; evaluated with nominal parameter values for measles in the UK.

a serological type observation varies only between -5.26×10^{-5} and 2.41×10^{-4}.

Figures 5.11 and 5.12 show the resulting dynamic sensitivity functions for a prevalence/incidence observation where $\omega_M = 1$ and $6\,\mathrm{yr}^{-1}$ respectively (i.e. average duration of maternally acquired immunity of 12 and 2 months). In this instance

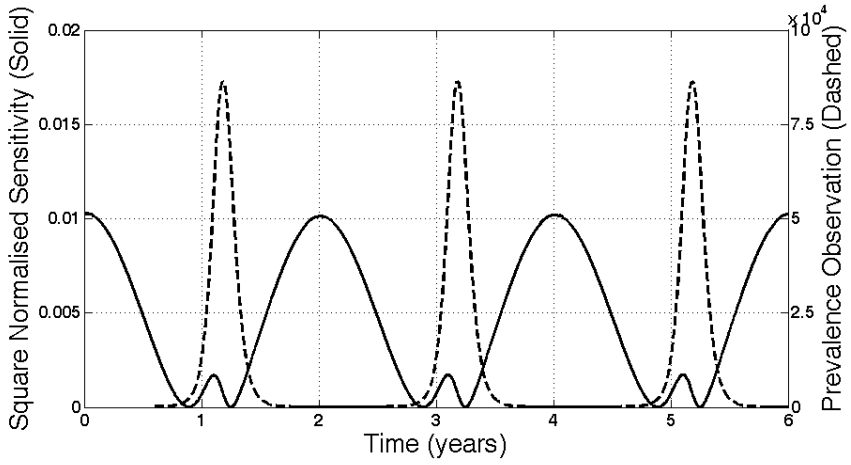

Figure 5.11: Normalised sensitivity (squared) with respect to ω_M, for a prevalence or incidence observation of a seasonally forced MSIR model, computed with the nominal UK measles parameter set and $\omega_M = 1\,\mathrm{yr}^{-1}$

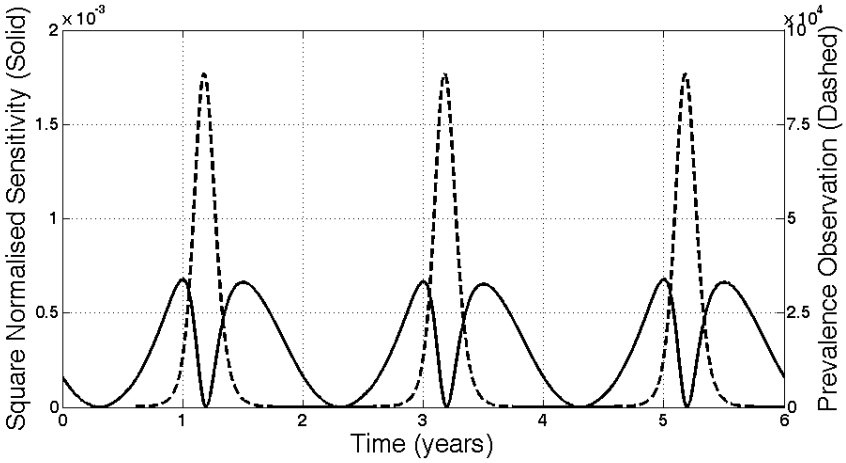

Figure 5.12: Normalised sensitivity (squared) with respect to ω_M, for a prevalence or incidence observation of a seasonally forced MSIR model, computed with the nominal UK measles parameter set and $\omega_M = 6\,\mathrm{yr}^{-1}$

the normalised sensitivity functions are found to be amplified with decreasing ω_M (increasing duration of protection). It can be seen from the outputs of the two simulations that the peak sum of squares deviation to a unit change in $\ln \omega_M$ is more than 10 times greater for an average duration of 12 months than for 2 months.

In all cases the point of maximum (magnitude) normalised sensitivity does not necessarily align with the biennial peak in the corresponding observation. This is an interesting result as it suggests, for example, that prevalence or incidence data collected for validating this particular characteristic of the MSIR model, would not be optimally sampled around the time of maximum epidemic behaviour. It can also be seen that there are regions for all output types where the sensitivity to ω_M is positive and negative, and hence two points during each biennial cycle where the normalised sensitivity of $y(t, p)$ is equal to zero.

Further analysis of the resulting sensitivity matrix for all examples show that it has full rank (i.e. $S^T S$ is non-singular), indicating that the MSIR model is sensitivity identifiable (see Definition 2 in Section 5.1.2) at p_0 corresponding to the UK measles parameter set. This result is consistent with those of a structural identifiability analysis given in (4.42), see Section 4.4, since the unknown observation

Table 5.2: Principal component analysis of the normalised sensitivity matrix corresponding to a MSIR model with seasonal forcing. Computed at nominal parameter values for pre-vaccine measles in the UK and sampled at 0.01 year intervals over a 10 year period.

No.	Eigenvalue	μ	N	β_0	β_1	ϕ	v	ω_M
1	561135	0.236	-0.022	0.270	-0.044	-0.927	-0.095	0.002
2	312054	0.560	-0.115	0.710	0.108	0.323	0.230	0.001
3	7952.76	0.366	0.395	-0.009	-0.306	0.174	-0.766	0.003
4	1074.88	0.300	0.594	-0.269	0.672	-0.065	0.170	-0.002
5	32.7887	-0.187	-0.423	0.146	0.662	0.032	-0.567	0.064
6	0.07314	-0.378	0.309	0.357	0.048	0.001	-0.047	-0.794
7	0.00054	0.479	-0.451	-0.450	0.003	-0.000	-0.002	-0.605

gain, k, is neglected i.e. $k = 1$, and the parameters μ and ω_M are distinguishable from their nominal values.

For completeness, the relative influences of all MSIR model parameters are examined by means of a singular value decomposition of the normalised $S^T S$ matrix, see Section 5.1.2 and the work by Vajda et al. [1985]. Table 5.2 shows the magnitude of the resulting principle components and the relative contributions of each individual model parameter.

It can be seen that the magnitude of the principal components range between 5.4×10^{-4} and 5.6×10^{5}. The parameter ω_M is clearly the least influential parameter in the model, making significant contributions (i.e. absolute value greater than 0.2 [Vajda et al., 1985]) to only the two smallest components. In this instance an elemental value of 0.002 corresponds to a 0.0004% contribution to the sum of squares deviation in $y(t, p)$, in the direction of the largest eigenvalue. It can also be noted that despite a tenfold increase in the peak sum of squares deviation for $\omega_M = 1\,\mathrm{yr}^{-1}$, see Figure 5.12, the resulting PCA reveals no greater contribution to all but the smallest principal component. In contrast, all other model parameters appear to be well defined by the chosen outputs, with significant influence over at

least one of the three major components.

5.4.2 Seasonally Forced Models with Incomplete Immunity

In order to extend the analysis using nominal values for hRSV, the process of seasonal forcing is applied to an appropriate epidemic model with incomplete immunity. An existing example of a seasonally forced model of this type is the 17 compartment, time domain, ODE based MSEIRS4 model, proposed by Weber et al. [2001]. It has been developed as a more realistic representation of the epidemiological mechanisms associated with reinfection and accumulating acquired immunity, observed with hRSV.

The model has been chosen for analysis in this work because it is very closely related to the MSIRS2 model structure proposed in Section 3.3.1 and has also been previously fitted to four separate sets of empirical data [Weber et al., 2001]. A formal sensitivity analysis can therefore be performed using fitted nominal values, in order to study the influence of maternally acquired immunity on observations of primary infection, and hence, the determinability of ω_M. It should be noted that this is not intended as a critique of the work published by Weber et al. [2001], given that the flow rate coefficient ω_M is not a fitted parameter in their parameter estimation, and the influence of maternal immunity was not the focus of their study, or the subject of any inference from the results.

The set of system equations corresponding to the MSEIRS4 model are given in Appendix A. The first four infections in the natural history of the disease are distinguished by separate state variables (i.e. $S_i(t)$, $E_i(t)$, $I_i(t)$ and $R_i(t)$ for $i = 1, \ldots, 4$), where $E_i(t)$, for $i = 1, \ldots, 4$, represents a latent incubation period with an average duration of ζ^{-1}. In this instance, baseline susceptibility decreases

Table 5.3: MSEIRS4 model parameters for hRSV in Gambia, Florida, Finland & Singapore [Weber et al., 2001]; values for μ, v, ω_M, ω_R, & ζ given in yr^{-1}.

Location	μ	β_0	β_1	ϕ	v	ω_M	ω_R	ζ	σ_1	σ_2	σ_3
Gambia	0.041	256	0.20	0.26	36	13	1.8	91	0.50	0.35	0.25
Florida	0.016	268	0.13	0.03	36	13	1.8	91	0.50	0.35	0.25
Finland	0.013	192	0.39	0.19	36	13	1.8	91	0.50	0.35	0.25
Singapore	0.016	260	0.12	0.00	36	13	1.8	91	0.50	0.35	0.25

with successive experience of infection, following a temporary period of full protection upon recovery from each infection. Therefore, it can be noted that the MSIRS2 model, given by (3.20)-(3.26), can be derived from the MSEIRS4 model by neglecting the incubation stages and considering only the first two infections.

The analysis is performed using the nominal set of fitted parameter values, extracted from the work by Weber et al. [2001], corresponding to hRSV in The Gambia, see Table 5.3. In a similar manner to the MSIR example, the sensitivity matrix is generated numerically once the simulation has satisfactorily converged to a stable endemic limit cycle. Sample points are again taken at uniform 0.01 year intervals, for 10 complete annual cycles. Figures 5.13 and 5.14 show the resulting deviation in the sum of squares function, $Q(\alpha)$, due to a unit change in $\ln \omega_M$, for primary prevalence or incidence and serological type outputs respectively. The dynamic sensitivity functions are given with respect to time, and presented against their corresponding output functions.

It is found that the sensitivity of ω_M for all output types is periodic with a time period of 1 year. Near identical results are obtained for prevalence and incidence outputs (peak absolute value of 0.078), however, the normalised sensitivity of ω_M for a serological observation is found to be significantly smaller in magnitude (peak absolute value of 0.005) and peaked at slightly different points in time. There are again also two points during each epidemic period where the sensitivity of $y(t, p)$ with respect to ω_M is equal to zero. The point of maximum sensitivity for all out-

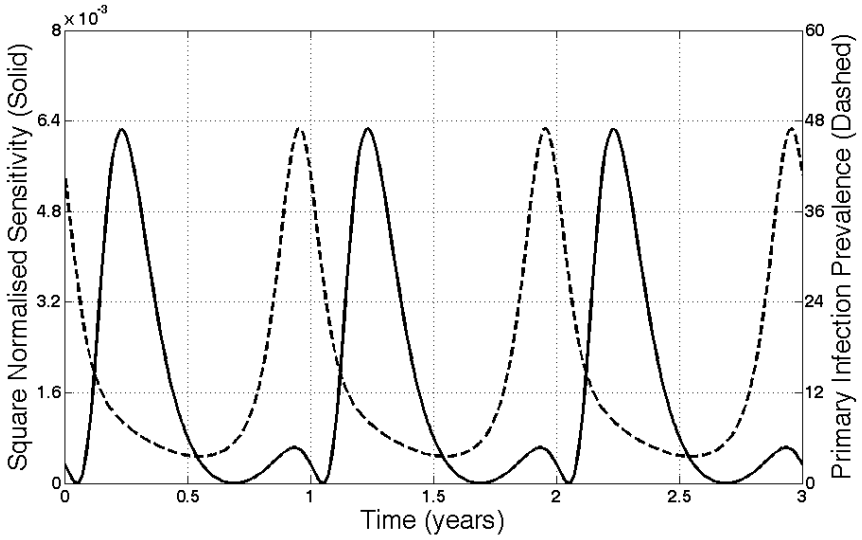

Figure 5.13: Resulting sum of squares deviation, $Q(\alpha)$, in a prevalence/incidence observation of a seasonally forced MSEIRS4 model, to a unit change in $\ln \omega_M$ (normalised sensitivity squared); evaluated at nominal values for hRSV in The Gambia.

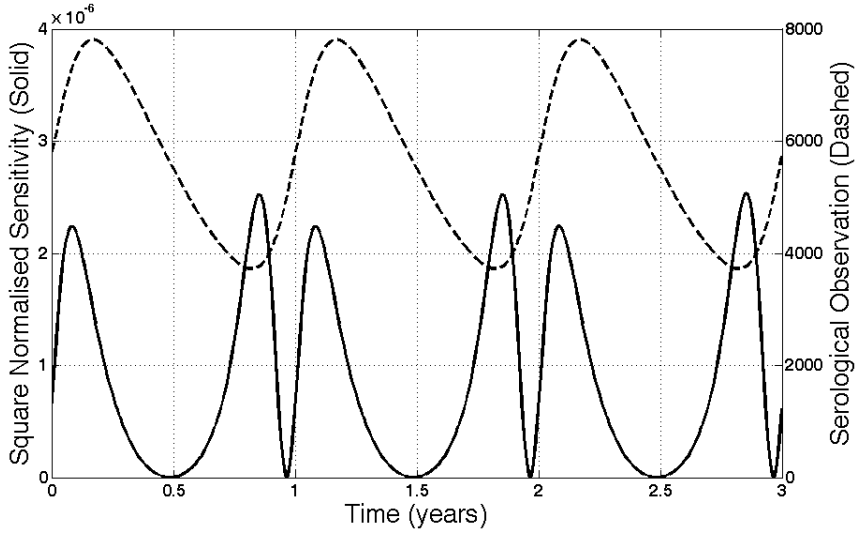

Figure 5.14: Sum of squares deviation to a unit change in $\ln \omega_M$ (normalised sensitivity squared), for a serological observation of a seasonally forced MSEIRS4 model; evaluated with nominal parameter values for hRSV in The Gambia.

puts does not necessarily align with the annual peak in the corresponding observation, although their position relative to the annual epidemic cycle is comparable to that of the measles example shown in Figures 5.9 and 5.10.

It can also be noted that by removing seasonal forcing from the model (i.e. setting $\beta_1 = 0$), hence forcing the system to converge to a fixed point endemic equilibrium, the analysis gives rise to a steady state normalised sensitivity value in the region of 0.0014 for a prevalence or incidence observation of primary infection. This value appears to be consistent with the results shown in Figure 5.3, which correspond to the normalised sensitivity of an unforced MSIRS2 model, at endemic equilibrium, with nominal values for hRSV in the UK.

The MSEIRS4 system is found to be sensitivity identifiable, i.e. the sensitivity matrix, S, has full rank for all three observations, however, through a singular value decomposition of S^TS, it is also shown that ω_M is again poorly defined by time series infection dynamics. It can be seen from Table 5.4, which shows the individual parameter contributions to the resulting principal components of $Q(\alpha)$, that ω_M contributes to only the 5th, 6th, 7th and 8th principal components, which are between 10^4 and 10^8 times smaller than the largest.

Similar results were also obtained for parameter sets estimated using epidemic data from Finland, Florida and Singapore [Weber et al., 2001], suggesting that the regional variation in parameter values observed in these cases does not have a significant impact on sensitivity.

Table 5.4: Principal component analysis of the normalised sensitivity matrix corresponding to a MSEIRS4 model with nominal values for hRSV in The Gambia. Evaluated using a 0.01 year sampling interval over ten complete annual cycles.

No.	Eigenvalue	μ	β_0	β_1	ϕ	v	ω_M	ω_R	ζ	σ_1	σ_2	σ_3
1	1.9×10^{4}	-0.123	-0.590	0.141	-0.161	0.576	0.001	-0.270	-0.039	-0.029	-0.0248	-0.430
2	1.1×10^{3}	0.372	-0.327	-0.276	-0.440	-0.577	0.018	0.011	-0.183	-0.012	-0.0163	-0.344
3	1.2×10^{2}	-0.696	0.149	-0.427	-0.457	0.083	0.011	0.254	-0.173	0.010	0.0029	-0.007
4	1.9×10^{1}	0.048	0.287	0.686	-0.647	-0.011	-0.001	0.058	0.150	-0.012	-0.0052	-0.003
5	2.7×10^{0}	-0.365	0.130	0.323	0.375	-0.329	0.227	0.159	-0.088	0.016	-0.0201	-0.641
6	3.2×10^{-2}	0.036	0.416	-0.276	-0.105	0.036	0.451	-0.654	0.259	-0.049	-0.0264	-0.193
7	1.7×10^{-2}	-0.339	-0.475	0.130	-0.024	-0.335	0.363	-0.124	0.381	0.294	0.1197	0.369
8	3.0×10^{-4}	0.265	-0.0084	0.022	-0.026	0.269	0.752	0.342	-0.380	0.128	0.0474	0.114
9	3.0×10^{-5}	0.083	-0.106	-0.147	-0.002	0.088	0.174	0.449	0.621	-0.549	-0.1546	-0.108
10	2.8×10^{-6}	-0.180	-0.119	0.178	0.021	-0.178	0.128	-0.270	-0.403	-0.715	-0.2016	0.294
11	4.6×10^{-10}	0.004	0.012	-0.001	-0.001	0.004	-0.010	-0.008	-0.011	-0.284	0.9575	-0.043

5.5 Conclusions & Discussion

A formal sensitivity analysis has been applied to a set of contrasting ODE epidemic models, with various observation structures, for two common viral diseases. The objective has been to assess the determinability of parameters associated with passive immunity from MAb, and hence, also estimate the magnitude of their influence over the static, dynamic and seasonal characteristics of system behaviour.

The analysis has indicated that the corresponding sensitivity of community-wide transmission levels is potentially increased by processes associated with a greater duration of protection from MAb, higher fertility rates and partial immunity. It has also been shown for homogeneous cases that changes in the rate that maternally protected neonates become fully susceptible has a much greater influence on epidemiological measures recorded with respect to age than with respect to time.

A potential limitation of the analysis in this work has arisen from the consideration of only homogeneous transmission, immunity and fertility etc. It is possible that greater output sensitivity may be generated from small perturbations in ω_M if, for example, the peak age of transmission occurs close to that of the average duration of waning maternal antibody. However, the analysis of heterogeneous PDE based systems is found to be substantially more challenging using techniques associated with automatic differentiation and the accuracy of most numerical methods do not permit the implementation of finite differencing given that time domain sensitivities are found to be in the region of 10^{-3}.

Implications for the Estimation of MAb Parameters

All worked examples have consistently shown near identical normalised sensitivity results, corresponding to changes in ω_M, for observations of incidence and preva-

lence in either domain. This suggests that it is not critical which of the two data types are used with respect to parameter estimation within these model structures. In addition, no examples were found where it may be beneficial to utilise a serological type observation recorded with respect to time.

In all dynamic and static age domain analyses it has been shown that there are key regions, both in the annual epidemic cycle (i.e. with respect to time) and in the average age profile, that correspond to peak, and conversely, zero sensitivity to variation in all unknown model parameters. This indicates that the use of prior experimental design and optimal sampling could be of great benefit in maximising confidence during parameter estimation and potentially minimising unnecessary data collection. In the age domain, analysis of the considered models has shown comparable peak values in normalised sensitivity for serological and prevalence/incidence outputs. However, these peaks tend not to occur at the same points in age, and have contrasting dependencies on the basic reproduction number and nominal value of ω_M. Similarly in the time domain, maximal output sensitivity to ω_M appears in all cases not to coincide with the annual or biennial epidemic peak in infection and differs again between observations of prevalence/incidence and serology.

A comparison of results corresponding to equilibrium observations of systems with constant and seasonally varying transmission suggests that changes in ω_M can potentially have a more significant impact on dynamic behaviour than on overall levels of infection. However, in all dynamic time domain examples the parameter was still clearly found to be one of the least sensitive in the model. Consequently, MSIR framework models with time domain output structures are likely to be inappropriate for estimating characteristics associated with maternally acquired immunity. Moreover, through the use of techniques such as subset selection, these models may be acceptably reduced by omitting the immunising effects of MAb if the purpose of the model is to achieve reasonable estimates for other parameters such as those associated with transmission.

More promisingly, analysis has shown that maternally acquired immunity has a much greater influence on epidemiological observations recorded with respect to age than with respect to time. However, the results of a structural identifiability analysis, described in Chapter 4, have shown that these parameters are not uniquely determined by age domain output structures. One possible resolution to this problem might be to simultaneously fit equivalent model structures to both age and time domain data sets; although this is likely to involve dedicated epidemiological studies beyond those which are typically conducted for the two infections discussed in this work. In addition, the particularly young age in peak sensitivity of all age domain observations could be a major hindrance in the selection of suitably high fidelity sample points in this region.

Chapter 6

Model Analysis & Numerical Simulation

The role of maternally acquired immunity within the observed characteristics of many infectious diseases remains largely unclear. Models have been proposed in Chapter 3 that aim to describe some of the fundamental epidemiological processes associated with MAb, such that their influence over a broad range of system behaviour may be explored. It is the objective of this chapter to provide additional analysis of these models and present examples of their use in assessing the potential impact of mass maternal immunisation on systems with differing epidemiological characteristics.

In the absence of appropriate data, the scope of this work is unable to extend to the validation of quantitative predictions regarding intervention outcomes for specific infections. Instead, the aim is to provide a more qualitative analysis using a range of typical values extracted from the literature (see Section 3.5). It is intended that the work highlights some of the potential effects of mass maternal immunisation on static, dynamic and seasonal characteristics of infection, and to encourage the discussion of how prospective interventions of this type may be more optimally

implemented in future public health policy. Specific areas of interest include:

- The potential impact of maternally targeted intervention on the incidence of neonatal infection and the average age of primary contraction.
- Possible outcomes regarding population-wide prevalence of infection.
- How the potential success of maternal immunisation might be subject to:
  - The force of infection / average age at primary infection.
  - Processes associated with reinfection, including the distribution/dominance of primary and secondary infectivity.
  - Heterogeneity in the population age profile and transmission function.
- The potential interaction of mass maternal immunisation with early childhood targeted vaccines.
- The dynamic consequences of system perturbation due to rapid implementation of an intervention campaign.
- Seasonal targeting of prospective intervention strategies for systems with temporal forcing.

To address these issues, Section 6.1 presents a continuation of the preliminary steady state analysis described in Section 3.3.5, where a number of ODE-based time domain models are used to explore the impact of various combinations of passive and active intervention effort on the overall prevalence of infection. Relations are elicited for varying degrees of antibody interaction between vaccines, reinfection and discrete age dependent fertility/mortality.

A more detailed analysis of potential age specific infection patterns resulting from maternal immunisation is presented in Section 6.2. The analysis uses various implementations of the continuous age domain model described in Section 3.4.2,

with MAb titre distribution characteristics elicited from the literature for hRSV. Finally, in Section 6.3, a number of the proposed models are used to explore the consequences of intervention on the time dynamic behaviour of systems with and without seasonal forcing.

6.1 Time Domain Steady State Analysis

In keeping with the work flow of previous chapters, the following section considers the characteristics of ODE-based time domain models residing at a fixed point equilibrium. In this instance, the effects of temporal variation are neglected and age dependency is included only in the discrete compartmentalised form described in Section 3.4.1. The analysis is performed in order to gain insight into the potential dependencies of population-wide infection levels on prospective intervention strategies.

Analytic solutions are found according to Section 6.2.1 using the symbolic manipulation package MATHEMATICA (version 7.0.0). However, solutions to systems more complex than those previously considered in the preliminary analysis of Section 3.3.5 are typically too expansive to include explicitly. In these cases, key relations are illustrated graphically using typical parameter values and appropriate intervals of variation.

6.1.1 Fundamental MSIR

The foundation for all prior analyses in this work has been the fundamental MSIR model shown by Figure 3.1. In this instance, the model is considered with the addition of maternal (passive) and potentially interacting childhood (active birth

targeted) immunisation as described in Section 3.3.3. The system equations are derived from the full incomplete immunity model (3.33)-(3.38) by removing the state variables corresponding to secondary infection (i.e. $S_2(t)$ and $I_2(t)$) and setting the parameter ω_R equal to zero. It should be recalled that the proportions P_m and P_v correspond to the application of maternal and birth targeted immunisation respectively, which are applied in terms of the net birth rate, μN. The interaction between neonatal immunity derived from the two intervention types and natural infection experience of the mother is described by the parameter ϑ.

The system has a single, stable equilibrium point corresponding to either eradication or endemic persistence of the infectious agent. In the absence of any intervention, these equilibrium points are delineated by the bifurcation point, $R_0 = 1$. For $R_0 > 1$ and under suboptimal intervention, an endemic level of infection transmission is observed, which is subsequently dependent on the proportions P_m, P_v and ϑ. Evaluating this equilibrium using nominal values for pre-vaccine measles in the UK (Table 3.1), a series of relations between endemic prevalence of infection and various combinations of intervention effort, with and without antibody interaction, are elicited and shown in Figure 6.1.

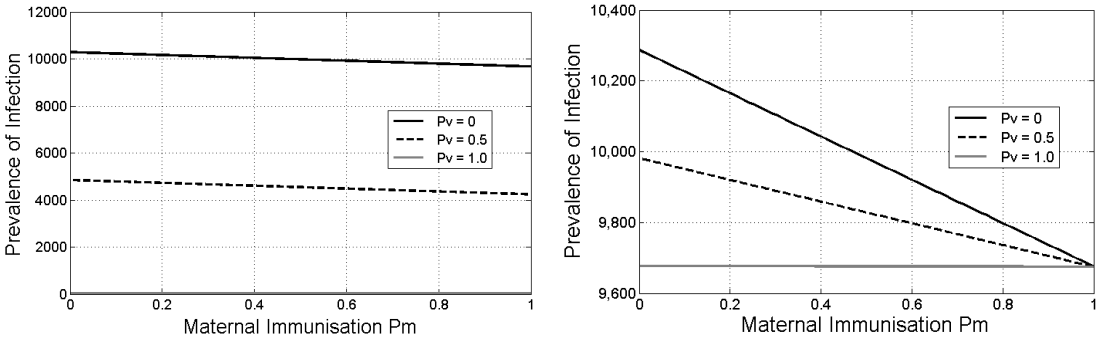

(a) Primary infection profiles for $\vartheta = 0$. (b) Primary infection profiles for $\vartheta = 1$.

Figure 6.1: Endemic prevalence of infection for specific proportions of birth targeted vaccination, P_v, and antibody interaction, ϑ, with respect to maternal immunisation, P_m, and evaluated at nominal parameter values for pre-vaccine measles in the UK.

It can be seen from the two graphs in Figure 6.1 that the model predicts both

interventions would have a positive impact on reducing the transmission of the pathogen. In the absence of antibody interaction, i.e. $\vartheta = 0$, Figure 6.1(a) shows that in this example it is possible to force the disease free equilibrium to become stable and eradicate the infectious agent. However, for high values of ϑ, the efficacy of birth targeted vaccination is significantly reduced. In Figure 6.1(b), high levels of antibody interaction are seen to prevent the eradication of the infection by means of the considered intervention strategy.

Following the analysis in Section 2.2.1, an eradication threshold for ϑ can be found, above which, too few newborns successfully respond to the active vaccine and herd immunity can no longer be achieved. The system Jacobian matrix is evaluated at the disease free equilibrium, with maximum maternal and birth targeted immunisation (i.e. P_m, $P_v = 1$). This gives rise to a set of eigenvalues:

$$\begin{aligned} \lambda_1 &= -2\mu, \\ \lambda_2 &= -(\omega_M + \vartheta\mu), \\ \lambda_3 &= -v - 2\mu + \frac{\vartheta\beta\omega_M}{2(\vartheta\mu + \omega_M)}, \end{aligned} \tag{6.1}$$

which are always negative and real provided the interaction parameter adheres to the following inequality:

$$\vartheta < \frac{2(v + 2\mu)\omega_M}{\beta\omega_M - 2v\mu - 4\mu^2}. \tag{6.2}$$

Evaluating (6.2) with respect to the UK measles parameter set (Table 3.1), it is found that for eradication of the infection to be possible, $\vartheta < 0.11$.

From Figure 6.1(b) it can be seen that for $\vartheta = 1$, the minimum prevalence of infection that can be achieved is 9675 cases (a reduction of 611 cases or 5.94%). This limit in efficacy occurs since only newborns born to fully susceptible mothers will benefit from either of the two immunisations. As population immunity is raised, the number of successful birth targeted vaccinations quickly diminish, restricting

the impact of the intervention. If maternal immunisation is successfully applied to all pregnant women, i.e. $P_m = 1$, then all newborns will be protected by MAb and potentially none will respond to the active vaccine. This result emphasizes the efforts of Williams et al. [1995] and Nicoara et al. [1999] who discuss the importance of targeting childhood vaccination beyond the average duration of MAb.

An expression approximating the average age at primary infection predicted by the model may be derived similarly to those of the MSIR (3.19) and MSIR with maternal immunisation only (3.61), and given in the following form:

$$A_v \approx \frac{\hat{\mu_M}}{\hat{\mu_M} + \hat{\mu_S}}(\omega^{-1} + \lambda^{-1}) + \frac{\hat{\mu_M}}{\hat{\mu_M} + \hat{\mu_S}}(\lambda^{-1}), \tag{6.3}$$

where

$$\begin{aligned} \hat{\mu_M} &= \mu(1-(1-\vartheta)P_v)\left[\hat{Ab^+} + P_m\hat{Ab^-}\right], \\ \hat{\mu_S} &= \mu(1-P_v)(1-P_m)\hat{Ab^-}. \end{aligned}$$

The function is based on a weighted average of the corresponding proportions of seropositive (Ab^+) and seronegative Ab^- newborns, excluding those who successfully respond to the active (birth targeted) vaccine and avoid primary infection. The resulting relations between the average age at primary infection, the two forms of intervention and their interactions are illustrated by Figure 6.2, which is evaluated again with respect to the UK measles parameter set (Table 3.1). It should be noted, with respect to Figure 6.2(a), that for values of P_m, P_v and ϑ that result in the eradication of the infectious agent, an average age at primary infection can no longer be calculated.

It can be seen from the two graphs in Figure 6.2 that again both interventions have a positive impact on the average age at primary infection. However, in cases where there are high levels of antibody interaction the benefits of active immunisation are substantially limited.

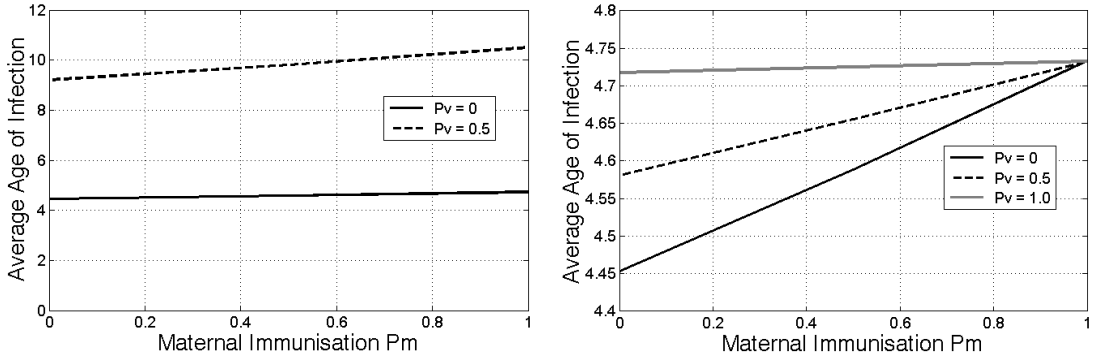

(a) Average age of infection for $\vartheta = 0$. (b) Average age of infection for $\vartheta = 1$.

Figure 6.2: Average age at primary infection for specific proportions of birth targeted vaccination, P_v, and antibody interaction, ϑ, with respect to maternal immunisation, P_m; evaluated at nominal parameter values for pre-vaccine measles in the UK.

All results in this section suggest that if the detrimental effects of antibody interaction are reduced then active immunisation is by far the most effective intervention with respect to wider population infection. However, the characteristics that have been discussed in this section are potentially accentuated by the solid and lifelong immunity assumed by the MSIR model. In this case, a particularly high proportion of the population is seen to reside in a seropositive state, leading to naturally high levels of MAb among newborns.

6.1.2 Models with Incomplete Immunity

To explore the outcomes of intervention implemented within systems where active immunity is incomplete, the analysis is applied to the MSIRS2 model structure proposed in Section 3.3.3. The model is described by the set of system equations (3.33)-(3.39), where it can be recalled that the additional state variables $S_2(t)$ and $I_2(t)$ correspond to characteristics associated with altered secondary infections. The parameters ω_R, σ and γ describe, respectively, the rate of loss of active immunity, a reduced risk of secondary infection and a reduction in secondary infectivity.

As discussed in Section 3.3.1, in cases such as hRSV it is often unclear whether the more significant source of transmission is from primary or secondary infectivity. In the MSIRS2 model, higher values of σ and γ result in a greater prevalence of reinfection, which may subsequently dominate the behaviour of the system and the overall force of infection. In contrast to the MSIR example, rapid waning of active immunity yields lower numbers of seropositive individuals throughout the childbearing population, leading also to fewer numbers of children born with protective levels of MAb. The objective of this analysis is therefore to explore whether the static influence of maternal immunisation over wider population transmission is affected by the balance of primary and secondary infection.

The MSIRS2 system is found to have a single, stable equilibrium point corresponding to either eradication or endemic persistence of the infection. Provided that the invasion threshold is met, an endemic level of transmission is observed, which is subsequently dependent on the intervention parameters, P_m, P_v and ϑ. The equilibrium is evaluated at nominal parameter values for hRSV (Table 3.2), where the secondary infection parameters, ω_R, σ and γ, and the transmission parameter, β, are varied to encompass a spectrum of infectivity biases, whilst maintaining a constant force of infection.

The resulting relations between the endemic prevalence of primary infection and various combinations of intervention effort, for primary and reinfection dominated transmission, with and without antibody interaction, are shown in Figure 6.3. For Figures 6.3(a) and 6.3(b) the secondary infection parameters are set to: $\omega_R = 1.8\,\mathrm{yr}^{-1}$ (average duration of immunity of 6.67 months), $\sigma = 1$ and $\gamma = 1$, which correspond to the upper interval values given by Table 3.3(C). In order to maintain a typical force of infection for hRSV of $\lambda = 0.84\,\mathrm{yr}^{-1}$, the transmission parameter is set to $\beta = 152\,\mathrm{yr}^{-1}$.

For comparison, Figures 6.3(c) and 6.3(d) show the relations that result from parameterising the model such that it emulates an MSIR type structure, where

only primary infection contributes to the overall force of infection. In this instance, $\omega_R = 0\,\mathrm{yr}^{-1}$ (lifelong immunity), $\sigma = 0$, $\gamma = 0$, and subsequently, $\beta = 2490\,\mathrm{yr}^{-1}$ (see Table 3.3(A)).

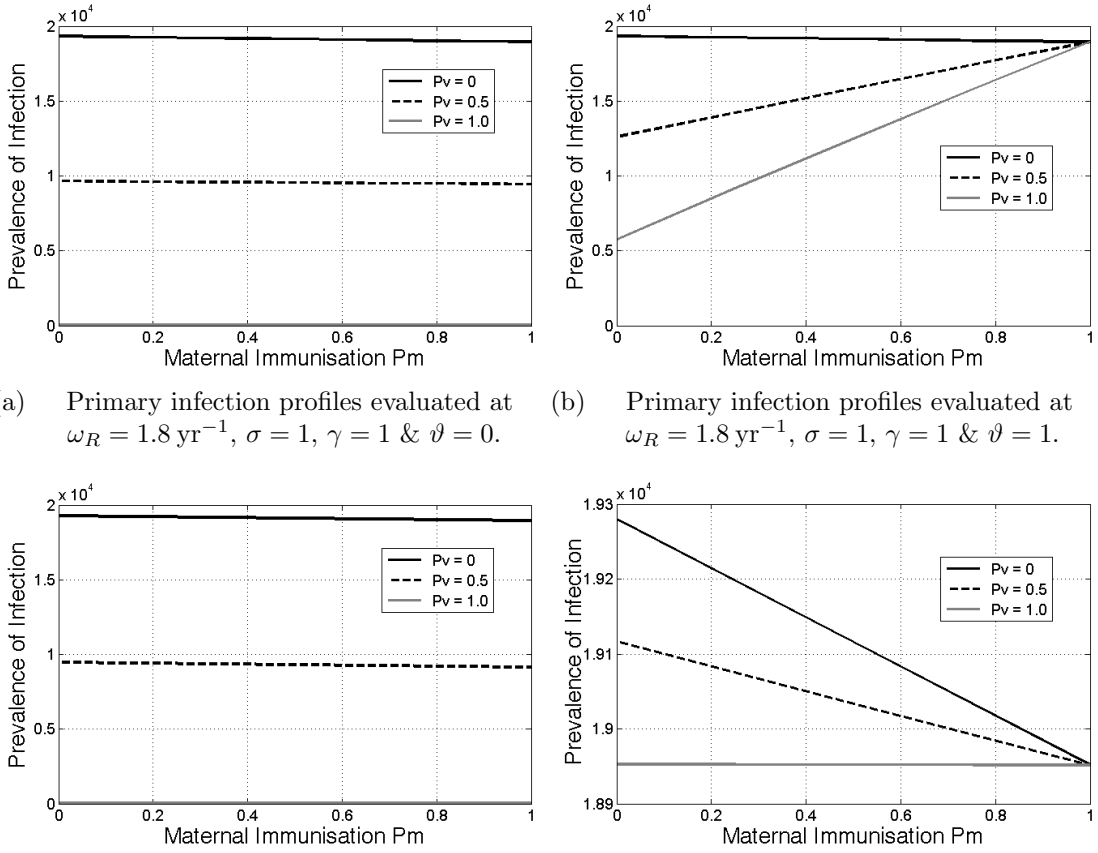

(a) Primary infection profiles evaluated at $\omega_R = 1.8\,\mathrm{yr}^{-1}$, $\sigma = 1$, $\gamma = 1$ & $\vartheta = 0$.

(b) Primary infection profiles evaluated at $\omega_R = 1.8\,\mathrm{yr}^{-1}$, $\sigma = 1$, $\gamma = 1$ & $\vartheta = 1$.

(c) Primary infection profiles evaluated at $\omega_R = 0\,\mathrm{yr}^{-1}$, $\sigma = 0$, $\gamma = 0$ & $\vartheta = 0$.

(d) Primary infection profiles evaluated at $\omega_R = 0\,\mathrm{yr}^{-1}$, $\sigma = 0$, $\gamma = 0$ & $\vartheta = 1$.

Figure 6.3: Endemic prevalence of primary infection for specific proportions of birth targeted vaccination, P_v, and antibody interaction, ϑ, with respect to maternal immunisation, P_m. Evaluated at parameter values corresponding to reinfection-dominant, (a)-(b), or primary infection-dominant, (c)-(d), transmission.

The results indicate that, when applied independently, both the active and passive immunisation methods yield a positive impact on the prevalence of primary infection. For high values of ϑ, the efficacy of the active vaccine is once again inhibited through its interaction with MAb. However, in the absence of maternal immunisation, i.e. $P_m = 0$, it can be seen that the childhood vaccine is considerably more effective within the reinfection system than the MSIR (primary infection) system.

This is likely to be a result of waning population immunity, which subsequently leads to a reduction in the number of seropositive newborns. It should also be noted that since the transmission parameter, β, is reduced in order to maintain a constant force of infection in the presence of greater secondary infectivity, the basic reproduction number, R_0, is subsequently decreased.

When a combination of the two interventions is applied with high levels of interaction, it can be seen from Figure 6.3(d) that the MSIR-type system displays qualitatively similar results to that of the measles example shown in Figure 6.1(b). In this instance, birth targeted vaccination is predominantly limited by naturally occurring levels of MAb, such that it is still beneficial to implement the passive vaccine. However, in the reinfection example (Figure 6.3(b)), where natural levels of MAb are low, maternal immunisation has a significantly detrimental effect on the efficacy of the active vaccine. This implies that in situations where maternal immunisation is likely to interact with an existing or prospective childhood vaccine, its application should be considered with caution.

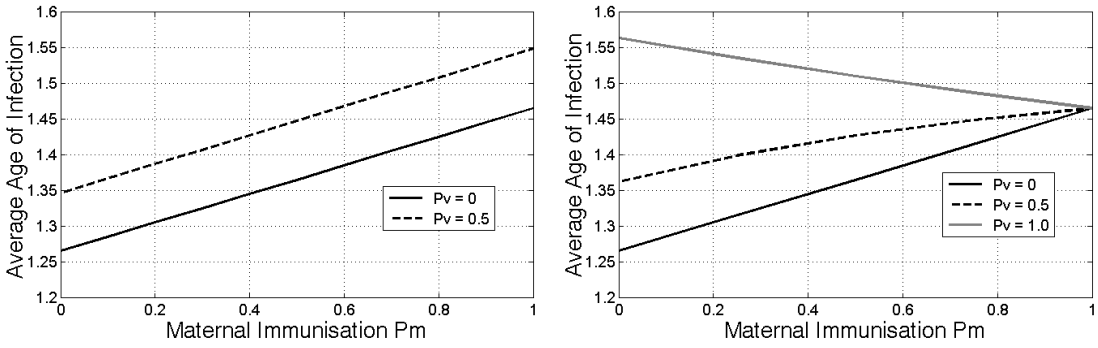

(a) Average age of infection for $\vartheta = 0$.

(b) Average age of infection for $\vartheta = 1$.

Figure 6.4: Average age at primary infection for specific proportions of birth targeted vaccination, P_v, and antibody interaction, ϑ, with respect to maternal immunisation, P_m; evaluated at nominal parameter values for hRSV where $\omega_R = 1.8\text{yr}^{-1}$, $\sigma = 1$ and $\gamma = 1$.

The resulting relations between the average age at primary infection and the applied interventions are calculated for the reinfection example using equation (6.3) and shown in Figure 6.4. In contrast to the results shown in Figure 6.3(b), it can

be seen from Figure 6.4(b) that for $\vartheta = 1$, maternal immunisation has a beneficial impact on the average age at primary infection at $P_v = 0$ and $P_v = 0.5$. Comparing the two graphs at $P_v = 0.5$ suggests that the implementation of mass maternal immunisation may have a positive influence on the average age at primary infection, despite raising overall prevalence.

6.2 Static Analysis Age Domain

In order to obtain a more detailed description of infection patterns in neonatal and young infant age classes, it is necessary to consider the evolution of the system state variables continuously with respect to age. Section 3.4.2 describes an alternatively derived PDE-based MSIR model structure that also includes a more empirical representation of MAb titres among newborns. The model is therefore focussed more directly on waning neonatal immunity and infection, rather than that of the population as a whole. The dependency of the maternally protected population is decoupled from the dynamics of susceptibility and immunity in the wider population, and determined purely from static serological observations.

The objective of this section is to demonstrate how the model may be used in order to explore specifically how the implementation of mass maternal immunisation might affect the age profile of primary infection incidence and the number of cases among infants below a target age. Static age profiles are extracted from numerical simulations generated using typical values and characteristics derived from the literature, and a number of speculative age varying transmission functions that emulate potential routes of infection.

6.2.1 Methods & Application

The model is initially considered as a fundamental MSIR system, without the additional complexities of sup-optimal immunity and altered secondary infections. Recalling from Section 3.4.2, the system is defined by the following set of nonlinear partial differential equations:

$$\frac{\partial M(t,a)}{\partial t} + \frac{\partial M(t,a)}{\partial a} = -Q(t,a) - \mu_d(a)M(t,a), \tag{6.4}$$

$$\frac{\partial S(t,a)}{\partial t} + \frac{\partial S(t,a)}{\partial a} = Q(t,a) - \big[\lambda(t,a)+\mu_d(a)\big]S(t,a), \tag{6.5}$$

$$\frac{\partial I(t,a)}{\partial t} + \frac{\partial I(t,a)}{\partial a} = \lambda(t,a)S(t,a) - \big[v(a)+\mu_d(a)\big]I(t,a), \tag{6.6}$$

$$\frac{\partial R(t,a)}{\partial t} + \frac{\partial R(t,a)}{\partial a} = v(a)I(t,a) - \mu_d(a)R(t,a), \tag{6.7}$$

where

$$\lambda(t,a_s) = \frac{1}{N}\int_0^\infty \beta(t,a_s,a_i)\; I(t,a_i)\; da_i. \tag{6.8}$$

The boundary conditions correspond to the current birth rates of seronegative and seropositive newborns, given by,

$$M(t,0) = \int_\tau^\infty C(t,Ab)\; dAb, \qquad S(t,0) = \int_0^\tau C(t,Ab)\; dAb, \qquad I(t,0) = 0, \tag{6.9}$$

where the function $C(t,Ab)$ describes a random distribution of cord log antibody titres. The rate at which maternally protected newborns become fully susceptible to infection is then described by the expression:

$$Q(a) = \omega_M\; C(\omega_M a+\tau)\; e^{-\int_0^a \mu_d(\alpha)d\alpha}. \tag{6.10}$$

The work by Williams et al. [1995] suggests the use of a Gaussian distribution as an appropriate model for population MAb titres in measles and this assumption

is also adopted in this work. Nominal characteristics for maternally acquired antibodies are derived according to those observed for hRSV by Cox et al. [1998], where similar characteristics have also been reported by Ochola et al. [2009]. In this instance, the static cord titre distribution $\hat{C}(Ab)$ has mean, $\bar{C} = 3.0$ log AU, and standard deviation, $\sigma_C = 0.39$, where the rate of MAb decay, ω_M, is 3.67 yr^{-1}, and the threshold for susceptibility, τ is 1.7 log AU.

Since the dependency of newborn serology is decoupled from that of the child bearing population, the process of age dependent fertility is not considered and a constant inflow of births is represented by the integral of $\hat{C}(Ab)$ with respect to Ab. The resulting birth rate coefficient is subsequently assumed to be equal to that used in previous examples such as for the UK ($\mu = 0.014$) or The Gambia ($\mu = 0.041$).

An age dependent mortality function, $\mu_d(a)$, is chosen to emulate Type I survivorship, that is where mortality rates are greatest among older individuals. The resulting population age distribution, $N(a)$, is generally regarded as a better approximation to human populations than that of Type II survivorship (where $\mu_d(a)$ is a constant coefficient), particularly for populations in more developed countries [Anderson and May, 1991]. For simplicity, this is implemented as a step function of the form:

$$\mu_d(a) = \begin{cases} 0 & \text{for} \quad a \leq L, \\ \infty & \text{for} \quad a > L, \end{cases} \tag{6.11}$$

where $L = \mu^{-1}$ corresponds to the average life expectancy. In the context of the model, which is focussed predominantly on primary infection in neonatal age classes, the most significant aspect of this assumption is the resulting neglection of infant mortality. Again this is reasonable for the consideration of developed populations, where mortality rates in the first year of life are typically less than 1%, however, it may be less appropriate for communities in developing regions.

Maternal immunisation is applied to the model according to Section 3.4.3, where a function $V_M(Ab)$ (a random distribution of scalar increases in log AU) is used to manipulate the initial cord log antibody titre distribution, $C(t, Ab)$, such that,

$$C_v(t, Ab) \;=\; (1 - P_m)C(t, Ab) + P_m \int_0^{Ab} \frac{C(t, z)V_M(Ab/z)}{\bar{C}} dz. \tag{6.12}$$

The distorting function, $V_M(Ab)$, is again assumed to be Gaussian, where $\bar{V}_M$ and σ_{V_M} denote the mean and standard deviation of this distribution, respectively. As in previous examples, the parameter P_m corresponds to the proportion of pregnant women who successfully respond to the vaccine. The best documented example of a candidate vaccine trial of this type for hRSV is that presented by Munoz et al. [2003]. The study reports a 4 fold increase in the geometric mean concentrations of hRSV IgG Ab in infants born to vaccine recipients compared to those of mothers who received a placebo. However, an increase of only $0.5 \log 2$ AU was observed for neutralising antibodies. In the model, the immunising effects on the mother are neglected since in the MSIR example virtually all individuals are already immune by the time they reach child bearing age.

As continually discussed throughout this work, in reality, pathogen transmission is often a highly heterogeneous process with potentially complex interdependencies on social interaction, physiological development and immunological experience of the host. However, estimation of these functions from empirical observation is critically impeded by the issues of indeterminacy described in Section 2.4.1. The most practicable approach to this problem has arisen from the combined works of Grenfell and Anderson [1985], who present a maximum-likelihood methodology for estimating age-related changes in the rate of infection, $\lambda(a)$, from serological data, and that of May and Anderson [1984], and Schenzle [1984], who impose constraints on the structure of $\beta(a_s, a_i)$ such that it may be estimated explicitly.

The technique presented by Grenfell and Anderson [1985] initially involves modelling the average force of infection as an arbitrary degree polynomial of the form:

$$\lambda(a) \;=\; \begin{cases} \displaystyle\sum_{i=0}^{k} b_i\, a^i & \text{for} \quad M < a \leq L, \\ 0 & \text{for} \quad a \leq M, \end{cases} \tag{6.13}$$

where L and M denote the upper and lower age limits, respectively, and k is the order of the expression. The resulting cumulative distribution of seropositive individuals, given by the function:

$$F(a) \;=\; \begin{cases} 1 - \exp\left[-\displaystyle\sum_{i=0}^{k} \left(b_i\, \frac{a^{i+1} - M^{i+1}}{i+1} \right) \right] & \text{for} \quad M < a \leq L, \\ 0 & \text{for} \quad a \leq M, \end{cases} \tag{6.14}$$

is then fitted to empirical age serological profile data, in order to estimate the polynomial coefficients, b_i, for $i = 0, \ldots, k$. In the original work, the method is applied to a number of datasets corresponding to records of measles incidence in the UK and USA, for which the estimated rates of infection consistently rise to a peak at around 10 years of age and decline thereafter [Grenfell and Anderson, 1985]. In addition, the results from a series of further studies for pertussis, measles, mumps, rubella, chicken pox and scarlet fever are collated in the book by Anderson and May [1991]. The review reports a striking similarity in the age-specific force of infection, with a consistent peak in $\lambda(a)$ occurring between 5-15 years of age across the range of studied infections.

Unfortunately, the lower age limit, M, is included in functions (6.13) and (6.14) in order to avoid obscurity due to the presence of maternally acquired antibodies. It is found that the estimation of $\lambda(a)$ in this age region is significantly hindered by ambiguity between genuine seroconversion due to experience of infection and residual MAb. In this instance, longitudinal serological data, such as that discussed in the work by Ochola et al. [2009], is required in order to detect increasing Ab titres that are indicative of an active immune response. However, the inference of infection rates from analyses of this nature is still limited by restrictions on serum

sampling frequencies, measurement error and confidence in the interpretation of results below the limit of quantification. Consequently, in order to further the analysis in this work, a series of example transmission functions are speculated in order to characterise potential patterns of infection resulting from common and vertical age biased social mixing, and decreasing susceptibility due to physiological development among young infant age classes.

6.2.2 Simulation Results

Simulation of the system is performed in order to give insight into the potential effects of maternal immunisation on age specific infection patterns among young infants. Average age profiles of incidence and serology are presented for various intervention characteristics and age specific transmission functions. The full PDE model structure, given by (6.4)-(6.9), is solved according to Appendix B using simple numerical methods based on an explicit 3rd order backwards difference scheme [Chapra and Canale, 2002]. More sophisticated algorithms have been presented for problems of this nature, see for example the work by White [2000], however, the simple approach is adopted in this work for ease of implementation and to minimise time required for computation. The techniques are considered to be appropriate since the outcomes of the analysis are largely qualitative in nature.

Constant Transmission Function

The model is first considered in the most simple case with non-seasonal and homogeneous transmission. The transmission function is therefore assumed to be constant with respect to time and age, where a nominal value of $\beta = 2490\,\text{yr}^{-1}$ is chosen to give a typical force of infection, $\lambda = 0.84\,\text{yr}^{-1}$, for hRSV. In the absence of maternal immunisation, the simulation results are qualitatively comparable to

the age serological profile data presented by Cox et al. [1998] (Figure 6.5). The model predicts a peak in the proportion of the population susceptible (nadir in proportion seropositive) of around 80%, occurring at 0.60 years (7.2 months) of age, and around 90% of individuals having experienced infection by 3 years of age.

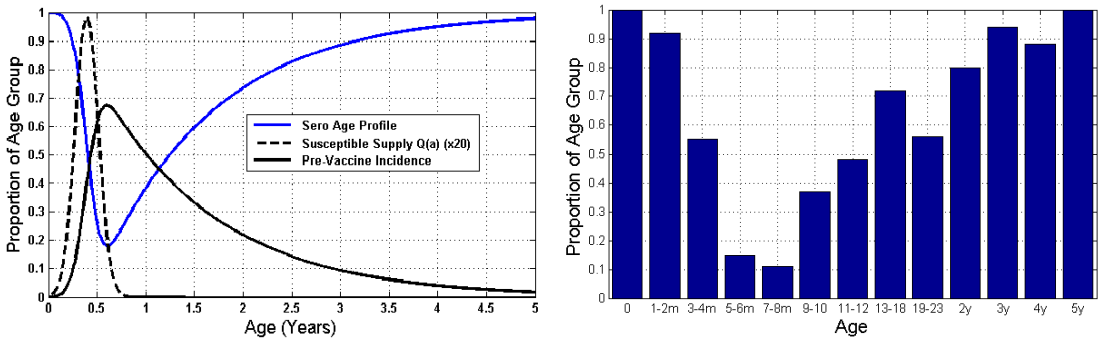

(a) PDE Model Simulation (b) hRSV Age Serological Data

Figure 6.5: Comparison between simulation results for the PDE MSIR model with non-seasonal and homogeneous transmission, and age serological survey data presented in the work by Cox et al. [1998], where incidence is presented as a proportion of the net birth rate, μN.

It can be seen from Figure 6.5(a) that the peak ages for incidence and susceptible supply occur at around 0.60 years (7.2 months) and 0.35 years (4.3 months) of age, respectively. Since the distribution $\hat{C}(Ab)$ is assumed to be Gaussian, the peak age of susceptible supply also corresponds to the estimated average duration of protection afforded by MAb. This prediction is notably higher than that documented in the original work by Cox et al. [1998], where a simpler first order elimination model is used to estimate an average duration of around 0.27 years (3.3 months).

The average age at primary infection is calculated using (2.39) and found to be 1.57 years (18.8 months), which is 0.32 years (3.8 months) greater than that predicted by the ODE models examined in Section 6.1 (Figure 6.4). The proportion of newborns who become susceptible below a specified age may be found by evaluating the integral expression given by (3.94). For the parameter values applied to the model, it is estimated that only 0.04% of newborns are born immediately susceptible to infection. However, it is also shown that 91.6% of infants are likely

to become susceptible before the age of 6 months. In order to protect all individuals at risk of infection in this age region, an immunologically interacting vaccine would need to invoke an effective response in mothers with antibody titres of at least 3.54 log AU.

A non-interacting maternal immunisation campaign is applied to the model according to Section 6.2.1 and a series of simulations performed in order to examine the impact of the intervention. Results obtained for a range of values for the mean vaccine efficacy, $\bar{V}_M$, (with standard deviation, $\sigma_{V_M} = 0.25$) and the effective vaccination coverage, P_m, are presented in Figure 6.6 and Table 6.1. It should be noted that since $\bar{C} = 3.0$ log AU, mean vaccine efficacies of $\bar{V}_M = 1.46$ and $\bar{V}_M = 1.60$ correspond roughly to a 4- or 6- fold average increase in antibody titre, respectively.

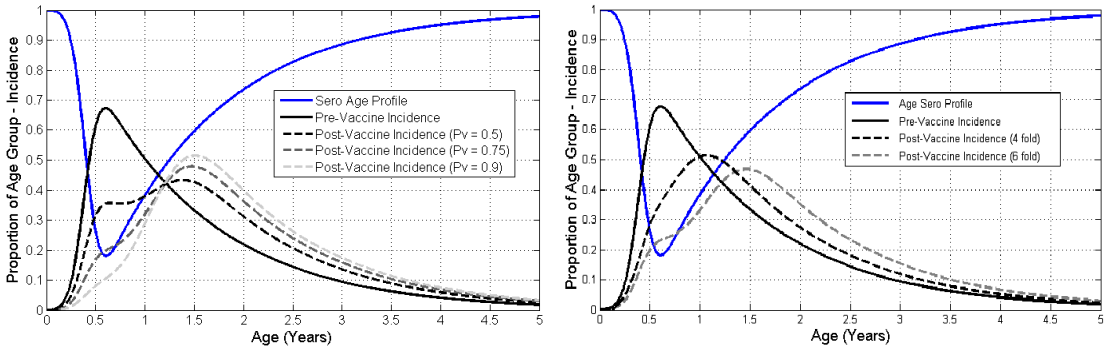

(a) Responses to various P_m, at $\bar{V}_M = 1.46$ (b) Responses to various $\bar{V}_M$, at $P_m = 0.75$

Figure 6.6: Predicted outcomes of mass maternal immunisation applied to a fundamental decoupled MSIR model structure with non-seasonal and homogeneous transmission; evaluated for various values of vaccine coverage and efficacy, where incidence is presented as a proportion of the net birth rate, μN.

In response to the intervention, the simulations show an upward spreading of the incidence age profile, leading to a moderate rise in the average age at primary infection (Figure 6.6). There is also a significant reduction in the proportion of individuals acquiring infection below 1 year and below 6 months of age, with notably more success in the younger of the two age groups (see Table 6.1). In this context, the results concur that maternal immunisation is a potentially efficacious

intervention strategy with respect to reducing neonatal infection. However, it can also be seen that the predicted distortion in the susceptible age profile consequently leads to a decrease in the peak value. Hence, passive immunisation may prove detrimental to the task of targeting active childhood vaccination to the nadir in seropositivity (peak age of susceptibility), thereby increasing the degree of potential interaction. This effect appears to be more pronounced for midrange vaccination coverage, where neither the vaccinated or unvaccinated characteristic curves dominate the resulting age profile.

Table 6.1: Predicted outcomes of mass maternal immunisation applied to a fundamental decoupled MSIR model structure with homogeneous transmission; evaluated for various values of vaccine coverage and efficacy.

Proportion of Coverage P_m	Mean Vaccine Efficacy $\bar{V}_M$	Average Age at Infection (years)	Proportion Infected < 6 months	< 1 year
0	N/A	1.57	9.4%	39.7%
0.5	1.47	1.78	5.4%	27.6%
0.75	1.47	1.89	3.4%	21.7%
1	1.47	2.00	1.4%	15.8%
0.75	1.23	1.74	5.5%	29.5%
0.75	1.47	1.89	3.4%	21.7%
0.75	1.60	1.98	2.8%	18.0%

The results in Table 6.2 show the effects of differing degrees of variance for the vaccine response distribution. It can be seen that greater variability in vaccine response appears to advance the increase in average age at primary infection, but also leads to less effective prevention of infection among the proportion of individuals under 6 or 12 months of age.

It should also be noted that the overall prevalence of infection, calculated from the integral of $J(a)$ with respect to a, remains unchanged following the implementation of the vaccine. This result is contrary to that predicted by the ODE models in Section 6.1 (see Figure 6.3), and is a consequence of neglecting the immunising response of the mother, and of the inclusion of an age-specific mortality function

Table 6.2: Predicted outcomes of mass maternal immunisation applied to a fundamental decoupled MSIR model structure with homogeneous transmission, for various values of vaccine coverage and variance in efficacy.

Proportion of Coverage P_m	Standard Deviation Vaccine Efficacy σ_{V_M}	Average Age at Infection (years)	Proportion Infected < 6 months	< 1 year
0	N/A	1.57	9.4%	39.7%
0.25	0.1	1.67	7.1%	33.4%
0.25	0.25	1.682	7.4%	33.7%
0.25	0.5	1.70	7.7%	33.5%
0.75	0.1	1.88	2.6%	20.8%
0.75	0.25	1.89	3.4%	21.7%
0.75	0.5	1.96	4.6%	21.4%

based on simplified Type II survivorship. It indicates that in homogeneous systems with low infant mortality rates, maternal immunisation does not reduce the overall prevalence of infection, unless there is significant herd immunity resulting from vaccination of the mother.

Constant Common Age Transmission Bias

The first heterogeneous transmission profile to be considered is a diagonally symmetric, non-decreasing function of age, that is constant with respect to time (see Figure 6.7(a)). The function corresponds to a situation where the primary route of transmission is biased towards more frequent mixing between similar aged individuals. Social interactions that potentially spread infection are often more common between individuals of similar ages due to common social development and the structure of the education system. Simulation results are shown in Figure 6.7(b), where mass maternal immunisation is applied with a mean vaccine efficacy of 1.47 (approximately a 4 fold average increase in MAb) and a coverage, $P_m = 0.75$.

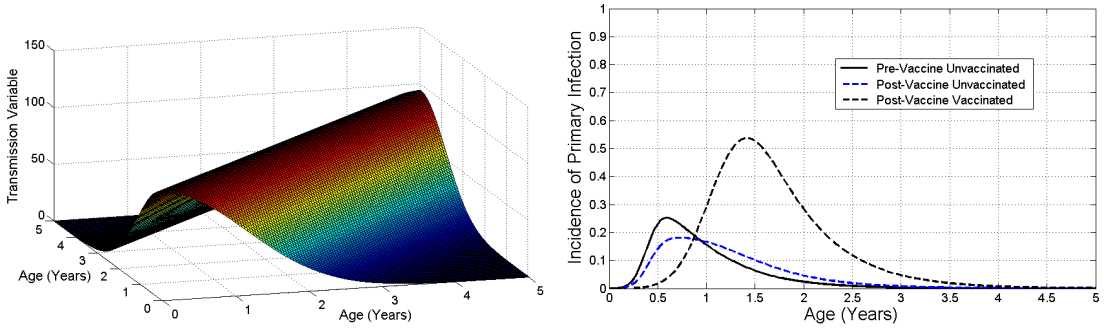

(a) Transmission Function (b) Incidence Age Profile

Figure 6.7: Simulation results comparing pre- and post-mass maternal immunisation incidence age profiles obtained using a decoupled MSIR model structure with common age biased transmission; evaluated for $\bar{V}_M = 1.47$, $\sigma_{V_M} = 0.25$ and $P_m = 0.75$, where incidence is presented as a proportion of the net birth rate, μN.

The model suggests that if transmission is higher among similar aged individuals, then raising the average age of infection among vaccinated individuals subsequently reduces the force of infection acting on unvaccinated individuals at younger ages and increases it at later ages. This leads to a lower incidence of infection in younger (unvaccinated) age classes, subsequently raising the average age of infection. Therefore, in this instance it can be noted that maternal immunisation is potentially beneficial for the infant population as a whole, including those that are not directly immunised by the vaccine. The overall prevalence of infection is again found to be unaffected by the intervention.

Vertical Age Transmission Bias

In the second example, the transmission function is biased such that the primary source of infection for relatively well protected neonates and very young children is from older age groups, for example through interaction with elder siblings residing in a higher risk (school or preschool) age class. The resulting transmission profile (shown in Figure 6.8(a)) is diagonally symmetric, constant in time, but increasing with respect to age. Simulation results corresponding to the static system response to immunisation are displayed in Figure 6.8.

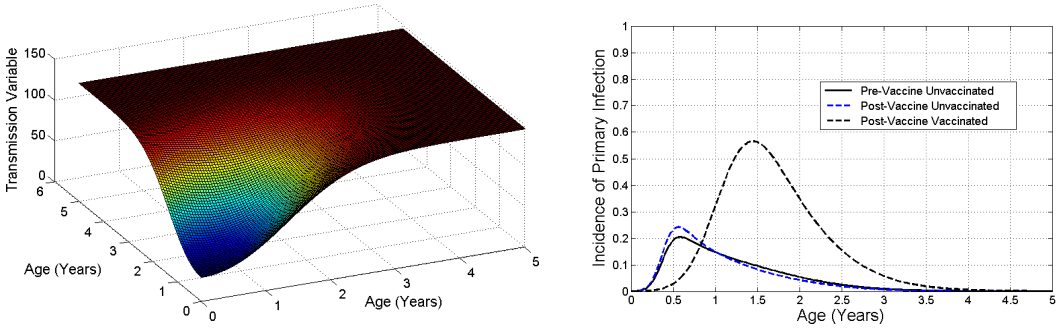

(a) Transmission Function (b) Incidence Age Profile

Figure 6.8: Simulation results comparing pre- and post-mass maternal immunisation incidence age profiles obtained using a decoupled MSIR model structure with vertical age biased transmission; evaluated for $\bar{V}_M = 1.47$, $\sigma_{V_M} = 0.25$ and $P_m = 0.75$, where incidence is presented as a proportion of the net birth rate, μN.

In this case, the force of infection applied to younger unvaccinated infants may be increased as a result of increasing the average age of infection in the vaccinated proportion. The simulation results shown in Figure 6.8 suggest that the implementation of a maternal immunisation campaign to a system of this type may in fact prove detrimental to those individuals who do not directly receive the vaccine, consequently reducing their average age at primary infection. The total proportion of individuals ultimately infected for pre- and post-vaccine implementations are compared as previously described and again suggest no significant impact from the intervention.

Non Symmetrical Decreasing Transmission Bias

The final heterogeneous transmission example corresponds to a situation where the susceptibility of the infant decreases with increasing age. This relation could be the result of some aspect of physiological development, for example, larger and more robust airways. The transmission function, shown in Figure 6.9(a), is therefore assumed to be non-diagonally symmetric and represents an age specific change in the host rather than social mixing patterns. Simulation results for the vaccinated and unvaccinated age profiles of primary incidence are shown in Figure 6.9(b).

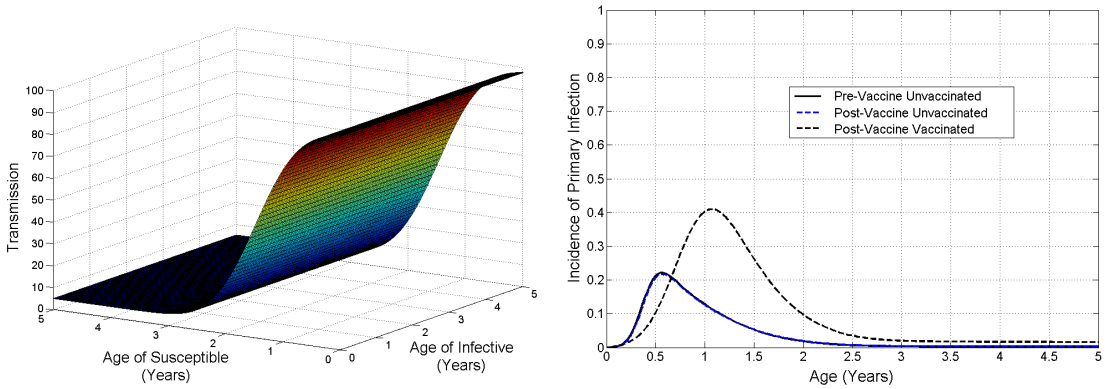

(a) Transmission Function (b) Incidence Age Profile

Figure 6.9: Simulation results comparing pre- and post-mass maternal immunisation incidence age profiles obtained using a decoupled MSIR model structure with non-symmetrical decreasing transmission; evaluated for $\bar{V}_M = 1.47$, $\sigma_{V_M} = 0.25$ and $P_m = 0.75$, where incidence is presented as a proportion of the net birth rate, μN.

The simulation suggests there is little difference in the risk experienced by pre- and post-vaccine unvaccinated individuals. However, the total proportion of individuals infected in the post-vaccine system (area under incidence age profile) is found to be 0.74, which is notably lower than the pre-vaccine proportion of 0.87. This indicates that maternal immunisation may result in reduced prevalence of infection in this type of system. However, in practical terms the decrease in $\beta(a_s, a_i)$ must originate from an initial value high enough to facilitate a very low average age at primary infection, to a final value low enough to sufficiently reduce basic reproduction, and within relatively close proximity of the region between pre- and post-vaccine average duration of MAb.

6.3 Times Series Analysis of Dynamic & Seasonal Responses

The static based analyses reported in the previous sections of this chapter have indicated that maternal immunisation is unlikely to notably affect long term pop-

ulation infection levels unless there exists some specific pattern of heterogeneity within neonatal and young infant age classes. However, interventions of this type do have a direct influence over the rate of susceptible supply, which is a key factor in the observed dynamic behaviour of epidemic systems. The two main objectives of this section are to demonstrate how MSIR framework models may be used to establish, firstly, whether stimulating greater neonatal immunity through maternal immunisation has the potential to significantly perturb stable endemic systems, and secondly, whether interventions of this type may benefit from seasonal targeting in cases where recurrent epidemic behaviour is driven by temporal forcing.

Time dynamic behaviour is simulated using the MSIRS2 ODE model with maternal immunisation (3.27)-(3.32) and the decoupled PDE system (3.81)-(3.85), which is extended to also include additional state variables corresponding to secondary infection. As in previous examples, the MSIRS2 model is solved using the `ode45` algorithm in MATLAB and the PDE model according to Section 6.2.1 where state variable solutions are integrated with respect to age in order to isolate population wide time series dynamics. Parameter values are set corresponding to those elicited in Section 3.5 for hRSV with varying degrees of reinfection. In the PDE model the transmission function, $\beta(t, a_s, a_i)$, is considered to be constant with respect to age and mortality is assumed to follow the Type I survivorship function given by (6.11). The cord log antibody titre distribution, $\hat{C}(Ab)$, and the vaccine response function, $V_M(Ab)$, are parameterised as in Section 6.2.1, such that they emulate the observations of Cox et al. [1998], and Munoz et al. [2003].

6.3.1 Dynamic Consequences of Intervention

Recalling from Section 2.1.2, it is discussed that unforced epidemic systems, particularly those with a short duration of infection and relatively slow rate of susceptible supply, have a strong propensity to oscillate following perturbation away from a

stable endemic steady state [Anderson and May, 1991]. In this instance, rapid implementation of public health interventions that lead to an appreciable reduction in population susceptibility have the potential to evoke significant epidemic behaviour while the system converges back to endemic equilibrium [Scherer and McLean, 2002].

In the absence of infant mortality, the total inflow of susceptible individuals is found to converge to that of the population net birth rate, μN. Assuming that the implementation of a mass maternal immunisation campaign yields a positive distortion of the cord antibody titre distribution, the intervention will result in an increase in the average duration of immunity between unvaccinated and vaccinated generations of newborns. This leads to a temporary decrease in susceptible supply, with magnitude and duration dependent on the efficacy of the vaccine and the proportion of pregnant mothers to which it is applied. Since maternally acquired immunity is passive and ultimately wanes with age, any reduction in susceptible supply invoked by higher MAb titres is unsustainable and will quickly return to its pre-vaccine rate. The resulting characteristic disturbance is illustrated in Figure 6.10(a), where simulation results are obtained for both the ODE and PDE versions of the MSIRS2 model evaluated at parameter values corresponding to hRSV with intermediate secondary infection (Tables 3.2 and 3.3(D)) and $P_m = 0.75$.

It can be seen from Figure 6.10(a) that both models predict a significant decrease in the rate of susceptible supply as a direct result of the immunisation. This leads to a reduction in the incidence of infection, which, when the rate of susceptible supply returns to its original value, allows for a rapid increase in the number of available susceptibles. This in turn triggers a series of epidemics as shown in Figure 6.10(b). In the ODE based system the rate at which maternally protected neonates become fully susceptible to infection is governed by simple first order elimination kinetics. This incurs an immediate response to the intervention that

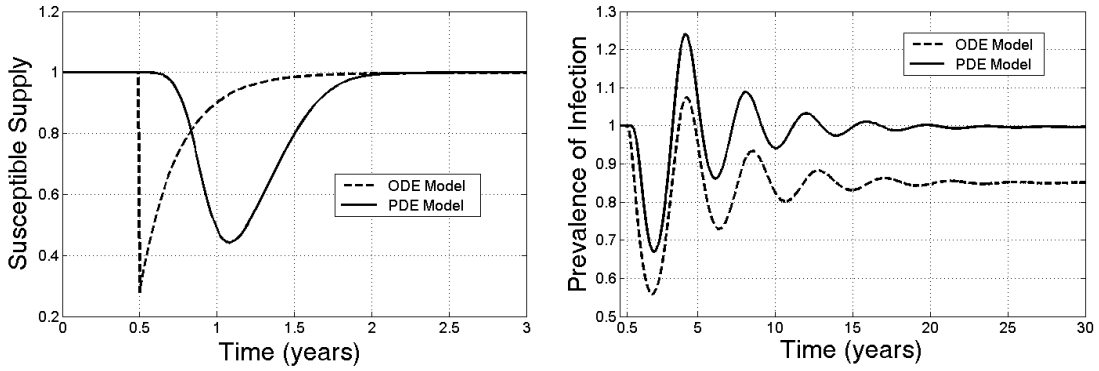

(a) Perturbation of Susceptible Supply (b) Predicted Dynamic Response

Figure 6.10: MSIRS2 ODE (coupled) and PDE (empirical/decoupled) model predictions for the dynamic response to perturbation from rapid implementation of a maternally targeted vaccine at $t = 0.5$ years. Susceptible supply and primary infection prevalence presented as a proportion of their steady state values.

converges exponentially back to its pre-vaccine rate (Figure 6.10(a)). In contrast, the PDE model prediction is determined by the resulting distortion of the cord titre distribution and the manner in which MAb wanes with age. This gives rise to a more gradual response curve with a notable delay in peak reduction caused by the propagation of seropositive individuals born prior to the intervention.

The epidemic oscillations observed following the implementation of the vaccine (Figure 6.10(b)) are the result of complex endemic steady state eigenvalues, as discussed in Section 2.1.2. Further investigation reveals that the observed differences in dynamics predicted by the two models result largely from the neglection of immunity acquired by the mother in the PDE model, rather than from decoupling the dependency of passive neonatal immunity on the wider population. The implications of this assumption also account for the offset in final value infection prevalence observed between the two models. This reiterates the suggestion that in homogeneous systems only the active response of the mother is likely to reduce overall population infection through herd immunity.

For comparison, Figure 6.11 shows the resulting dynamic response of the two models with parameter values corresponding to hRSV with varying infectivity

bias (see Table 3.3(B) and (C)). It can be seen from Figure 6.11(b) that increasing reinfection tends to reduce the highly oscillatory behaviour observed with more primary infection dominant systems, such as that shown in Figure 6.11(a). This illustrates that there is likely to be less risk of rebound epidemics associated with the rapid implementation of mass maternal immunisation in systems that display frequent reinfection of the host.

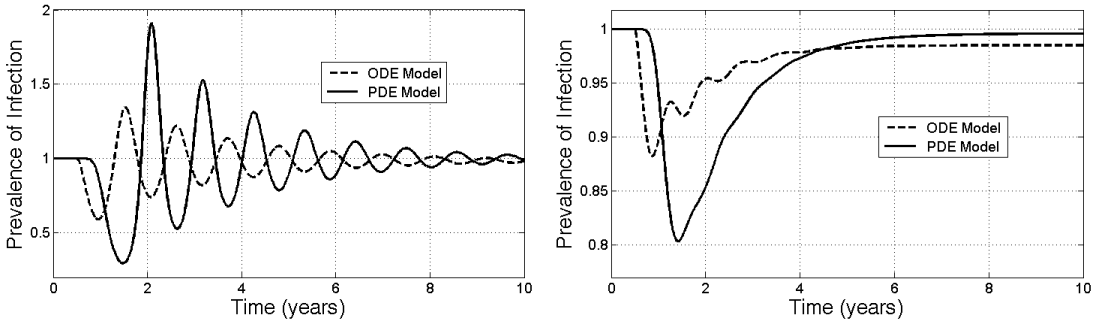

(a) Primary infection dynamics evaluated at $\beta_0 = 2490\text{yr}^{-1}$, $\omega_R = 1.8\text{yr}^{-1}$, $\sigma = 1$, $\gamma = 0$.

(b) Primary infection dynamics evaluated at $\beta_0 = 152\,\text{yr}^{-1}$, $\omega_R = 1.8\,\text{yr}^{-1}$, $\sigma = 1$, $\gamma = 1$.

Figure 6.11: MSIRS2 ODE and PDE system responses to perturbation by mass maternal immunisation at $t = 0.5$ years, presented as a proportion of pre-vaccine steady state values. Evaluated at parameter values corresponding to primary infection dominant, (a), or reinfection dominant, (b), transmission.

It should be noted that these characteristics may be evaluated in more detail through an eigenvalue analysis of the endemic steady state as described in Sections 2.1.2 and 3.3.5. It is also important to note that in cases where long term population infection levels are largely unaffected by the intervention, any subsequent oscillatory behaviour will result in epidemic peaks of infection that exceed pre-vaccination endemic levels.

6.3.2 Seasonality

Recalling from Section 2.1.3, many common infections tend to display large seasonal epidemics at endemic equilibrium, which are presumed to be sustained by

some form of temporal variation within the transmission function, $\beta(t)$ [Altizer et al., 2006]. In many cases such as measles and polio, pulse vaccination strategies are employed, whereby a vaccine is repeatedly administered independently of age and over very short periods of time [Nokes and Swinton, 1995]. Consequently, work such as that by Grassly and Fraser [2006] has sought to optimise the timing of periodic interventions with respect to the seasonal epidemic cycle, in order to maximise the impact of the vaccine.

Since maternal immunisation has been shown to directly influence the supply of susceptible individuals, it seems intuitive that there may be some notable advantage to seasonal targeting of the intervention in the context of systems with periodic temporal forcing. This is additionally supported given that the average duration of maternally acquired immunity is short with respect to typical epidemic time periods. Individuals who are immunised at such a time that their natural MAb titre would have waned shortly following an annual epidemic are unlikely to benefit from the vaccine if they are not significantly exposed to infection again until the following year. In this case it is hypothesised that immunisation should be targeted to those individuals who are likely to experience their first annual epidemic at around the time that low MAb titres wane to a susceptible level.

In order to assess the implications of alternative, seasonally targeted maternal immunisation strategies, the ODE MSIRS2 model, given by (3.27)-(3.32), is extended such that the proportional application of the intervention, $P_m(t)$, becomes a function of time. In the simplest case, maternal immunisation is administered during a single fixed period within each epidemic cycle. The relative timing of the immunisation pulse is then varied with respect to the epidemic interval in order to optimise the efficacy of the intervention. Temporal variation in the transmission of infection is included within the model as in previous examples using the sinusoidal function given by (2.14). The model is also further extended into a number of discrete age classes according to Section 3.4.1, such that the number of primary infections below a specific target age may be evaluated.

Simulation results are obtained using a two age class model structure, where the ageing parameter, $k_1 = 2\text{yr}^{-1}$, is set such that primary infection prevalence may be estimated among children under 6 months of age. For simplicity, all other model parameters are assumed to be the same for both age classes and are set according to Tables 3.2 and 3.3(C) for hRSV with high levels of reinfection. Simulation results corresponding to an ideal ($P_m(t) = 1$) annual maternal immunisation campaign with a duration of 3 months are shown in Figure 6.12(a).

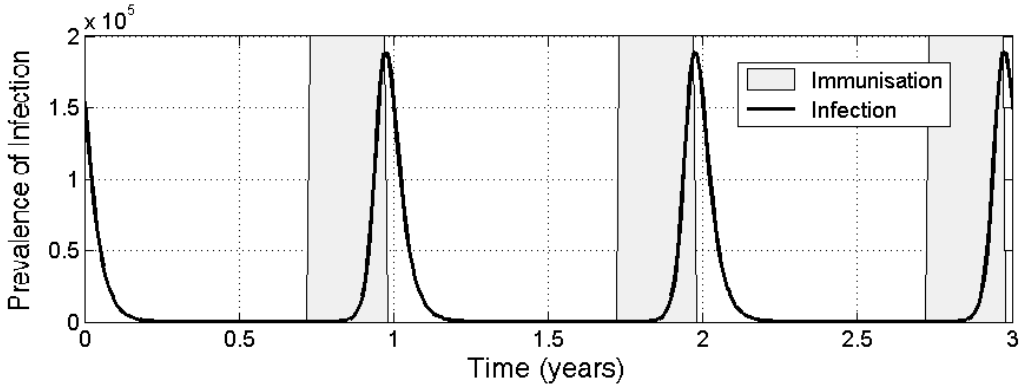

(a) Primary infection prevalence under 6 months of age with optimal maternal immunisation.

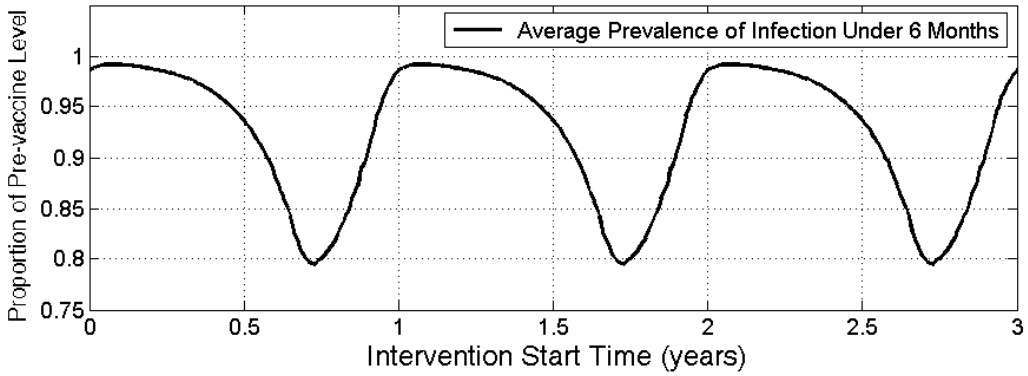

(b) Proportion of pre-vaccine primary infection level with respect to intervention timing.

Figure 6.12: Simulation results for a seasonally forced MSIRS2 model with variably timed 3 month pulse maternal immunisation. Evaluated at parameter values for hRSV with highly prevalent reinfection.

It can be seen from Figure 6.12(b) that the reduction in primary infection prevalence achieved varies between 0.8% and 20.5% depending on the timing of the intervention with respect to the epidemic cycle. This compares to a maximum reduction of 29.1%, which may be obtained with an untargeted intervention strat-

egy applied constantly throughout the year. The results suggest that the optimal implementation of a three month pulse strategy is during the period immediately prior to the annual epidemic peak of primary infection. This also coincides with the peak in population susceptibility, which additionally minimises the interaction between the vaccine and active immunity of the mother acquired from natural infection. It should be noted from Figure 6.12(b) that the impact of this particular intervention decreases rapidly either side of the optimum and that in practice, the epidemic peak of infection may be difficult to accurately predict three months in advance.

The analysis suggests that the potential benefit of seasonal targeting for a particular system is dependent on the ratio between the resulting increase in average duration of maternally acquired immunity and the inter-epidemic time period. For example, in cases such as hRSV infection in Finland, where seasonal epidemics are biennial, a significant reduction in vaccine effort may be achieved through pulse implementation. However, for infections where the inter-epidemic time period is similar or less than the potential increase in duration of MAb, the prospective benefits in efficacy are likely to be reduced.

Simulation results have clearly shown that there are likely to be potential benefits to pulse implementation of maternally targeted vaccines in seasonal systems. However, addition complexities such as the physical delay between vaccine administration to the mother and the birth of her offspring are required to be included in forthcoming versions of the model in order to facilitate more accurate predictions of optimal timing. In addition, it should be noted that the specificity of a particular strategy may also be diminished by variability in factors such as cord antibody titre and vaccine response distributions, consistency in the timing of epidemic peaks and again the duration of time between vaccine administration and full term.

6.4 Conclusions & Discussion

A series of MSIR framework models have been proposed for the study of population-level epidemiological processes associated with maternally acquired immunity. A preliminary analysis of this framework has been performed in order to gain insight into the potential outcomes and consequences of mass maternal immunisation, and to illustrate the importance of the subject. The discussed models have been shown to qualitatively repeat empirical observations of unvaccinated epidemic systems and their applicability in studying the wider implications of maternally targeted intervention has been demonstrated. It is hoped that the framework will ultimately contribute to the assessment and optimal implementation of future public health policy within this context.

Simulation of the models using nominal parameterisations have concurred that maternally targeted vaccines have the potential to appreciably reduce the incidence of infection among neonatal age classes. In cases such as hRSV, where a particularly low average age at primary infection is typically observed, interventions of this nature may prove invaluable to efforts aimed at alleviating the burden of disease within these age groups. However, it is anticipated that the potential consequences of mass maternal immunisation for the wider population are more variable and depend on a number of epidemiological factors such as age specific transmission characteristics and reinfection.

Population Level Outcomes

A series of static analyses have suggested that overall population infection levels may only be notably reduced by maternal immunisation if susceptibility, infectivity or survivorship decreases significantly between the pre- and post-vaccine average durations of maternally acquired immunity. In all static simulation examples,

the average age at primary infection and the prevalence of infection in younger ages for the vaccinated proportion of newborns showed improvements. However, the indirect consequences of immunisation to unvaccinated individuals appears to vary depending on the characteristic heterogeneity of the transmission function. Example transmission patterns have been illustrated that give rise to both beneficial and detrimental influences on infection among the remaining unvaccinated neonatal population.

Time series-based analyses have demonstrated that mass maternal immunisation has a direct impact on the rate that maternally protected infants become susceptible to infection. Simulation results suggest that any subsequent decrease in susceptibility arising from the intervention is ultimately only temporary. However, rapid implementation of a maternally targeted vaccine does have the potential to cause significant perturbations in susceptible supply that may notably alter the time course of the infection. Since a considerable decrease in long term prevalence is unlikely, any rebound epidemics that occur are likely to exceed endemic pre-intervention infection levels, posing an additional risk to newborns who remain unvaccinated.

The work has also provided evidence contributing to the question of whether maternally acquired immunity is a prominent driving force on seasonal epidemic cycles. For hRSV, studies such as those by Saux et al. [2003] and Stensballe et al. [2009] have reported significant seasonal variations in maternally derived antibody titres in newborns, and a strong correlation between neutralising MAb and seasonality of infection among infants under 6 months of age. This suggests that if variations in hRSV-neutralising MAb are reflective of those throughout the wider population, a coupled cyclic dependency between neonatal and population wide immunity may play an important role in the seasonality of hRSV in temperate climates [Stensballe et al., 2009]. However, simple comparisons between coupled and decoupled model structures in this work suggest, at least in the homogeneous case, that the dependency of immunity among newborns on that of the wider population does

not have a significant impact on dynamics. This is an interesting result since it indicates that for the presented examples, temporal variation in MAb may not have a significant influence on population wide patterns of infection.

The outcome is additionally supported in Section 6.3.2 for systems with high levels of reinfection, where minimal changes in seasonal epidemic behaviour are observed despite repeated variation in the maternally protected population induced by pulse maternal immunisation. However, the application of maternal immunisation to seasonally forced MSIR models, without processes of reinfection, has frequently given rise highly aberrant and possibly chaotic patterns of infection. Dramatic changes in the periodicity of epidemic cycles have been empirically observed following active intervention in cases such as measles [Bolker and Grenfell, 1996] and simple compartmental based models have been shown to qualitatively repeat these observations in work such as that by Earn et al. [2000]. However, due to the inherently complex and nonlinear nature of these processes, it is not certain that the transitions between regular and irregular dynamics are correctly described by the models presented in this work. Subsequently, the apparent suggestion that maternal immunisation has the potential to destabilise long term recurrent epidemic cycles of childhood diseases remains inconclusive without more formal validation.

Interaction and Optimisation

The study has highlighted the potential significance of antibody interaction with respect to the success of combined (maternally and childhood targeted) intervention strategies. For many childhood infections circulating within developed populations there is a sufficient window of opportunity to implement mass age targeted (childhood) vaccination campaigns that both avoid interaction with MAb and succeed in preventing a significant amount of susceptibility to natural infection. However, in more developing settings, where transmission rates among pre-school children are often much higher, and with more virulent infections such as hRSV,

it is not always possible to delay vaccination beyond the complete duration of MAb. In situations such as these, the upward distortion in susceptible age profile resulting from the implementation of mass maternal immunisation, may prove additionally detrimental to the success of childhood vaccines targeted at the peak age of susceptibility.

The analysis of intervention strategies applied to models with seasonal forcing has illustrated the potential merit for pulsed implementation of maternally administered vaccines. This study has found that the likely benefit for seasonal targeting is dependent on the ratio between the resulting increase in average duration of passively acquired immunity and the inter-epidemic time period. It has been shown through simulation of the model that the optimal time for intervention is immediately prior to the annual epidemic peak of infection. However, additional factors including the duration of time to full term and variability in determinants such as cord antibody titre, vaccine response and epidemic timing must also be considered in order to achieve a fully optimal strategy.

Chapter 7

Final Discussion & Future Research

The objective of this work has been to consider the population level influences of maternally acquired immunity and the potential outcomes and consequences of mass maternal immunisation. A series of lumped system models have been proposed as part of a general mathematical model framework for studying a number of distinct problems within this context. The analysis and simulations presented in Chapter 6 have demonstrated the applicability of these models to real world scenarios and raised a number of pertinent questions regarding the safe and optimal implementation of maternally targeted interventions. The work has also considered the impact of maternally acquired immunity on aspects of model validation through the application of formal methods such as structural identifiability, indistinguishability and sensitivity analysis. It is found in Chapters 4 and 5 that the confident estimation of model parameters through fitting to real data is likely to be a markedly non-trivial task.

Maternal Immunisation

A qualitative analysis of the proposed models has shown that maternally targeted vaccination has the potential to appreciably reduce the incidence of infection among neonatal and young infant age classes. In all static simulation examples the models have predicted notable improvements in both the average age at primary infection and the prevalence of infection among infants under 6 months of age. In cases such as hRSV, where a particularly low average age at primary infection is typically observed, these results may prove invaluable to efforts aimed at alleviating the burden of disease among the very young. The efficacy of the intervention is found to be dependent on successful seroconversion of the mother, sufficient transfer of antibodies before birth and the duration of maternally acquired antibodies within the newborn. Variability in these characteristics is currently included within the model, however, an intuitive progression from this work would be to consider variation in the neutralising characteristics of MAb.

Low levels of neutralising MAb are likely to result in partial immunity, similar to that described in altered secondary infection models [White et al., 2007], which could have significant implications on the outcome of neonatal infection. The problem may also be extended to consider the effects of cross reaction between multiple strain variants as described in the work by White et al. [1998]. A common epidemiological observation of hRSV are complex patterns of homologous and heterologous infection and a seasonal alternation between two dominant genotypes [White et al., 2005]. It is hypothesised in the review by Cane [2001] that these observed patterns may in fact be governed by high levels of maternal antibody present after an epidemic of a particular strain. An interesting subject of further research may be to explore these interactions using compartmental based models and to consider the implications of control by maternally targeted vaccines.

A static analysis of age dependent model structures with heterogeneous transmission functions has been used to highlight characteristic examples where the

implementation of mass maternal immunisation may have beneficial or detrimental consequences to unvaccinated newborns and to the population as a whole. It is suggested by the model that a substantial change in social interaction, physiological development or survivorship is required within the region of 3 to 9 months of age in order to induce a significant impact on long term infection characteristics. A valuable route of future research may therefore be towards better characterisation of neonatal and young infant transmission patterns, perhaps through the identification of key factors such as the start of nursery or the typical composition of households, i.e. mixing with elder siblings etc.

Time series-based simulations suggest that the greatest risks associated with mass maternal immunisation reside in the form of short term dynamics resulting from rapid implementation of the vaccine and the potential interaction with childhood targeted interventions. It is found that maternal immunisation has a temporary but direct impact on the rate of susceptible supply, where significant perturbations may notably alter the time course of the infection. In cases where the long term population wide prevalence of infection remains largely unchanged, any rebound epidemics are likely to exceed pre-intervention endemic levels. The work dictates that sufficient care must be taken to ensure that interventions are not aggressively implemented within highly oscillatory systems.

It is also strongly suggested that the potential interactions between maternally and childhood targeted vaccines are exhaustively considered. The subsequent distortion in the susceptible age profile resulting from the implementation of mass maternal immunisation may prove detrimental to the success of childhood vaccines targeted at the peak age of susceptibility. This could be particularly problematic in cases where there is a narrow window of opportunity between the duration of MAb and the average age at primary infection. A potential opportunity for future application of the proposed models may be in the optimisation of combined intervention strategies, where, for example, the benefits of seasonally pulsed administration could be further utilised to minimise interaction between vaccines.

Model Validation

The proposed model framework has been shown to qualitatively repeat empirical observations of unvaccinated epidemic systems, however, further validation of these models, and particularly those including processes of intervention, is a markedly non-trivial task. A structural identifiability analysis of fundamental ODE models within the proposed framework has shown that key parameters are not uniquely determined by age domain observations of infection. Furthermore, it has been shown that homogeneous time-series models are highly insensitive to processes associated with maternally acquired immunity and that the addition of vaccination tends to have an additionally detrimental effect on parameter identifiability. It is suggested that further validation of these models through fitting to population data will require very specific longitudinal based studies that provide both age and time domain records of infection and serology. The outcome of a formal sensitivity analysis has also highlighted the necessity for optimal sampling during the collection of such data. It is hoped that the outcome of this work may be of use in guiding the design of future studies in order to maximise the amount of information gained from parameter estimation.

Bibliography

D. Alonso, A. J. McKane, and M. Pascual. Stochastic amplification in epidemics. *J R Soc Interface*, 4(14):575–582, 2007.

S. Altizer, A. Dobson, P. Hosseini, P. Hudson, M. Pascual, and P. Rohani. Seasonality and the dynamics of infectious diseases. *Ecol Lett*, 9(4):467–484, 2006.

R. M. Anderson. The concept of herd immunity and the design of community-based immunization programmes. *Vaccine*, 10(13):928–935, 1992.

R. M. Anderson and B. T. Grenfell. Control of congenital rubella syndrome by mass vaccination. *Lancet*, 2(8459):827–828, 1985.

R. M. Anderson and R. M. May. Vaccination against rubella and measles: quantitative investigations of different policies. *J Hyg (Lond)*, 90(2):259–325, 1983.

R. M. Anderson and R. M. May. Age-related changes in the rate of disease transmission: implications for the design of vaccination programmes. *J Hyg (Lond)*, 94(3):365–436, 1985.

R. M. Anderson and R. M. May. *Infectious Diseases of Humans: Dynamics and Control*. Oxford University Press, 1991.

H. Andersson. *Stochastic epidemic models and their statistical analysis*. Spinger, New York, 2000.

G. E. B. Archer, A. Saltelli, and I. M. Sobol. Sensitivity measures, ANOVA-like

techniques and the use of bootstrap. *J Statist Comput Simul*, 58(2):99–120, 1997.

M. Ballow, K. L. Cates, J. C. Rowe, C. Goetz, and C. Desbonnet. Development of the immune system in very low birth weight (less than 1500 g) premature infants: concentrations of plasma immunoglobulins and patterns of infections. *Pediatr Res*, 20(9):899–904, 1986.

H. T. Banks and A. Cintrón-Arias. Parameter selection methods in inverse problem formulation. Technical report, Center for Research in Scientific Computation, Feb 2010.

H. T. Banks, S. Dediu, and S. E. Ernstberger. Sensitivity functions and their uses in inverse problems. *J Inv Ill-posed Problems*, 15:638–708, 2007.

J. Batzel, G. Baselli, R. Mukkamala, and K. H. Chon. Modelling and disentangling physiological mechanisms: linear and nonlinear identification techniques for analysis of cardiovascular regulation. *Phil Trans R Soc A*, 367(1892):1377–1391, 2009.

D. J. Bearup, N. D. Evans, and M. J. Chappell. The input-output relationship approach to structural identifiability analysis. *Proc UKACC Int Conf Control*, pages 132–137, 2010.

R. Bellman and K. J. Åström. On structural identifiability. *Math Biosci*, 7(3-4): 329–339, 1970.

G. Bellu, M. P. Saccomani, S. Audoly, and L. D'Angiò. Daisy: A new software tool to test global identifiability of biological and physiological systems. *Comput Methods Programs Biomed*, 88(1):52–61, 2007.

B. M. Bolker and B. T. Grenfell. Impact of vaccination on the spatial correlation and persistence of measles dynamics. *Proc Natl Acad Sci U S A*, 93(22):12648–12653, 1996.

O. Boubaker and A. Fourati. Structural identifiability of non linear systems: an overview. *Proc IEEE ICIT*, 3:1244–1248, 2004.

F. Boulier, D. Lazard, F. Ollivier, and M. Petitot. Computing representations for radicals of finitely generated differential ideals. *Appl Algebra Engrg Comm Comput*, 20(1):73–121, 2009.

A. H. Brandenburg, J. Groen, H. A. van Steensel-Moll, E. C. Claas, P. H. Rothbarth, H. J. Neijens, and A. D. Osterhaus. Respiratory syncytial virus specific serum antibodies in infants under six months of age: limited serological response upon infection. *J Med Virol*, 52(1):97–104, 1997.

P. A. Cane. Molecular epidemiology of respiratory syncytial virus. *Rev Med Virol*, 11(2):103–116, 2001.

V. Capasso. *Mathematical Structures of Epidemic Systems*. Springer-Verlag, 1993.

M. J. Chappell, K. R. Godfrey, and S. Vajda. Global identifiability of the parameters of nonlinear systems with specified inputs: a comparison of methods. *Math Biosci*, 102(1):41–73, 1990.

S. C. Chapra and R. P. Canale. *Numerical Methods for Engineers: With Software and Programming Applications.* McGraw-Hill, 4th edition, 2002.

C. Cobelli and J. J. DiStefano III. Parameter and structural identifiability concepts and ambiguities: a critical review and analysis. *Am J Physiol*, 239(1):7–24, 1980.

S. M. Cook, R. I. Glass, C. W. LeBaron, and M. S. Ho. Global seasonality of rotavirus infections. *Bull World Health Organ*, 68(2):171–177, 1990.

B. T. Costa-Carvalho, H. M. Vieria, R. B. Dimantas, C. Arslanian, C. K. Naspitz, D. Sol, and M. M. Carneiro-Sampaio. Transfer of IgG subclasses across placenta in term and preterm newborns. *Braz J Med Biol Res*, 29(2):201–204, 1996.

M. J. Cox, R. S. Azevedo, P. A. Cane, E. Massad, and G. F. Medley. Seroepidemiological study of respiratory syncytial virus in São Paulo State, Brazil. *J Med Virol*, 55(3):234–239, 1998.

J. E. Crowe. Influence of maternal antibodies on neonatal immunization against respiratory viruses. *Clin Infect Dis*, 33(10):1720–1727, 2001.

A. R. Curtis and W. P. Sweetenham. *FACSIMILE/CHEKMAT Users' Manual.* Harwell Laboratory Report AERE 12805, 1987.

B. Damien, S. Huiss, F. Schneider, and C. P. Muller. Estimated susceptibility to asymptomatic secondary immune response against measles in late convalescent and vaccinated persons. *J Med Virol*, 56(1):85–90, 1998.

H. Davies. *Introductory immunobiology.* Chapman Hall, London, 2nd edition, 1997.

D. Degenring, C. Froemelb, G. Diktac, and R. Takors. Sensitivity analysis for the reduction of complex metabolism models. *J Process Control*, 14(7):729–745, 2004.

O. Diekmann, J. A. Heesterbeek, and J. A. Metz. On the definition and the computation of the basic reproduction ratio R0 in models for infectious diseases in heterogeneous populations. *J Math Biol*, 28(4):365–382, 1990.

K. Dietz. The estimation of the basic reproduction number for infectious diseases. *Stat Methods Med Res*, 2(1):23–41, 1993.

N. N. Dougherty and H. C. Meissner. Respiratory syncytial virus immunoprophylaxis: impact on epidemiology. *Paediatr Drugs*, 2(2):127–132, 2000.

D. J. Earn, P. Rohani, B. M. Bolker, and B. T. Grenfell. A simple model for complex dynamical transitions in epidemics. *Science*, 287(5453):667–670, 2000.

W. J. Edmunds, G. F. Medley, D. J. Nokes, C. J. O'Callaghan, H. C. Whittle, and A. J. Hall. Epidemiological patterns of hepatitis B virus (HBV) in highly endemic areas. *Epidemiol Infect*, 117(2):313–325, 1996.

W. J. Edmunds, C. J. O'Callaghan, and D. J. Nokes. Who mixes with whom? A method to determine the contact patterns of adults that may lead to the spread of airborne infections. *Proc Biol Sci*, 264(1384):949–957, 1997.

J. A. Englund. Passive protection against respiratory syncytial virus disease in infants: the role of maternal antibody. *Pediatr Infect Dis J*, 13(5):449–453, 1994.

J. A. Englund. Maternal immunization with inactivated influenza vaccine: rationale and experience. *Vaccine*, 21(24):3460–3464, 2003.

J. A Englund and W. P. Glezen. Maternal immunization with Haemophilus influenzae type b vaccines in different populations. *Vaccine*, 21(24):3455–3459, 2003.

J. A. Englund, W. P. Glezen, and P. A. Piedra. Maternal immunization against viral disease. *Vaccine*, 16(14-15):1456–1463, 1998.

N. D. Evans, M. J. Chapman, K. R Godfrey, and M. J. Chappell. Identifiability of uncontrolled nonlinear rational systems. *Automatica*, 38:1799–1805, 2002.

N. D. Evans, M. J. Chapman, K. R. Godfrey, and M. J. Chappell. Structural indistinguishability between uncontrolled (autonomous) nonlinear analytic systems. *Automatica*, 40:1947–1953, 2004.

N. D. Evans, L. J. White, M. J. Chapman, K. R Godfrey, and M. J. Chappell. The structural identifiability of the susceptible infected recovered model with seasonal forcing. *Math Biosci*, 194(2):175–197, 2005.

A. R. Falsey and E. E. Walsh. Respiratory syncytial virus infection in adults. *Clin Microbiol Rev*, 13(3):371–384, 2000.

A. R. Falsey, H. K. Singh, and E. E. Walsh. Serum antibody decay in adults following natural respiratory syncytial virus infection. *J Med Virol*, 78(11): 1493–1497, 2006.

C. P. Farrington and H. J. Whitaker. Estimation of effective reproduction numbers for infectious diseases using serological survey data. *Biostatistics*, 4(4):621–632, 2003.

C. P. Farrington, M. N. Kanaan, and N. J. Gay. Estimation of the basic reproduction number for infectious diseases from age-stratified serological data. *Appl Statist*, 50(3):251–292, 2001.

P. E. Fine and J. A. Clarkson. Measles in England and Wales–I: An analysis of factors underlying seasonal patterns. *Int J Epidemiol*, 11(1):5–14, 1982.

M. Fink. myAD: Fast automatic differentiation code in MATLAB. 2006. URL `http://gosh.gmxhome.de/`.

M. Fink, A. Attarian, and H. Tran. Subset selection for parameter estimation in an HIV model. *Proc Appl Math Mech*, 7(1):1121501–1121502, 2007.

M. Fink, J. J. Batzel, and H. Tran. A respiratory system model: Parameter estimation and sensitivity analysis. *Cardiovasc Eng*, 8(2):120–134, 2008.

S. A. Forth and R. Ketzscher. High-level interfaces for the MAD (MATLAB automatic differentiation) package. *Proc 4th European Congress on Computational Methods in Applied Sciences & Engineering*, 2004.

H. A. Gans, A. M. Arvin, J. Galinus, L. Logan, R. DeHovitz, and Y. Maldonado. Deficiency of the humoral immune response to measles vaccine in infants immunized at age 6 months. *JAMA*, 280(6):527–532, 1998.

K. Glass and B. T. Grenfell. Waning immunity and subclinical measles infections in England. *Vaccine*, 22(29-30):4110–4116, 2004.

W. P. Glezen and M. Alpers. Maternal immunization. *Clin Infect Dis*, 28(2): 219–224, 1999.

K. R. Godfrey. *Compartmental models and their application.* Academic Press, N.Y., 1983.

K. R. Godfrey and M. J. Chapman. Identifiability and indistinguishability of linear compartmental models. *Math Comput Simulation*, 32(3):273–295, 1990.

K. R. Godfrey and J. J. DiStefano III. Identifiability of Model Parameters. In *Identifiability of Parametric Models (eds. E. Walter)*. Pergamon, 1987.

K. R. Godfrey and W. R. Fitch. The deterministic identifiability of nonlinear pharmacokinetic models. *J Pharmacokinet Biopharm*, 12(2):177–191, 1984.

K. R. Godfrey, M. J. Chapman, and S. Vajda. Identifiability and indistinguishability of nonlinear pharmacokinetic models. *J Pharmacokinet Biopharm*, 22(3): 229–251, 1994.

M. G. M. Gomes, L. J. White, and G. F. Medley. Infection, reinfection, and vaccination under suboptimal immune protection: epidemiological perspectives. *J Theor Biol*, 228(4):539–549, 2004.

N. C. Grassly and C. Fraser. Seasonal infectious disease epidemiology. *Proc Biol Sci*, 273(1600):2541–2550, 2006.

D. Greenhalgh, O. Diekmann, and M. C. de Jong. Subcritical endemic steady states in mathematical models for animal infections with incomplete immunity. *Math Biosci*, 165(1):1–25, 2000.

B. Greenwood. Maternal immunisation in developing countries. *Vaccine*, 21(24): 3436–3441, 2003.

B. T. Grenfell and R. M. Anderson. The estimation of age-related rates of infection from case notifications and serological data. *J Hyg (Lond)*, 95(2):419–436, 1985.

J. R. Groothuis, E. A. Simoes, M. J. Levin, C. B. Hall, C. E. Long, W. J. Rodriguez, J. Arrobio, H. C. Meissner, D. R. Fulton, R. C. Welliver, D. R. Fulton, R. C. Welliver, D. A. Tristram, G. R. Siber, G. A. Prince, M. Van Raden, and V. G. Hemming. Prophylactic administration of respiratory syncytial virus immune globulin to high-risk infants and young children. *N Engl J Med*, 329(21): 1524–1530, 1993.

S. Gupta, R. M. Anderson, and R. M. May. Networks of sexual contacts: implications for the pattern of spread of HIV. *AIDS*, 3(12):807–817, 1989.

M. Hacimustafaoglu, S. Celebi, E. Aynaci, M. Sinirtas, N. Koksal, A. Kucukerdogan, I. Ercan, G. Goral, and I. Ildirim. The progression of maternal RSV antibodies in the offspring. *Arch Dis Child*, 89(1):52–53, 2004.

C. B. Hall, R. G. Douglas, and J. M. Geiman. Respiratory syncytial virus infections in infants: Quantitation and duration of shedding. *J Pediatr*, 89(1):11–15, 1976.

C. B. Hall, E. E. Walsh, C. E. Long, and K. C. Schnabel. Immunity to and frequency of reinfection with respiratory syncytial virus. *J Infect Dis*, 163(4): 693–698, 1991.

R. Harpaz. Completeness of measles case reporting: review of estimates for the United States. *J Infect Dis*, 189 Suppl 1:185–190, 2004.

J. Hawker, N. Begg, I. Blair, R. Reintjes, and J. Weinberg. *Communicable Disease Control Handbook*. Blackwell, 2nd edition, 2005.

K. M. Heal, M. L. Hansen, and K. M. Rickard. *Maple V Learning Guide (Release 5).* Springer, Berlin, New York, 1998.

C. M. Healy and C. J Baker. Prospects for prevention of childhood infections by maternal immunization. *Curr Opin Infect Dis*, 19(3):271–276, 2006.

A. C. Hearn. *REDUCE Users Manual 3.6.* RAND, Santa Monica, 1995.

J. H. Hemmes, K. C. Winkler, and S. M. Kool. Virus survival as a seasonal factor in influenza and polimyelitis. *Nature*, 188:430–431, 1960.

R. Hermann and A. J. Krener. Nonlinear controllability and observability. *IEEE Trans Automat Control*, 22(3):728–740, 1977.

E. Hubert. Differential algebra for derivations with nontrivial commutation rules. *J Pure Appl Algebra*, 200(1-2):163 – 190, 2005.

S. Huiss, B. Damien, F. Schneider, and C. P. Muller. Characteristics of asymptomatic secondary immune responses to measles virus in late convalescent donors. *Clin Exp Immunol*, 109(3):416–420, 1997.

J. A. Jacquez. The inverse problem for compartmental systems. *Math Comput Simulation*, 24(6):252–459, 1982.

J. A. Jacquez. *Compartmental Analysis in Biology and Medicine*. BioMedware, 3rd edition, 1996.

C. A. Janeway and P. Travers. *Immunobiology: The Immune System In Health and Disease*. Garland Science Publishing, 2005.

V. A. A. Jansen, N. Stollenwerk, H. J. Jensen, M. E. Ramsay, W. J. Edmunds, and C. J. Rhodes. Measles outbreaks in a population with declining vaccine uptake. *Science*, 301(5634):804, 2003.

F. Kappel, J .J. Batzel, M. Bachar, and P. Kotanko. A mathematical model comparing solute kinetics in low- and high-BMI hemodialysis patients. Technical report, Institute for Mathematics and Scientific Computing, Univeristy of Graz, Mar 2009.

M. J. Keeling and B. T. Grenfell. Individual-based perspectives on R_0. *J Theor Biol*, 203(1):51–61, 2000.

M. J. Keeling and B. T. Grenfell. Understanding the persistence of measles: reconciling theory, simulation and observation. *Proc Biol Sci*, 269(1489):335–343, 2002.

M. J. Keeling, P. Rohani, and B. T. Grenfell. Seasonally forced disease dynamics explored as switching between attractors. *Physica D*, 148(3-4):317–335, 2001.

A. S. Kemp and D. E. Campbell. The neonatal immune system. *Semin Neonatal*, 1(2):67–75, 1996.

W. O. Kermack and A. G. McKendrick, editors. *Contributions to the mathematical theory of epidemics, Part I*, volume 115 of *Proc R Soc A*, 1927.

J. P. C. Kleijnen. Sensitivity analysis and related analyses: A review of some statistical techniques. *J Statist Comput Simul*, 57:111–142, 1997.

E. G. Knox. Strategy for rubella vaccination. *Int J Epidemiol*, 9(1):13–23, 1980.

E. Kreyszig. *Advanced Engineering Mathematics*. Wiley, 2006.

M. Krusemeyer. Why does the Wronskian work? *Amer Math Monthly*, 95(1): 46–49, 1988.

F. E. H. Lee, E. E Walsh, A. R. Falsey, R. F. Betts, and J. J. Treanor. Experimental infection of humans with A2 respiratory syncytial virus. *Antiviral Res*, 63(3): 191–196, 2004.

L. Ljung and T. Glad. On global identifiability for arbitrary model parametrizations. *Automatica*, 30(2):265–276, 1994.

G. Margaria, E. Riccomagno, M. J. Chappell, and H. P. Wynn. Differential algebra methods for the study of the structural identifiability of rational function statespace models in the biosciences. *Math Biosci*, 174(1):1–26, 2001.

G. Margaria, E. Riccomagno, and L. J. White. Structural identifiability analysis of some highly structured families of statespace models using differential algebra. *J Math Biol*, 49(5):433–454, 2004.

R. M. May and R. M. Anderson. Spatial heterogeneity and the design of immunization programs. *Math Biosci*, 72(1):83–111, 1984.

H. McCallum, N. Barlow, and J. Hone. How should pathogen transmission be modelled? *Trends Ecol Evol*, 16(6):295–300, 2001.

G. F. Medley and D. J. Nokes. Mathematical Models of Vaccination. In *Topley & Wilson's Microbiology and Microbial Infections - 10th Edition: Immunology (eds. S. H. E. Kaufmann & M. E. Steward)*, pages 947–966, London, 2005. Hodder Arnold.

G. F. Medley, N. A. Lindop, W. J. Edmunds, and D. J. Nokes. Hepatitis-B virus endemicity: heterogeneity, catastrophic dynamics and control. *Nat Med*, 7(5): 619–624, 2001.

F. R. Mooi and S. C. de Greeff. The case for maternal vaccination against pertussis. *Lancet Infect Dis*, 7(9):614–624, 2007.

A. W. Mounts, T. Ando, M. Koopmans, J. S. Bresee, J. Noel, and R. I. Glass. Cold weather seasonality of gastroenteritis associated with norwalk-like viruses. *J Infect Dis*, 181(2):284–287, 2000.

K. Mulholland. Maternal immunization for the prevention of bacterial infection in young infants. *Vaccine*, 16(14-15):1464–1467, 1998.

K. Mulholland, R. O. Suara, G. Siber, D. Roberton, S. Jaffar, J. N'Jie, L. Baden, C. Thompson, R. Anwaruddin, L. Dinan, W. P. Glezen, N. Francis, B. Fritzell, and B. M. Greenwood. Maternal immunization with Haemophilus influenzae type b polysaccharide-tetanus protein conjugate vaccine in The Gambia. *JAMA*, 275(15):1182–1188, 1996.

F. M. Munoz and J. A. Englund. A step ahead: Infant protection through maternal immunization. *Pediatr Clin North Am*, 47(2):449–463, 2000.

F. M. Munoz, P. A. Piedra, and W. P. Glezen. Safety and immunogenicity of respiratory syncytial virus purified fusion protein-2 vaccine in pregnant women. *Vaccine*, 21(24):3465–3467, 2003.

I. A. Nestorov. Sensitivity analysis of pharmacokinetic and pharmacodynamic systems: I. A structural approach to sensitivity analysis of physiologically based pharmacokinetic models. *J Pharmacokinet Biopharm*, 27(6):577–596, 1999.

C. Nicoara, K. Zch, D. Trachsel, D. Germann, and L. Matter. Decay of passively acquired maternal antibodies against measles, mumps, and rubella viruses. *Clin Diagn Lab Immunol*, 6(6):868–871, 1999.

D. J. Nokes and R. M. Anderson. The use of mathematical models in the epidemiological study of infectious diseases and in the design of mass immunization programmes. *Epidemiol Infect*, 101(1):1–20, 1988.

D. J. Nokes and J. Swinton. The control of childhood viral infections by pulse vaccination. *IMA J Math Appl Med Biol*, 12(1):29–53, 1995.

R. Ochola, C. S., G. Fegan, P. D. Scott, G. F. Medley, P. A. Cane, and D. J. Nokes. The level and duration of RSV-specific maternal IgG in infants in Kilifi Kenya. *PLoS One*, 4(12):e8088, 2009.

M. M. Ogilvie, A. S. Vathenen, M. Radford, J. Codd, and S. Key. Maternal antibody and respiratory syncytial virus infection in infancy. *J Med Virol*, 7(4): 263–271, 1981.

P. L. Ogra. Respiratory syncytial virus: the virus, the disease and the immune response. *Paediatr Respir Rev*, 5((Suppl A)):119–126, 2004.

K. Ogungbenro, A. Dokoumetzidis, and L. Aarons. Application of optimal design methodologies in clinical pharmacology experiments. *Pharm Stat*, 8(3):239–252, 2009.

H. F. Pabst, D. W. Spady, R. G. Marusyk, M. M. Carson, L. W. Chui, M. R. Joffres, and K. M. Grimsrud. Reduced measles immunity in infants in a well-vaccinated population. *Pediatr Infect Dis J*, 11(7):525–529, 1992.

I. R. Pedersen, C. H. Mordhorst, G. Glikmann, and H. von Magnus. Subclinical measles infection in vaccinated seropositive individuals in arctic Greenland. *Vaccine*, 7(4):345–348, 1989.

R. W. Pitcher-Wilmott, P. Hindocha, and C. B. Wood. The placental transfer of IgG subclasses in human pregnancy. *Clin Exp Immunol*, 41(2):303–308, 1980.

H. Pohjanpalo. System identifiability based on the power series expansion of the solution. *Math Biosci*, 41(6):21–33, 1978.

J. M. Puck, W. P. Glezen, A. L. Frank, and H. R. Six. Protection of infants from infection with influenza A virus by transplacentally acquired antibody. *J Infect Dis*, 142(6):844–849, 1980.

H. Rabitz, M. Kramer, and D. Dacol. Sensitivity analysis in chemical kinetics. *Ann Rev Phys Chem*, 34:419–461, 1983.

P. D. Reuman, E. M. Ayoub, and P. A. Small. Effect of passive maternal antibody on influenza illness in children: a prospective study of influenza A in mother-infant pairs. *Pediatr Infect Dis J*, 6(4):398–403, 1987.

J. F. Ritt. *Differential Algebra*. American Mathematical Society, New York, 1950.

M. P. Saccomani, S. Audoly, and L. D'Angiò. Parameter identifiability of nonlinear systems: the role of initial conditions. *Automatica*, 39(4):619–632, 2003.

F. Saji, Y. Samejima, S. Kamiura, and M. Koyama. Dynamics of immunoglobulins at the feto-maternal interface. *Rev Reprod*, 4(2):81–89, 1999.

H. Sarvas, I. Seppl, S. Kurikka, R. Siegberg, and O. Mkel. Half-life of the maternal IgG1 allotype in infants. *J Clin Immunol*, 13(2):145–151, 1993.

H. Sato, P. Albrecht, D. W. Reynolds, S. Stagno, and F. A. Ennis. Transfer of measles, mumps, and rubella antibodies from mother to infant: its effect on measles, mumps, and rubella immunization. *Am J Dis Child*, 133(12):1240–1243, 1979.

L. Sattenspiel, J. Koopman, C. Simon, and J. A. Jacquez. The effects of population structure on the spread of the HIV infection. *Am J Phys Anthropol*, 82(4):421–429, 1990.

N. Le Saux, I. Gaboury, and N. MacDonald. Maternal respiratory syncytial virus antibody titers: season and children matter. *Pediatr Infect Dis J*, 22(6):563–564, 2003.

D. Schenzle. An age-structured model of pre- and post-vaccination measles transmission. *IMA J Math Appl Med Biol*, 1(2):169–191, 1984.

A. Scherer and A. McLean. Mathematical models of vaccination. *Br Med Bull*, 62 (1):187–199, 2002.

C. A. Siegrist. Mechanisms by which maternal antibodies influence infant vaccine responses: review of hypotheses and definition of main determinants. *Vaccine*, 21(24):3406–3412, 2003.

I. Smets, K. Bernaerts, J. Sun, K. Marchal, J. Vanderleyden, and J. Van Impe. Sensitivity function-based model reduction: A bacterial gene expression case study. *Biotechnol Bioeng*, 80(2):195–200, 2002.

L. G. Stensballe, H. Ravn, K. Kristensen, T. Meakins, P. Aaby, and E. A. F. Simoes. Seasonal variation of maternally derived respiratory syncytial virus antibodies and association with infant hospitalizations for respiratory syncytial virus. *J Pediatr*, 154(2):296–298, 2009.

C. V. Sumaya and R. S. Gibbs. Immunization of pregnant women with influenza A/New Jersey/76 virus vaccine: reactogenicity and immunogenicity in mother and infant. *J Infect Dis*, 140(2):141–146, 1979.

S. B. Thacker, K. Choi, and P. S. Brachman. The surveillance of infectious diseases. *JAMA*, 249(9):1181–1185, 1983.

R. Tomović. *Sensitivity Analysis of Dynamic Systems*. McGraw Hill, 1963.

S. Vajda. Structural identifiability of linear, bilinear, polynomial and rational systems. In *Proc 9th IFAC World Congress, Budapest, Hungary*, pages 107–112, 1984.

S. Vajda, P. Valko, and T. Turányi. Principal component analysis of kinectic models. *Int J Chem Kinet*, 17(1):55–81, 1985.

S. Vajda, K. R. Godfrey, and H. Rabitz. Similarity transformation approach to identifiability analysis of nonlinear compartmental models. *Math Biosci*, 93(2): 217–248, 1989.

B. A. M. van der Zeijst, M. I. Dijkman, W. Luytjes, A. J. W. van Alphen, and G. P. J. M. van den Dobbelsteen. On the design of national vaccination programmes. *Vaccine*, 25(16):3143–3145, 2007.

J. Vandelaer, M. Birmingham, F. Gasse, M. Kurian, C. Shaw, and S. Garnier. Tetanus in developing countries: an update on the Maternal and Neonatal Tetanus Elimination Initiative. *Vaccine*, 21(24):3442–3445, 2003.

T. A. Waldmann and W. Strober. Metabolism of immunoglobulins. *Prog Allergy*, 13:1–110, 1969.

E. Walter. *Identifiability of state space models*. Springer, Berlin, 1982.

A. Weber, M. Weber, and P. Milligan. Modeling epidemics caused by respiratory syncytial virus (RSV). *Math Biosci*, 172(2):95–113, 2001.

H. J. Whitaker and C. P. Farrington. Estimation of infectious disease parameters from serological survey data: the impact of regular epidemics. *Stat Med*, 23(15): 2429–2443, 2004.

L. J. White. *A theoretical study of the effects of immunity on infectious disease transmission*. PhD thesis, University of Warwick, 2000.

L. J. White, M. J. Cox, and G. F. Medley. Cross immunity and vaccination against multiple microparasite strains. *IMA J Math Appl Med Biol*, 15(3):211–233, 1998.

L. J. White, N. D. Evans, T. J. Lam, Y. H. Schukken, G. F. Medley, K. R. Godfrey, and M. J. Chappell. The structural identifiability and parameter estimation of a multispecies model for the transmission of mastitis in dairy cows. *Math Biosci*, 174(2):77–90, 2001.

L. J. White, M. Waris, P. A. Cane, D. J. Nokes, and G. F. Medley. The transmission dynamics of groups A and B human respiratory syncytial virus (hRSV) in England & Wales and Finland: seasonality and cross-protection. *Epidemiol Infect*, 133(2):279–289, 2005.

L. J. White, J. N. Mandl, M. G M Gomes, A. T. Bodley-Tickell, P. A. Cane, P. Perez-Brena, J. C. Aguilar, M. M. Siqueira, S. A. Portes, S. M. Straliotto, M. Waris, D. J. Nokes, and G. F. Medley. Understanding the transmission

dynamics of respiratory syncytial virus using multiple time series and nested models. *Math Biosci*, 209(1):222–239, 2007.

WHO. Maternal and neonatal tetanus elimination by 2005: strategies for achieving and maintaining elimination. *World Health Organization: Geneva*, 2002.

B. G. Williams, F. T. Cutts, and C. Dye. Measles vaccination policy. *Epidemiol Infect*, 115(3):603–621, 1995.

S. Wolfram. *The Mathematica Book*. Wolfram Media/Cambridge University Press, Cambridge, UK, 1999.

J. W. T. Yates, N. D. Evans, and M. J. Chappell. Structural identifiability analysis via symmetries of differential equations. *Automatica*, 45(11):2585–2591, 2009.

K. Zaman, E. Roy, S. E. Arifeen, M. Rahman, R. Raqib, E. Wilson, S. B. Omer, N. S. Shahid, R. F. Breiman, R. E. Breiman, and M. C. Steinhoff. Effectiveness of maternal influenza immunization in mothers and infants. *N Engl J Med*, 359 (15):1555–1564, 2008.

R. M. Zinkernagel. Maternal antibodies, childhood infections, and autoimmune diseases. *N Engl J Med*, 345(18):1331–1335, 2001.

Appendix A

MSEIRS4 Model Equations

System of ordinary differential equations describing the MSEIRS4 model derived and evaluated for hRSV in the work by Weber et al. [2001].

$$
\begin{aligned}
\dot{M}(t) &= \mu Ab^{+}(t) - (\omega_M + \mu)M(t), \\
\dot{S}_1(t) &= \mu Ab^{-}(t) + \omega_M M(t) - \mu S_1(t) - \lambda_1(t)S_1(t), \\
\dot{E}_i(t) &= \lambda_i(t)S_i(t) - (\zeta + \mu)E_i(t), && i = 1, \ldots, 4, \\
\dot{I}_i(t) &= \zeta E_i(t) - (\nu + \mu)I_i(t), && i = 1, \ldots, 4, \\
\dot{R}_i(t) &= \nu I_i(t) - (\omega_R + \mu)R_i(t), && i = 1, \ldots, 4, \\
\dot{S}_j(t) &= \omega_R R_{j-1}(t) - \mu S_j(t) - \lambda_j(t)S_j(t), && j = 2, 3, \\
\dot{S}_4(t) &= \omega_R(R_3(t) + R_4(t)) - \mu S_4(t) - \lambda_4(t)S_4(t),
\end{aligned}
$$

where

$$
Ab^{+}(t) = \sum_{i=1}^{4} R_i(t), \qquad Ab^{-}(t) = 1 - Ab^{+}(t), \qquad I(t) = \sum_{i=1}^{4} I_i(t),
$$

$$
\begin{aligned}
\lambda_1(t) &= \beta_0(1 + \beta_1 \cos(2\pi t + \phi))I(t), & \lambda_2(t) &= \sigma_1 \lambda_1(t) \\
\lambda_3(t) &= \sigma_2 \lambda_1(t), & \lambda_4(t) &= \sigma_3 \lambda_1(t),
\end{aligned}
$$

Appendix B

Simulation Techniques for PDE Model Structures

Simulation of the PDE system in Chapter 6 is performed using simple numerical methods based on finite differencing. The domain space is divided into a uniform mesh with a constant step size, h, and boundary conditions determined by the model. The internal grid points are then estimated incrementally, for each age profile at increasing steps in time, using an explicit backwards difference scheme. Since time series dynamics are seen to evolve much more rapidly than average age profiles, a higher degree of accuracy is applied to calculations in the time domain. Therefore, partial derivatives with respect to age and time are substituted by 2nd and 3rd order finite differences, respectively, according to the following expressions:

$$\frac{dX(t,a)}{dt} = \frac{11X_{i,j} - 18X_{i-1,j} + 9X_{i-2,j} - 2X_{i-3,j}}{6h} + O(h^3), \tag{B.1}$$

$$\frac{dX(t,a)}{da} = \frac{3X_{i,j} - 4X_{i,j-1} + X_{i,j-2}}{2h} + O(h^2), \tag{B.2}$$

where $X_{i,j} = X(t_i, a_j)$.

In practice, additional complexities arise in the solving of epidemic PDE systems since the force of infection is directly dependent on the integral of the infective age profile, denoted $I(t)$. This means that mesh points for certain state variables cannot be solved explicitly since they are effectively dependent on their own solu-

tion. Therefore, for each increment in time, an estimate of $\lambda(t, a)$ is extrapolated from previous time points using a 2nd order Lagrange interpolating polynomial of the form:

$$L(t_i) \;=\; \sum_{i=0}^{k} y_i \ell_i(t) \qquad\qquad \ell_i(t) \;=\; \prod_{j=0,\, j\neq i}^{k} \frac{(t - t_j)}{(t_i - t_j)} \,. \tag{B.3}$$

Since the simulation time steps are uniformly spaced, the function can be reduced to the following expression:

$$I(t_i) \;=\; I(t_{i-3}) \;-\; 3\, I(t_{i-2}) \;+\; 3\, I(t_{i-1}) \,. \tag{B.4}$$

More sophisticated numerical methods have been presented to address this problem, for example in the work by White [2000], where a further iterative process, nested into the main routine, is executed at each increment in time in order to allow convergence to a solution for $\lambda(t, a)$. The simple extrapolation approach is adopted in this work for ease of implementation and to minimise time required for computation.

Integration of the state variable solutions, for example over an integer number of complete annual cycles to find an average age profile, is performed using Romberg integration; a Newton-Cotes type method based on repeated application of Richardson extrapolation to the trapezoidal rule (for more information see the book by Chapra and Canale [2002]).

Let $J_0^{(h)}$, $J_0^{(2h)}$ and $J_0^{(4h)}$ denote the integrals computed using the trapezoidal rule with step sizes h, $2h$ and $4h$ respectively, such that:

$$J_0^{(h)} \;=\; J + c_1 h^2 + c_2 h^4 + c_3 h^6 + \dots \,, \tag{B.5}$$

$$J_0^{(2h)} \;=\; J + c_1 (2h)^2 + c_2 (2h)^4 + c_3 (2h)^6 + \dots \,, \tag{B.6}$$

$$J_0^{(4h)} \;=\; J + c_1 (4h)^2 + c_2 (4h)^4 + c_3 (4h)^6 + \dots \,, \tag{B.7}$$

where J is the exact solution and the later terms correspond to the resulting error. More accurate integral estimates can then be obtained by combining (B.5)-(B.7)

such that subsequent error terms are eliminated according to the following process:

$$J_1^{(h)} = \frac{4J_0^{(h)} - J_0^{(2h)}}{3} = J - 4c_2h^4 - 20c_3h^6 + \dots , \tag{B.8}$$

$$J_1^{(2h)} = \frac{4J_0^{(2h)} - J_0^{(4h)}}{3} = J - 64c_2h^4 - 1280c_3h^6 + \dots , \tag{B.9}$$

$$J_2^{(h)} = \frac{16J_1^{(h)} - J_1^{(2h)}}{15} = J + 64c_3h^6 + \dots . \tag{B.10}$$

It can be seen from the final estimate (B.10) that the magnitude of the truncation error is significantly reduced with relatively little computational effort.

Error Estimation

An estimation of the error in the numerical solution is found by comparing simulation results corresponding to a homogeneous MSIR model to those generated from equivalent ODE-based systems with more computationally tractable solutions. A suitable test model is derived from the general MSIR system equations (3.3)-(3.7) by setting all model parameters to constant values and ensuring that $\mu_b = \mu_d = \mu$, such that equivalent time and age domain models are given by (3.14)-(3.17) and (3.45)-(3.48), respectively. The system of partial differential equations is then solved using the described methods with parameter values corresponding to hRSV without secondary infection (Tables 3.2 and 3.3(A)), and a step size of 0.0026 years.

In the absence of seasonal forcing, the steady state prevalence of infection estimated by the simulation is compared to the analytic solution given by (3.54). The resulting normalised error is found to be 3.9×10^{-4} for the PDE model and 4.3×10^{-8} for the ODE system obtained using the `ode45` algorithm in MATLAB.

In the age domain, the steady state average age profile predicted by the PDE model simulation is compared to an analytic solution derived from the equivalent age domain model (3.45)-(3.48), as shown in Section 3.3.4. The resulting error functions are displayed in Figure B.1. It can be seen from Figure B.1(b) that the peak normalised error has a magnitude of 0.096 and occurs directly after the first simulation step. The location of the maximum error coincides with the greatest rate of change in $I(a)$ and is also likely to be a result of there being only one previous age point on which to base the finite difference estimate. Following its

peak, the magnitude of the normalised error curve quickly decreases to a more reasonable level, where an average value of 6.3×10^{-4} is recorded over the first 12 months of age.

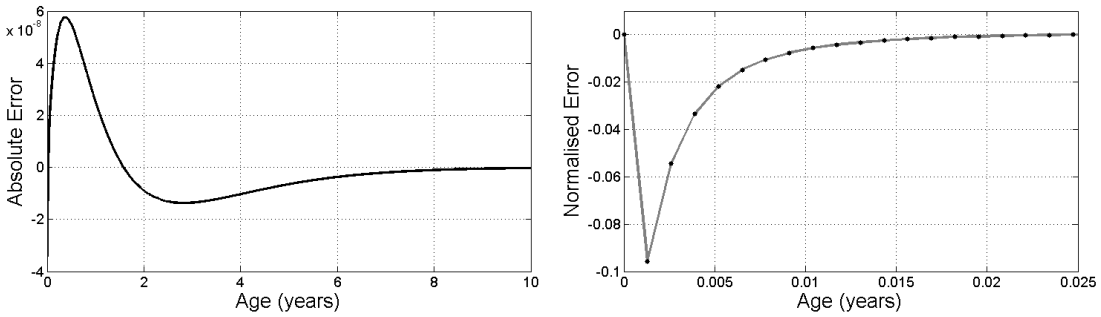

(a) Absolute Error (b) Normalised Error

Figure B.1: Variation in absolute and normalised error of the numerical solution to a homogeneous MSIR PDE model found using a 2nd/3rd order backwards difference scheme.

Finally, the resulting times series prediction generated by the addition of seasonal forcing is compared to that obtained by solving the ODE system (3.14)-(3.17) using a fourth order Runge-Kutta algorithm (MATLAB `ode45`) with a maximum step size of 0.001 years. The variation in normalised error over a complete annual cycle is shown in Figure B.2. It is found that the maximum normalised error is 0.0081, which occurs at the beginning of each annual epidemic, and the average error across one complete annual cycle is 0.0039.

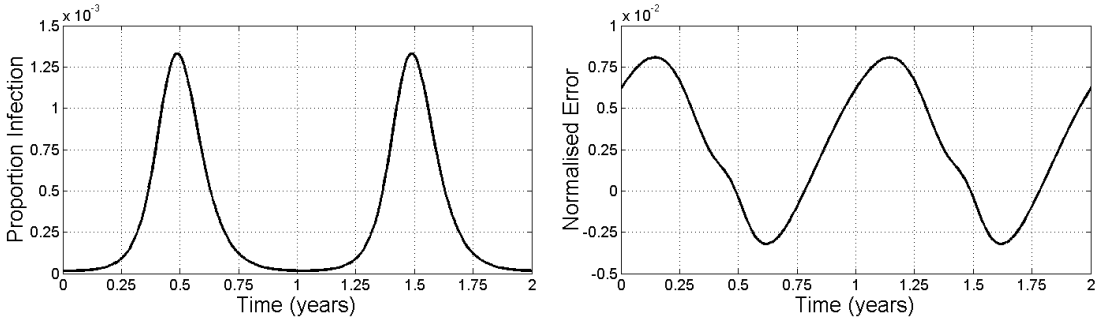

(a) Simulation Output (b) Normalised Error

Figure B.2: Time series variation in normalised error between numerical solutions of the homogeneous PDE and ODE MSIR models, using 2nd/3rd order backwards differencing and 4th order Runge-Kutta, respectively.

It should be noted that the estimated error is considered to be acceptable in the context of this work given that the outcomes of the analysis are largely qualitative in nature.